

Discovery and Preclinical Characterization of BIIB129, a Covalent, Selective, and Brain Penetrant BTK Inhibitor for the Treatment of Multiple Sclerosis

Martin K. Himmelbauer, Bekim Bajrami, Rebecca Basile, Andrew Capacci, Te Yu Chen, Colin K. Choi, Rab Gilfillan, Felix Gonzalez-Lopez de Turiso, Chungang Gu, Marc Hoemberger, Douglas S. Johnson, J. Howard Jones, Ekta Kadakia, Melissa Kirkland, Edward Y. Lin, Ying Liu, Bin Ma, Tom Magee, Srinivasa Mantena, Isaac E. Marx, Claire M. Metrick, Michael Mingueneau, Paramasivam Murugan, Cathy A. Muste, Prasad Nadella, Marta Nevalainen, Chelsea R. Parker Harp, Vatee Pattaropong, Alicia Pietrasiewicz, Robin J. Prince, Thomas J. Purgett, Joseph C. Santoro, Jurgen Schulz, Simone Sciabola, Hao Tang, H. George Vandever, Ti Wang, Zain Yousaf, Christopher J. Helal, Brian T. Hopkins†*

AUTHOR ADDRESS

† Biotherapeutics & Medicinal Sciences, Biogen, 225 Binney Street, Cambridge, Massachusetts 02142, United States

Brian T. Hopkins – Research & Development, Biogen, Cambridge, Massachusetts 02142, United States; orcid.org/ 0000-0002-2912-9954; Email: brian.hopkins@biogen.com

ASSOCIATED CONTENT

Table of Contents:

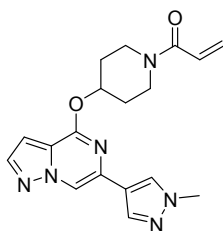
Synthetic Procedures	2
Assays	48
BTK Biochemical Activity Assay (BTK IC ₅₀)	48
Continuous-read Kinetic Enzyme Assay (log k _{inact} /K _i).....	48
CD69 Whole Blood Assay	48

Immortalized TMD8 Cell Assay.....	49
Protein Crystallography.....	49
Metabolite ID of compound 10.....	52
<i>In vitro</i> metabolism of compound 10 in rat and human liver microsomes.....	52
<i>In-vitro</i> metabolism of compound 10 in rat, dog, monkey and human hepatocytes.....	53
<i>In-vivo</i> metabolism of compound 10 in rat plasma, urine and bile.....	58
Metabolism of BIIB129 (25).....	61
Cross-Species <i>In Vitro</i> Metabolic Stability in Liver Microsomes and Hepatocytes.....	61
Metabolic Profile of BIIB129 (25) in Vitro:.....	62
<i>In-vivo</i> metabolism of BIIB129 (25) in rat plasma, urine and bile.....	65
PK/PD modeling.....	67
Prediction of Human PK Parameters of BIIB129 (25).....	67
Activity of BIIB129 (25) in the BioMAP Human Cell-Based Assay.....	69
Kinome Selectivity:.....	72
Determining Kinome Selectivity using <i>scanMAX</i> TM	72
Determining Kinome Selectivity using <i>KdELECT</i> TM	72
References:.....	75

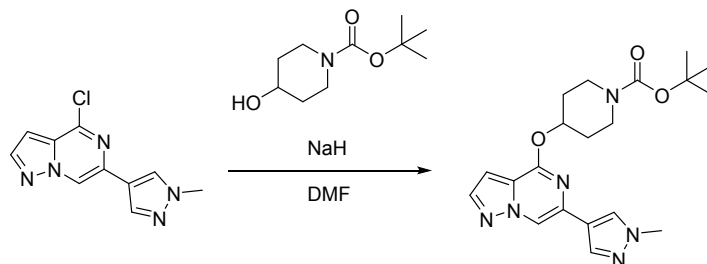
Synthetic Procedures

Compound 7:

1-(4-((6-(1-Methyl-1*H*-pyrazol-4-yl)pyrazolo[1,5-*a*]pyrazin-4-yl)oxy)piperidin-1-yl)prop-2-en-1-one

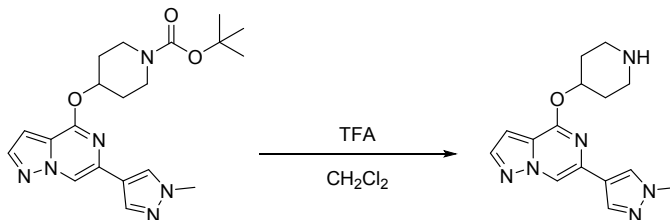


1. *Synthesis of tert-butyl 4-((6-(1-methyl-1*H*-pyrazol-4-yl)pyrazolo[1,5-*a*]pyrazin-4-yl)oxy)piperidine-1-carboxylate*



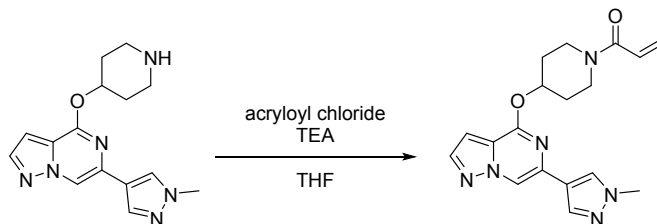
To a solution of *tert*-butyl 4-hydroxypiperidine-1-carboxylate (664 mg, 3.30 mmol) in DMF (10 mL) was added NaH (396 mg, 9.90 mmol, 60% purity) in four batches under vigorous stirring at 0 °C. After 45 min, 4-chloro-6-(1-methyl-1*H*-pyrazol-4-yl)pyrazolo[1,5-*a*]pyrazine (700 mg, 3.00 mmol) was added to the resulting pale-yellow suspension and stirring was continued at rt overnight. The mixture was diluted with EtOAc (30 mL) and water (15 mL) was added carefully. The aqueous phase was separated and extracted with EtOAc (10 mL). The combined organic phase was washed with brine (20 mL), dried over Na₂SO₄, filtered, and concentrated *in vacuo*. The resulting crude residue was purified by column chromatography (10 g SiO₂, 50% EtOAc in heptane) to afford *tert*-butyl 4-((6-(1-methyl-1*H*-pyrazol-4-yl)pyrazolo[1,5-*a*]pyrazin-4-yl)oxy)piperidine-1-carboxylate (1.30 g, 98% yield). LCMS (ESI⁺): *m/z* calcd. for C₂₀H₂₆N₆O₃ [M+H]⁺, 399.2; found, 399.2.

2. *Synthesis of 6-(1-methyl-1H-pyrazol-4-yl)-4-(piperidin-4-yloxy)pyrazolo[1,5-a]pyrazine*



To a vigorously stirred solution of *tert*-butyl 4-((6-(1-methyl-1*H*-pyrazol-4-yl)pyrazolo[1,5-*a*]pyrazin-4-yl)oxy)piperidine-1-carboxylate (1.2 g, 2.9 mmol) in CH₂Cl₂ (5.0 mL) was added TFA (6.7 g, 58.9 mmol, 4.5 mL) at rt. After stirring overnight, the resulting mixture was diluted with MeOH (1 mL) and purified on a 5 g SCX column (eluant: 2 M NH₃-MeOH) to afford the title compound 6-(1-methyl-1*H*-pyrazol-4-yl)-4-(piperidin-4-yloxy)pyrazolo[1,5-*a*]pyrazine (890 mg, 96% yield) as a white solid. LCMS (ESI⁺): *m/z* calcd. for C₁₅H₁₈N₆O [M+H]⁺, 299.2; found, 299.2.

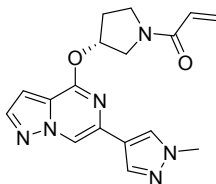
3. *Synthesis of (1-(4-((6-(1-methyl-1H-pyrazol-4-yl)pyrazolo[1,5-a]pyrazin-4-yl)oxy)piperidin-1-yl)prop-2-en-1-one*



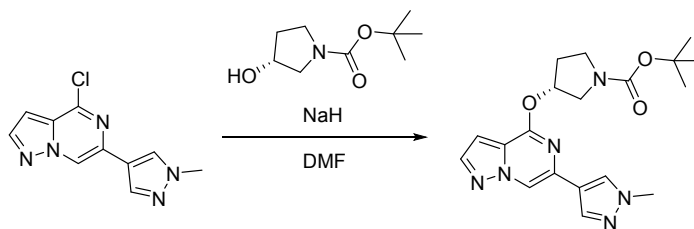
To a solution of 6-(1-methyl-1*H*-pyrazol-4-yl)-4-(piperidin-4-yloxy)pyrazolo[1,5-*a*]pyrazine (30 mg, 0.10 mmol) in THF (1 mL) was added acryloyl chloride (14 mg, 0.15 mmol, 13 μ L) followed by TEA (19 mg, 0.19 mmol, 27 μ L) at rt. After stirring overnight, the volatiles were removed and the residual material was purified by HPLC (Waters XSelect CSH C18, 5 μ m, 19 mm \times 100 mm column with mobile phase H₂O (A) and MeCN (B) and a gradient of 5 – 50% B (0.2% NH₄OH final v/v % modifier) with flow rate at 30 mL/min) to afford 1-(4-(((6-(1-methylpyrazol-4-yl)pyrazolo[1,5-*a*]pyrazin-4-yl)oxy)-1-piperidyl)prop-2-en-1-one (25 mg, 67% yield) as a clear oil. HRMS (ESI⁺): *m/z* calcd. for C₁₈H₂₀N₆O₂ [M+H]⁺, 353.1721; found, 353.1726. ¹H NMR (500 MHz, dimethyl sulfoxide-*d*₆): δ (ppm) 8.76 (s, 1H), 8.22 (s, 1H), 8.02 (s, 2H), 6.88 (d, *J* = 2.4 Hz, 2H), 6.19–6.07 (m, 1H), 5.75–5.67 (m, 1H), 5.65–5.54 (m, 1H), 3.95 (m, 2H), 3.89 (s, 3H), 3.69–3.46 (m, 2H), 2.20–2.03 (m, 2H), 1.86–1.68 (m, 2H).

Compound 8:

(*R*)-1-(3-(((6-(1-Methyl-1*H*-pyrazol-4-yl)pyrazolo[1,5-*a*]pyrazin-4-yl)oxy)pyrrolidine-1-yl)prop-2-en-1-one



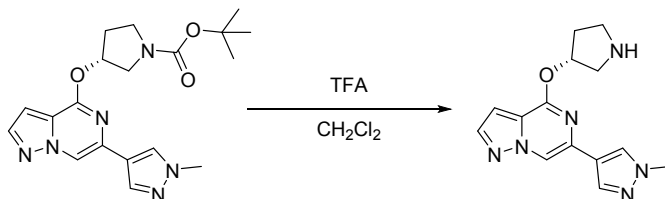
1. Synthesis of *tert*-butyl (*R*)-3-(((6-(1-methyl-1*H*-pyrazol-4-yl)pyrazolo[1,5-*a*]pyrazin-4-yl)oxy)pyrrolidine-1-carboxylate



To a solution of *tert*-butyl (*R*)-3-hydroxypyrrolidine-1-carboxylate (193 mg, 1.03 mmol) in DMF (3 mL) was added NaH (136 mg, 3.40 mmol, 60% purity) in four batches under vigorous stirring at 0 °C. After 45 min, 4-chloro-6-(1-methyl-1*H*-pyrazol-4-yl)pyrazolo[1,5-*a*]pyrazine (240 mg, 1.03 mmol) was added to the resulting pale-yellow suspension and stirring was continued at rt overnight. The mixture was

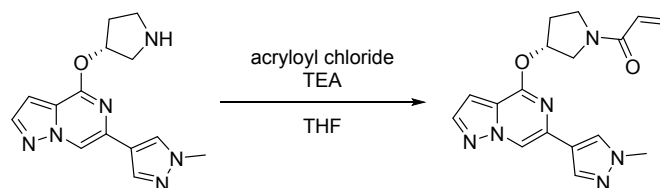
diluted with EtOAc (30 mL) and water (15 mL) was added carefully. The aqueous phase was separated and extracted with EtOAc (10 mL). The combined organic phase was washed with brine (20 mL), dried over Na₂SO₄, filtered, and concentrated *in vacuo*. The resulting crude residue was purified by column chromatography (10 g SiO₂, 50% EtOAc in heptane) to afford *tert*-butyl (*R*)-3-(((6-(1-methyl-1*H*-pyrazol-4-yl)pyrazolo[1,5-*a*]pyrazin-4-yl)oxy)pyrrolidine-1-carboxylate (345 mg, 83% yield). LCMS (ESI+): *m/z* calcd. for C₁₉H₂₄N₆O₃ [M+H]⁺, 385.2; found, 385.2.

2. *Synthesis of (R)-6-(1-methyl-1H-pyrazol-4-yl)-4-(5yrrolidine-3-yloxy)pyrazolo[1,5-a]pyrazine*



To a vigorously stirred solution of *tert*-butyl (*R*)-3-(((6-(1-methyl-1*H*-pyrazol-4-yl)pyrazolo[1,5-*a*]pyrazin-4-yl)oxy)pyrrolidine-1-carboxylate (326 mg, 0.85 mmol) in CH₂Cl₂ (5 mL) was dropwise added TFA (1.93 g, 17.0 mmol, 1.30 mL) at rt. After stirring overnight, the resulting mixture was diluted with MeOH (1 mL) and purified on a 5 g SCX column (eluant: 2 M NH₃-MeOH) to afford (*R*)-6-(1-methyl-1*H*-pyrazol-4-yl)-4-(5yrrolidine-3-yloxy)pyrazolo[1,5-*a*]pyrazine (230 mg, 91% yield) as a colorless oil. LCMS (ESI+): *m/z* calcd. for C₁₄H₁₆N₆O [M+H]⁺, 285.1; found, 285.1.

3. *Synthesis of (R)-1-(3-(((6-(1-methyl-1H-pyrazol-4-yl)pyrazolo[1,5-a]pyrazin-4-yl)oxy)5yrrolidine-1-yl)prop-2-en-1-one*

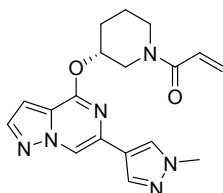


To a solution of (*R*)-6-(1-methyl-1*H*-pyrazol-4-yl)-4-(pyrrolidine-3-yloxy)pyrazolo[1,5-*a*]pyrazine (30 mg, 0.11 mmol) in THF (1 mL) was added acryloyl chloride (11 mg, 0.12 mmol, 10 μL) followed by TEA (21 mg, 0.21 mmol, 29 μL) at rt. After stirring overnight, the volatiles were removed *in vacuo* and the resulting crude residue was purified by HPLC (Waters Xselect CSH C18, 5 μm, 19 mm × 100 mm column with mobile phase H₂O (A) and MeCN (B) and a gradient of 5–50% B (0.2% NH₄OH final v/v % modifier) with flow rate at 30 mL/min) to afford (*R*)-1-(3-(((6-(1-methyl-1*H*-pyrazol-4-yl)pyrazolo[1,5-*a*]pyrazin-4-yl)oxy)5yrrolidine-1-yl)prop-2-en-1-one (28 mg, 74% yield) as a clear oil. HRMS (ESI+): *m/z* calcd. for C₁₇H₁₈N₆O₂ [M+H]⁺, 339.1564; found, 339.1571. ¹H NMR (500 MHz, dimethyl sulfoxide-*d*₆): δ (ppm) 8.79 (s, 1H), 8.25 (d, *J* = 3.1 Hz, 1H), 8.04–8.02 (dd, *J* = 10.1, 2.1 Hz, 1H), 6.88–6.83 (m,

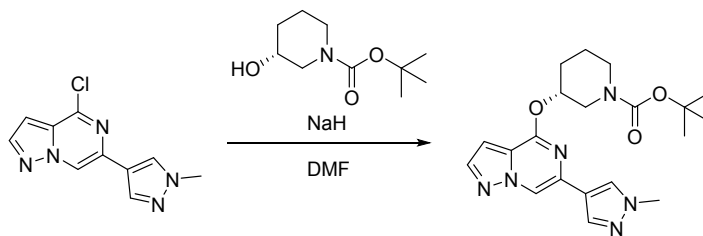
1H), 6.72–6.54 (m, 1H), 6.21–6.12 (m, 1H), 5.95–5.81 (m, 1H), 5.74–5.63 (m, 1H), 4.13–4.02 (m, 1H), 3.90 (s, 3H), 3.89–3.82 (m, 2H), 3.76 (s, 2H), 2.37 (br d, $J = 1.8$ Hz, 2H).

Compound 9:

(*R*)-1-(3-((6-(1-methyl-1*H*-pyrazol-4-yl)pyrazolo[1,5-*a*]pyrazin-4-yl)oxy)piperidin-1-yl)prop-2-en-1-one

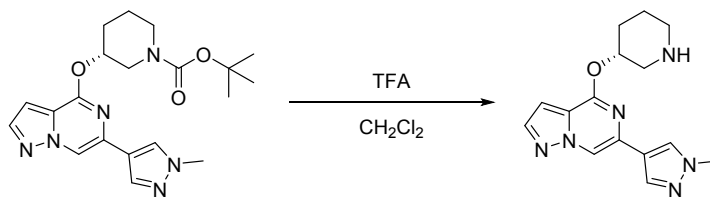


1. *Synthesis of tert-butyl (R)-3-((6-(1-methyl-1*H*-pyrazol-4-yl)pyrazolo[1,5-*a*]pyrazin-4-yl)oxy)piperidine-1-carboxylate*



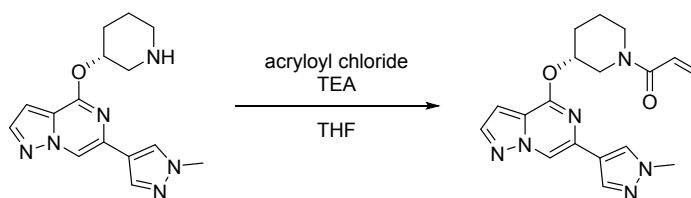
To a solution of *tert*-butyl (*R*)-3-hydroxypiperidine-1-carboxylate (221 mg, 1.10 mmol) in DMF (3 mL) was added NaH (132 mg, 3.30 mmol, 60% purity) in four batches under vigorous stirring at 0 °C. After 45 min, 4-chloro-6-(1-methyl-1*H*-pyrazol-4-yl)pyrazolo[1,5-*a*]pyrazine (234 mg, 1.00 mmol) was added to the resulting pale-yellow suspension and stirring was continued at rt overnight. The mixture was diluted with EtOAc (30 mL) and water (15 mL) was added carefully. The aqueous phase was separated and extracted with EtOAc (10 mL). The combined organic phase was washed with brine (20 mL), dried over Na₂SO₄, filtered, and concentrated *in vacuo*. The resulting crude residue was purified by column chromatography (10 g SiO₂, 50% EtOAc in heptane) to afford (*R*)-3-((6-(1-methyl-1*H*-pyrazol-4-yl)pyrazolo[1,5-*a*]pyrazin-4-yl)oxy)piperidine-1-carboxylate (390 mg, 88% yield) as a sticky colorless gum. LCMS (ESI⁺): m/z calcd. for C₂₀H₂₆N₆O₃ [M+H]⁺, 399.2; found, 399.2.

2. *Synthesis of (R)-6-(1-methyl-1H-pyrazol-4-yl)-4-(piperidin-3-yloxy)pyrazolo[1,5-a]pyrazine*



To a vigorously stirred solution of *tert*-butyl (*R*)-3-((6-(1-methyl-1*H*-pyrazol-4-yl)pyrazolo[1,5-*a*]pyrazin-4-yl)oxy)piperidine-1-carboxylate (390 mg, 0.98 mmol) in CH₂Cl₂ (3 mL) was added TFA (2.2 g, 19.6 mmol, 1.5 mL) at rt. After stirring overnight, the resulting mixture was diluted with MeOH (1 mL) and purified on a 5 g SCX column (eluant: 2 M NH₃-MeOH) to afford (*R*)-6-(1-methylpyrazol-4-yl)-4-(3-piperidyloxy)pyrazolo[1,5-*a*]pyrazine (270 mg, 88% yield) as a pale-yellow oil. LCMS (ESI+): *m/z* calcd. for C₁₅H₁₈N₆O [M+H]⁺, 299.1; found, 299.1.

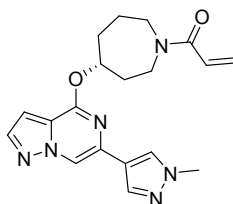
3. *Synthesis of (R)-1-(3-((6-(1-methyl-1H-pyrazol-4-yl)pyrazolo[1,5-a]pyrazin-4-yl)oxy)piperidin-1-yl)prop-2-en-1-one*



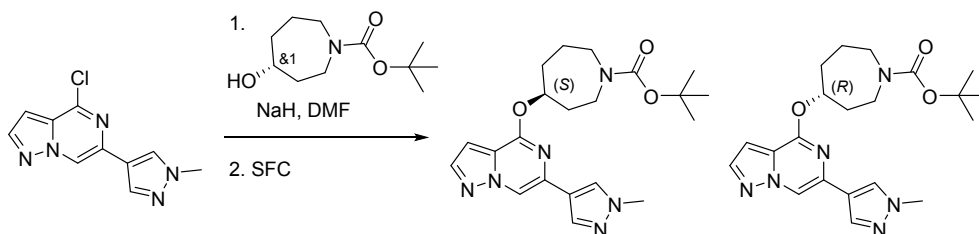
To a solution of (*R*)-6-(1-methylpyrazol-4-yl)-4-(3-piperidyloxy)pyrazolo[1,5-*a*]pyrazine (30 mg, 0.10 mmol) in THF (1 mL) was added acryloyl chloride (9 mg, 0.10 mmol, 8 μL) at rt. To the resulting white suspension was added TEA (12 mg, 0.12 mmol, 17 μL) at rt. After stirring overnight, the volatiles were removed *in vacuo* and the resulting crude residue was purified by HPLC (Waters XSelect CSH C18, 5 μm, 19 mm × 100 mm column with mobile phase H₂O (A) and MeCN (B) and a gradient of 5 – 50% B (0.2% NH₄OH final v/v % modifier) with flow rate at 30 mL/min) to afford (*R*)-1-(3-((6-(1-methyl-1*H*-pyrazol-4-yl)pyrazolo[1,5-*a*]pyrazin-4-yl)oxy)piperidin-1-yl)prop-2-en-1-one (23 mg, 62% yield) as a clear oil. HRMS (ESI+): *m/z* calcd. for C₁₈H₂₀N₆O₂ [M+H]⁺, 353.1721; found, 353.1730. ¹H NMR (500 MHz, dimethyl sulfoxide-*d*₆): δ (ppm) 8.77 (s, 1H), 8.20 (s, 1H), 8.01 (d, *J* = 2.4 Hz, 2H), 6.95-6.54 (m, 2H), 6.18-5.94 (m, 1H), 5.74-5.43 (m, 1H), 5.41-5.23 (m, 1H), 4.25-4.19 (m, 1H), 3.98-3.85 (m, 4H), 3.85-3.60 (m, 2H), 2.18-1.78 (m, 3H), 1.62-1.51 (m, 1H).

Compound 10:

(*R*)-1-(4-((6-(1-Methyl-1*H*-pyrazol-4-yl)pyrazolo[1,5-*a*]pyrazin-4-yl)oxy)azepan-1-yl)prop-2-en-1-one



1. Synthesis of *tert*-butyl (*S*)-4-((6-(1-methyl-1*H*-pyrazol-4-yl)pyrazolo[1,5-*a*]pyrazin-4-yl)oxy)azepane-1-carboxylate and *tert*-butyl (*R*)-4-((6-(1-methyl-1*H*-pyrazol-4-yl)pyrazolo[1,5-*a*]pyrazin-4-yl)oxy)azepane-1-carboxylate



To a solution of *tert*-butyl 4-hydroxyazepane-1-carboxylate (710 mg, 3.30 mmol) in DMF (10 mL) was added NaH (396 mg, 9.90 mmol, 60% purity) in four batches under vigorous stirring at 0 °C. After 45 min, 4-chloro-6-(1-methyl-1*H*-pyrazol-4-yl)pyrazolo[1,5-*a*]pyrazine (700 mg, 3.00 mmol) was added to the pale-yellow suspension and stirring was continued at rt overnight. The mixture was diluted with EtOAc (30 mL) and water (15 mL) was added carefully. The aqueous phase was separated and extracted with EtOAc (10 mL). The combined organic phase was washed with brine (20 mL), dried over Na₂SO₄, filtered, and concentrated *in vacuo*. The resulting crude residue was purified by column chromatography (10 g SiO₂, 50% EtOAc in heptane) to afford *tert*-butyl 4-(6-(1-methylpyrazol-4-yl)pyrazolo[1,5-*a*]pyrazin-4-yl)oxyazepane-1-carboxylate (1.3 g, 95% yield) as a yellow oil. The racemic material was resolved by chiral SFC purification (CHIRALPAK AD-H 30 x 250mm, 5 μm, 25% IPA with 0.1% DEA in CO₂, flow rate: 100 mL/min, ABPR 120 bar, MBPR 60 psi, column temp 40 °C) to afford two compounds of arbitrarily assigned stereochemistry:

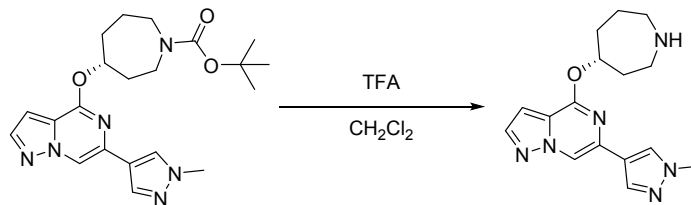
Peak 1: *tert*-butyl (*S*)-4-((6-(1-methyl-1*H*-pyrazol-4-yl)pyrazolo[1,5-*a*]pyrazin-4-yl)oxy)azepane-1-carboxylate (first eluting peak) ($R_f = 2.31$ min., 389 mg, 63% yield, 99.8% *ee*).

Peak 2: *tert*-butyl (*R*)-4-((6-(1-methyl-1*H*-pyrazol-4-yl)pyrazolo[1,5-*a*]pyrazin-4-yl)oxy)azepane-1-carboxylate (second eluting peak) ($R_f = 2.43$ min., 407 mg, 66% yield, 91.1% *ee*) as off-white solids.

LCMS (ESI+): m/z calcd. for C₂₁H₂₈N₆O₃ [M+H]⁺, 413.2; found, 413.2.

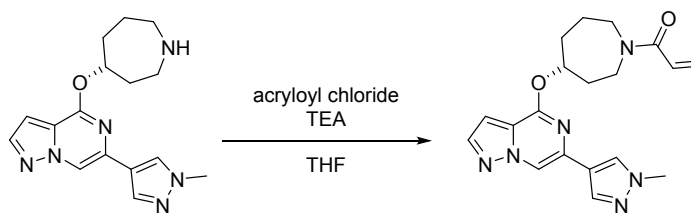
Note: The absolute stereochemistry of the product in these two peaks was later confirmed using a similar procedure but commercially available chiral *tert*-butyl (4*S*)-hydroxyazepane-1-carboxylate to afford a compound whose analytical data aligned with the first eluting peak *tert*-butyl (*S*)-4-((6-(1-methyl-1*H*-pyrazol-4-yl)pyrazolo[1,5-*a*]pyrazin-4-yl)oxy)azepane-1-carboxylate.

2. Synthesis of (*R*)-4-(azepan-4-yl)oxy)-6-(1-methylpyrazol-4-yl)pyrazolo[1,5-*a*]pyrazine



To a vigorously stirred solution of *tert*-butyl (*R*)-4-((6-(1-methyl-1*H*-pyrazol-4-yl)pyrazolo[1,5-*a*]pyrazin-4-yl)oxy)azepane-1-carboxylate (407 mg, 0.99 mmol) in CH₂Cl₂ (3 mL) was added TFA (2.25 g, 19.7 mmol, 1.51 mL) at rt. After stirring overnight, the resulting mixture was diluted with MeOH (1 mL) and purified on a 5 g SCX column (eluant: 2 M NH₃-MeOH) to afford (*R*)-4-(azepan-4-yloxy)-6-(1-methylpyrazol-4-yl)pyrazolo[1,5-*a*]pyrazine (250 mg, 77% yield) as a white solid. LCMS (ESI⁺): *m/z* calcd. for C₁₆H₂₀N₆O [M+H]⁺, 313.2; found, 313.2.

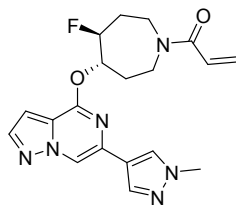
3. *Synthesis of (R)-1-(4-((6-(1-methyl-1H-pyrazol-4-yl)pyrazolo[1,5-a]pyrazin-4-yl)oxy)azepan-1-yl)prop-2-en-1-one*



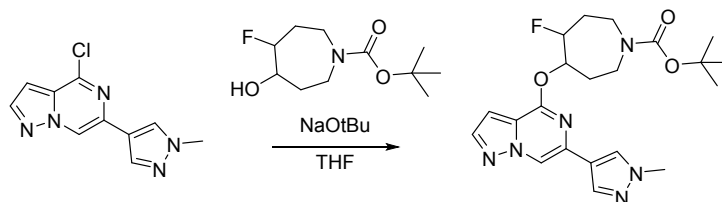
To a solution of (*R*)-4-(azepan-4-yloxy)-6-(1-methylpyrazol-4-yl)pyrazolo[1,5-*a*]pyrazine (30 mg, 0.10 mmol) in THF (1 mL) was added acryloyl chloride (17 mg, 0.19 mmol, 16 μ L) followed by TEA (19 mg, 0.19 mmol, 27 μ L) at rt. After stirring overnight, the volatiles were removed *in vacuo* and the resulting crude residue was purified by HPLC (Waters XSelect CSH C18, 5 μ m, 19 mm \times 100 mm column with mobile phase H₂O (A) and MeCN (B) and a gradient of 5 – 50% B (0.2% NH₄OH final v/v % modifier) with flow rate at 30 mL/min) to afford (*R*)-1-(4-((6-(1-methyl-1*H*-pyrazol-4-yl)pyrazolo[1,5-*a*]pyrazin-4-yl)oxy)azepan-1-yl)prop-2-en-1-one (9 mg, 23% yield) as a clear oil. HRMS (ESI⁺): *m/z* calcd. for C₁₉H₂₂N₆O₂ [M+H]⁺, 366.1800; found, 366.1800. ¹H NMR (500 MHz, dimethyl sulfoxide-*d*₆): δ (ppm) 8.73 (s, 1H), 8.18 (d, *J* = 18.9 Hz, 1H), 8.03-7.98 (m, 1H), 6.87-6.76 (m, 2H), 6.18 (ddd, *J* = 16.5, 3.7, 2.4 Hz, 1H), 5.75-5.65 (m, 1H), 5.58-5.45 (m, 1H), 3.88 (d, *J* = 1.8 Hz, 3H), 3.79-3.56 (m, 4H), 2.92-2.71 (m, 1H), 2.26-2.17 (m, 1H), 2.10-1.99 (m, 2H), 1.98-1.84 (m, 2H), 1.82-1.63 (m, 1H).

Compound 11:

1-((4*S*,5*S*)-4-Fluoro-5-((6-(1-methyl-1*H*-pyrazol-4-yl)pyrazolo[1,5-*a*]pyrazin-4-yl)oxy)azepan-1-yl)prop-2-en-1-one

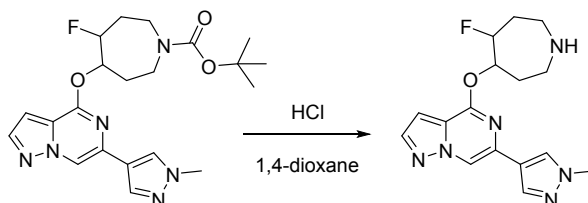


1. *Synthesis of tert-butyl-3-fluoro-4-((6-(1-methylpyrazol-4-yl)pyrazolo[1,5-a]pyrazin-4-yl)oxy)-azepane-1-carboxylate*



To a solution of *tert*-butyl-4-fluoro-5-hydroxy-azepane-1-carboxylate (500 mg, 2.14 mmol) in dry THF (20 mL) was added NaH (396 mg, 9.90 mmol, 60% purity) in four batches under vigorous stirring at 0 °C. After 15 min, 4-chloro-6-(1-methyl-1*H*-pyrazol-4-yl)pyrazolo[1,5-*a*]pyrazine (455 mg, 1.95 mmol) was added and stirring was continued at rt for 3.5 hrs. The mixture was diluted with EtOAc (30 mL) and water (15 mL) was added carefully. The aqueous phase was separated and extracted with EtOAc (10 mL). The combined organic phase was washed with brine (20 mL), dried over Na₂SO₄, filtered, and concentrated *in vacuo*. Column chromatography (24 g SiO₂, 0-35 % 3:1 EtOAc:EtOH in heptane) of the resulting residue afforded the desired compound (660 mg, 79%) as a colorless oil. LCMS (ESI⁺): *m/z* calcd. for C₂₁H₂₇N₆O₃F [M+H]⁺, 431.2; found 431.2. ¹H NMR (400 MHz, chloroform-*d*): δ (ppm) 8.14 (s, 1H), 7.87-7.65 (m, 3H), 6.71-6.65 (m, 1H), 5.68 (br d, *J* = 6.5 Hz, 1H), 5.10-4.80 (m, 1H), 3.88 (s, 3H), 3.80-3.33 (m, 4H), 2.40-1.95 (m, 4H), 1.43-1.38 (m, 9H).

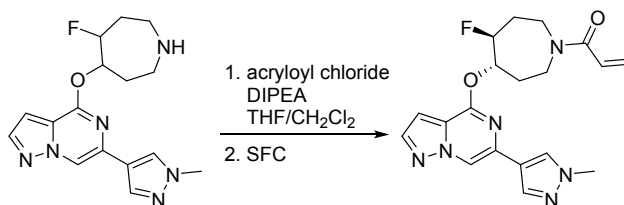
2. *Synthesis of 4-[5-fluoroazepan-4-yl]oxy-6-(1-methylpyrazol-4-yl)pyrazolo[1,5-a]pyrazine*



A 4 M solution of HCL in 1,4-dioxane (5.8 mL) was added to solid *tert*-butyl-4-fluoro-5-[6-(1-methylpyrazol-4-yl)pyrazolo[1,5-*a*]pyrazin-4-yl]oxy-azepane-1-carboxylate (660 mg, 1.53 mmol) in a reaction vial at rt. The resulting reaction mixture was stirred for 1 hr after which monitoring by LCMS indicated full consumption of starting material. The reaction mixture was carefully concentrated *in vacuo* to afford the title compound 4-(5-fluoroazepan-4-yl)oxy-6-(1-methylpyrazol-4-yl)pyrazolo[1,5-*a*]pyrazine

(500 mg, 99% yield) as an off-white solid which was used without further purification in the next step. LCMS (ESI+): m/z calcd. For $C_{16}H_{19}N_6OF$ $[M+H]^+$, 331.2; found 331.2.

3. *Synthesis of 1-((4S,5S)-4-fluoro-5-((6-(1-methyl-1H-pyrazol-4-yl)pyrazolo[1,5-a]pyrazin-4-yl)oxy)azepan-1-yl)prop-2-en-1-one*

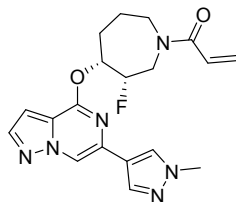


To a solution of 4-(5-fluoroazepan-4-yl)oxy-6-(1-methylpyrazol-4-yl)pyrazolo[1,5-*a*]pyrazine (500 mg, 1.51 mmol) in anhydrous THF (2 mL) and CH₂Cl₂ (5 mL) was added DIPEA (3.9 g, 30.37 mmol, 5.3 mL) followed by acryloyl chloride (301 mg, 3.33 mmol, 270 μ L) at 0 °C. The resulting reaction mixture was brought to rt. Complete consumption of starting material was observed by LCMS after 5 min. The reaction mixture was quenched by slow addition of sat. aq. NaHCO₃ (5 mL) and the biphasic mixture was loaded onto silica and purified by column chromatography (24 g SiO₂, 15-75 % 3:1 EtOAc:EtOH in heptane.) to afford 1-(4-fluoro-5-(6-(1-methylpyrazol-4-yl)pyrazolo[1,5-*a*]pyrazin-4-yl)oxy)azepan-1-yl)prop-2-en-1-one (360 mg, 62% yield). LCMS (ESI+): m/z calcd. for $C_{19}H_{21}N_6O_2F$ $[M+H]^+$, 384.2; found 385.2. ¹H NMR (400 MHz chloroform-*d*): δ (ppm) 8.25 (d, J = 1.0 Hz, 1H), 7.95-7.73 (m, 3H), 6.82-6.55 (m, 2H), 6.48-6.35 (m, 1H), 5.91-5.79 (m, 1H), 5.77-5.68 (m, 1H), 5.23-5.05 (m, 1H), 4.08-3.96 (m, 4H), 3.86-3.71 (m, 2H), 3.70-3.50 (m, 1H), 2.59-2.41 (m, 1H), 2.38-2.20 (m, 3H).

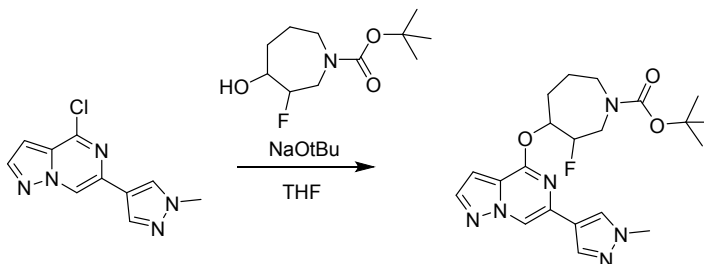
Two consecutive chiral SFC purifications A) (CHIRALPAK AD-H 30 x 250 mm, 5 μ m, 25% IPA with 0.1% DEA in CO₂, flow rate: 100 mL/min, ABPR 120 bar, MBPR 60 psi, column temp 40 °C) and B) (CHIRALPAK OX-H 30 x 250 mm, 5 μ m, 40% IPA with 0.1% DEA in CO₂, flow rate: 100 mL/min, ABPR 120 bar, MBPR 60 psi, column temp 40 °C) afforded the title compound 1-((4S,5S)-4-fluoro-5-((6-(1-methyl-1H-pyrazol-4-yl)pyrazolo[1,5-*a*]pyrazin-4-yl)oxy)azepan-1-yl)prop-2-en-1-one (R_f = 5.06 min., 7.5 mg, 2% yield, 98.6% *ee*). The absolute stereochemistry of the product was arbitrarily assigned. HRMS (ESI+): m/z calcd. for $C_{19}H_{21}FN_6O_2$ $[M+H]^+$, 385.1783; found, 385.1792. ¹H NMR (400 MHz, chloroform-*d*): δ (ppm) 8.16-8.15 (m, 1H), 7.84-7.64 (m, 3H), 6.72 (ddd, J = 10.2, 2.3, 0.8 Hz, 1H), 6.61-6.52 (m, 1H), 6.36 (ddd, J = 16.6, 6.3, 2.0 Hz, 1H), 5.70 (ddd, J = 10.5, 7.3, 2.0 Hz, 1H), 5.61-5.48 (m, 1H), 5.15-5.01 (m, 1H), 4.23-4.07 (m, 1H), 3.92 (d, J = 9.3 Hz, 3H), 3.81-3.75 (m, 1H), 3.55-3.51 (m, 1H), 3.36-3.24 (m, 1H), 2.52-2.41 (m, 1H), 2.33-2.01 (m, 3H).

Compound 12:

1-((3*S*,4*R*)-3-Fluoro-4-((6-(1-methyl-1*H*-pyrazol-4-yl)pyrazolo[1,5-*a*]pyrazin-4-yl)oxy)azepan-1-yl)prop-2-en-1-one

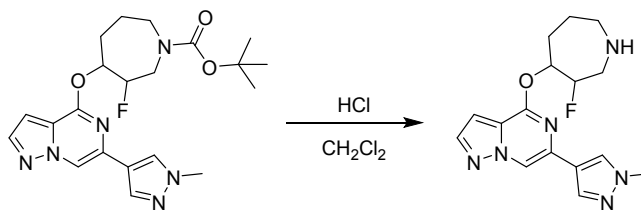


1. Synthesis of *tert*-butyl-3-fluoro-4-((6-(1-methylpyrazol-4-yl)pyrazolo[1,5-*a*]pyrazin-4-yl)oxy)-azepane-1-carboxylate



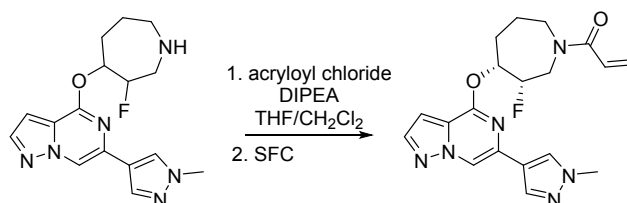
To a solution of *tert*-butyl-3-fluoro-4-hydroxy-azepane-1-carboxylate (514 mg, 2.20 mmol) in THF (8 mL) was added KO*t*Bu (289 mg, 3.00 mmol) at 0 °C. After 15 min, 4-chloro-6-(1-methyl-1*H*-pyrazol-4-yl)pyrazolo[1,5-*a*]pyrazine (468 mg, 2.00 mmol) was added carefully in portions to the cold heterogeneous mixture. The resulting reaction mixture was brought to rt and monitored by LCMS. After 3.5 hr, the reaction mixture was carefully quenched by slow addition of water (10 mL) and the biphasic mixture was extracted with EtOAc (3 x 20 mL). The combined organic phase was dried over Na₂SO₄, filtered, and concentrated *in vacuo*. The resulting residue was purified by column chromatography (24 g SiO₂, 0-35 % 3:1 EtOAc: EtOH in heptane.) to afford *tert*-butyl-3-fluoro-4-((6-(1-methylpyrazol-4-yl)pyrazolo[1,5-*a*]pyrazin-4-yl)oxy)-azepane-1-carboxylate (350 mg, 41% yield) as a colorless oil. LCMS (ESI⁺): *m/z* calcd. for C₂₁H₂₇N₆O₃F [M+H]⁺, 431.2; found, 431.2. ¹H NMR (400 MHz, methanol-*d*₄): δ (ppm) 8.49 (br s, 1H), 8.10-8.09 (m, 1H), 7.97 (d, *J* = 2.5 Hz, 1H), 7.95 (d, *J* = 2.5 Hz, 1H), 6.86 (dd, *J* = 2.3, 0.8 Hz, 1H), 5.69-5.61 (m, 1H), 4.99-4.83 (m, 1H), 3.97 (s, 3H), 3.93-3.48 (m, 4H), 2.22-2.14 (m, 1H), 1.97-1.88 (m, 3H), 1.53-1.49 (m, 9H).

2. Synthesis of 4-((3-fluoroazepan-4-yl)oxy)-6-(1-methyl-1*H*-pyrazol-4-yl)pyrazolo[1,5-*a*]pyrazine



To a solution of *tert*-butyl-3-fluoro-4-((6-(1-methylpyrazol-4-yl)pyrazolo[1,5-*a*]pyrazin-4-yl)oxy)azepane-1-carboxylate (240 mg, 0.56 mmol) in CH₂Cl₂ (2 mL) was added 4 M HCl in 1,4-dioxane (2.1 mL) at 0 °C. The resulting mixture was brought to rt and stirred for 1 hr, after which LCMS indicated complete conversion of starting material. The reaction mixture was carefully concentrated *in vacuo* to afford 4-((3-fluoroazepan-4-yl)oxy)-6-(1-methyl-1*H*-pyrazol-4-yl)pyrazolo[1,5-*a*]pyrazine (125 mg, 68% yield) which was used without further purification in the next step. LCMS (ESI+): *m/z* calcd. for C₁₆H₁₉N₆O [M+H]⁺, 331.2; found, 331.2.

3. *Synthesis of 1-((3*S*,4*R*)-3-fluoro-4-((6-(1-methyl-1*H*-pyrazol-4-yl)pyrazolo[1,5-*a*]pyrazin-4-yl)oxy)azepan-1-yl)prop-2-en-1-one*

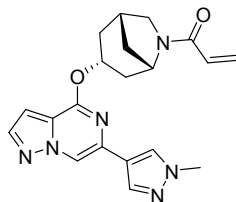


Step 1: DIPEA (515 mg, 3.98 mmol, 694 μL) and acryloyl chloride (88 mg, 0.97 mmol, 79 μL) were sequentially added dropwise to a solution of 4-((3-fluoroazepan-4-yl)oxy)-6-(1-methyl-1*H*-pyrazol-4-yl)pyrazolo[1,5-*a*]pyrazine (110 mg, 0.33 mmol) in CH₂Cl₂ (3 mL) under stirring at 0 °C. The resulting mixture was brought to rt and stirred for 10 min, after which LCMS indicated complete consumption of starting material. The reaction mixture was quenched by slow addition of sat. aq. NaHCO₃ (5 mL) and the biphasic mixture was loaded onto silica and purified by column chromatography (24 g SiO₂, 15-75 % 3:1 EtOAc: EtOH in heptane.) to afford 1-(3-fluoro-4-((6-(1-methyl-1*H*-pyrazol-4-yl)pyrazolo[1,5-*a*]pyrazin-4-yl)oxy)azepan-1-yl)prop-2-en-1-one (100 mg, 78% yield). LCMS (ESI+): *m/z* calcd. for C₁₉H₂₁N₆O₂F [M+H]⁺, 385.2; found, 385.2.

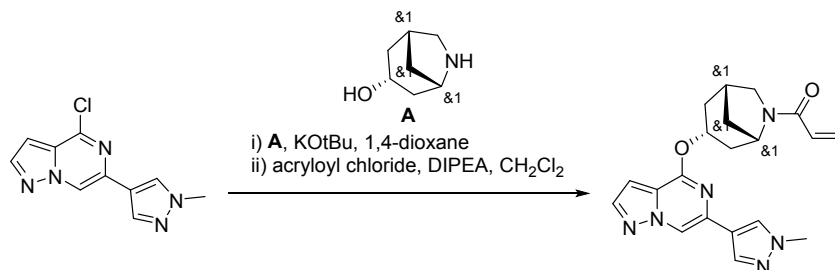
Step 2: The mixture of stereoisomers was resolved by chiral SFC purification (CHIRALPAK AD-H 30 x 250 mm, 5 μm, 25% IPA with 0.1% DEA in CO₂, flow rate: 100 mL/min, ABPR 120 bar, MBPR 60 psi, column temp 40 °C) to afford 1-((3*S*,4*R*)-3-fluoro-4-((6-(1-methyl-1*H*-pyrazol-4-yl)pyrazolo[1,5-*a*]pyrazin-4-yl)oxy)azepan-1-yl)prop-2-en-1-one as the second of four eluting peaks (*R_f* = 3.82 min., 55 mg, 28% yield, 98.6% *ee*). The absolute stereochemistry of the isolated compound was arbitrarily assigned. HRMS (ESI+): *m/z* calcd. for C₁₉H₂₁FN₆O₂ [M+H]⁺, 385.1783; found, 385.1789. ¹H NMR (400 MHz, chloroform-*d*): δ (ppm) 8.25-8.24 (m, 1H), 7.92-7.86 (m, 2H), 7.80-7.79 (m, 1H), 6.80-6.60 (m, 2H), 6.47-6.41 (m, 1H), 5.80-5.63 (m, 2H), 5.18-4.95 (m, 1H), 4.40-4.12 (m, 1H), 4.01-3.99 (m, 3H), 3.84-3.56 (m, 2H), 3.31-3.24 (m, 1H), 2.25-2.01 (m, 4H).

Compound 13:

1-((1*R*,3*R*,5*S*)-3-((6-(1-Methyl-1*H*-pyrazol-4-yl)pyrazolo[1,5-*a*]pyrazin-4-yl)oxy)-6-azabicyclo[3.2.1]octan-6-yl)prop-2-en-1-one

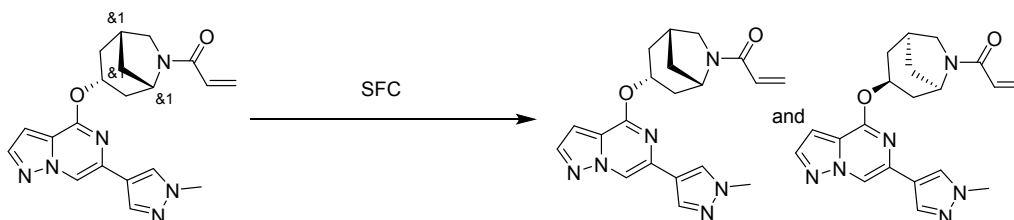


1. *Synthesis of rac-1-((1*R*,3*R*,5*S*)-3-((6-(1-methyl-1*H*-pyrazol-4-yl)pyrazolo[1,5-*a*]pyrazin-4-yl)oxy)-6-azabicyclo[3.2.1]octan-6-yl)prop-2-en-1-one*



To a solution of 4-chloro-6-(1-methyl-1*H*-pyrazol-4-yl)pyrazolo[1,5-*a*]pyrazine (200 mg, 0.86 mmol) and *rac*-(1*R*,3*R*,5*S*)-6-azabicyclo[3.2.1]octan-3-ol (120 mg, 0.94 mmol) in 1,4-dioxane (1.5 mL) was added KOtBu (1 M, 1 mL) at rt. After 5 min, the mixture was concentrated *in vacuo* and the resulting residue was dissolved in CH₂Cl₂ (1.5 mL) and DIPEA (332 mg, 2.57 mmol, 450 μL) was added. After 5 min, the mixture was cooled at -20 °C and acryloyl chloride (77 mg, 0.86 mmol, 69 μL) was added. After an additional 10 min, sat. aq. NaHCO₃ (10 mL) was added and the vigorously stirred biphasic mixture was brought to rt. The phases were separated, the aqueous layer was extracted with CH₂Cl₂ (2 x 10 mL) and the combined organic phase was concentrated to dryness. The crude reaction mixture was purified *via* column chromatography (10 g SiO₂, 3:1 EtOAc:EtOH in heptane) to afford *rac*-1-((1*R*,3*R*,5*S*)-3-((6-(1-methyl-1*H*-pyrazol-4-yl)pyrazolo[1,5-*a*]pyrazin-4-yl)oxy)-6-azabicyclo[3.2.1]octan-6-yl)prop-2-en-1-one (50 mg, 14% yield). LCMS (ESI+): *m/z* calcd. for C₂₀H₂₂N₆O₂ [M+H]⁺, 379.3; found, 379.3.

2. *Isolation of 1-((1*R*,3*R*,5*S*)-3-((6-(1-methyl-1*H*-pyrazol-4-yl)pyrazolo[1,5-*a*]pyrazin-4-yl)oxy)-6-azabicyclo[3.2.1]octan-6-yl)prop-2-en-1-one and 1-((1*S*,3*S*,5*R*)-3-((6-(1-methyl-1*H*-pyrazol-4-yl)pyrazolo[1,5-*a*]pyrazin-4-yl)oxy)-6-azabicyclo[3.2.1]octan-6-yl)prop-2-en-1-one*



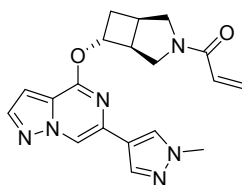
rac-1-((1*R*,3*R*,5*S*)-3-((6-(1-Methyl-1*H*-pyrazol-4-yl)pyrazolo[1,5-*a*]pyrazin-4-yl)oxy)-6-azabicyclo[3.2.1]octan-6-yl)prop-2-en-1-one (50 mg) was resolved by chiral SFC purification (CHIRALPAK IB 30 x 250mm, 5 μm, 20% EtOH in CO₂, flow rate: 100 mL/min, ABPR 120 bar, MBPR 40 psi, column temp 40 °C) to afford two compounds of arbitrarily assigned stereochemistry:

Peak 1: 1-((1*R*,3*R*,5*S*)-3-((6-(1-methyl-1*H*-pyrazol-4-yl)pyrazolo[1,5-*a*]pyrazin-4-yl)oxy)-6-azabicyclo[3.2.1]octan-6-yl)prop-2-en-1-one (compound **13**, *R_f* = 5.03 min., 21 mg, 41% yield, 100% *ee*)
 HRMS (ESI+): *m/z* calcd. for C₂₀H₂₂N₆O₂ [M+H]⁺, 379.1877; found, 379.1887. ¹H NMR (500 MHz, dimethyl sulfoxide-*d*₆): δ (ppm) 8.78-8.70 (m, 1H), 8.12-7.86 (m, 3H), 6.82-6.61 (m, 2H), 6.32 (ddd, *J* = 16.5, 8.6, 2.4 Hz, 1H), 5.76 (ddd, *J* = 10.2, 6.0, 2.8 Hz, 1H), 5.44-5.31 (m, 1H), 4.54-4.34 (m, 1H), 3.88 (d, *J* = 11.6 Hz, 3H), 3.70-3.62 (m, 1H), 3.60-3.38 (m, 1H), 3.07-2.60 (m, 2H), 2.38-2.21 (m, 1H), 1.90-1.74 (m, 3H), 1.66-1.39 (m, 1H).

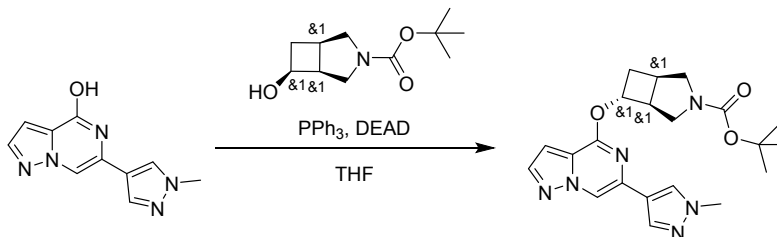
Peak 2: 1-((1*S*,3*S*,5*R*)-3-((6-(1-methyl-1*H*-pyrazol-4-yl)pyrazolo[1,5-*a*]pyrazin-4-yl)oxy)-6-azabicyclo[3.2.1]octan-6-yl)prop-2-en-1-one (*R_f* = 5.44 min., 22 mg, 41% yield, 91.2% *ee*).

Compound 14:

1-((1*R*,5*S*,6*R*)-6-((6-(1-Methyl-1*H*-pyrazol-4-yl)pyrazolo[1,5-*a*]pyrazin-4-yl)oxy)-3-azabicyclo[3.2.0]heptan-3-yl)prop-2-en-1-one



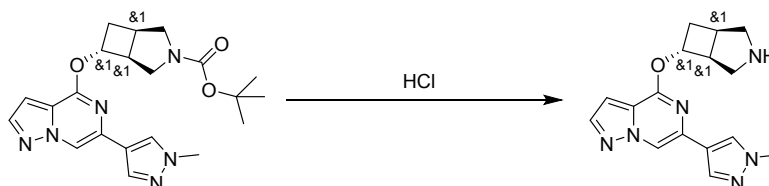
1. Synthesis of *rac*-*tert*-butyl (1*R*,5*S*,6*R*)-6-((6-(1-methyl-1*H*-pyrazol-4-yl)pyrazolo[1,5-*a*]pyrazin-4-yl)oxy)-3-azabicyclo[3.2.0]heptane-3-carboxylate



To a solution of PPh₃ (366 mg, 1.39 mmol) in THF (2 mL) was added a solution of DEAD (243 mg, 1.39 mmol, 220 μL) in THF (2 mL) at 0 °C. After 10 min, the resulting mixture was added *via* cannula to a slurry of 6-(1-methyl-1*H*-pyrazol-4-yl)pyrazolo[1,5-*a*]pyrazin-4-ol (250 mg, 1.16 mmol) and *rac*-*tert*-butyl (1*S*,5*R*,6*R*)-6-hydroxy-3-azabicyclo[3.2.0]heptane-3-carboxylate (300 mg, 1.41 mmol) in THF (3 mL) at 0 °C. After 5 min at 0 °C, the reaction mixture was heated at 35 °C for 20 hr, diluted with sat. aq. NaHCO₃ (10 mL) and extracted with MTBE (3 x 10 mL). The combined organic phase was concentrated

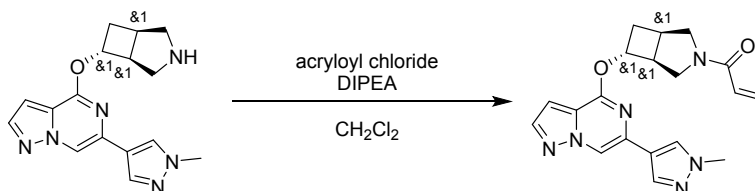
in vacuo, and the resulting residue was purified *via* column chromatography (24 g SiO₂, 0-90 % EtOAc in heptane) to afford *rac-tert-butyl (1R,5S,6R)-6-((6-(1-methyl-1H-pyrazol-4-yl)pyrazolo[1,5-a]pyrazin-4-yl)oxy)-3-azabicyclo[3.2.0]heptane-3-carboxylate* (455 mg, 62% yield). LCMS (ESI+): *m/z* calcd. for C₂₁H₂₆N₆O₃ [M+H]⁺, 411.2; found, 411.2.

2. *Synthesis of rac-4-(((1R,5S,6R)-3-azabicyclo[3.2.0]heptan-6-yl)oxy)-6-(1-methyl-1H-pyrazol-4-yl)pyrazolo[1,5-a]pyrazine*



A solution of *rac-tert-butyl (1R,5S,6R)-6-((6-(1-methyl-1H-pyrazol-4-yl)pyrazolo[1,5-a]pyrazin-4-yl)oxy)-3-azabicyclo[3.2.0]heptane-3-carboxylate* (455 mg, 0.72 mmol) in 1.25 M HCl in MeOH (5.8 mL) was heated at 40 °C for 5 hr. The reaction mixture was concentrated *in vacuo* and the crude material was taken up in EtOAc (5 mL) and concentrated to dryness. The material was taken up in CH₂Cl₂ (10 mL) resulting in a suspension which was passed through a filter. The solids were washed with CH₂Cl₂ (10 mL) and dissolved in MeOH (50 mL). The volatiles were removed and the resulting residue was taken up in EtOAc (5 mL) and concentrated *in vacuo* to afford *rac-4-(((1R,5S,6R)-3-azabicyclo[3.2.0]heptan-6-yl)oxy)-6-(1-methyl-1H-pyrazol-4-yl)pyrazolo[1,5-a]pyrazine* (67 mg, 27% yield, hydrochloride) as a white solid. LCMS (ESI+): *m/z* calcd. for C₁₆H₁₈N₆O [M+H]⁺, 311.2; found, 311.2. ¹H NMR (500 MHz, dimethyl sulfoxide-*d*₆): δ (ppm) 9.91 (br s, 1H), 9.62 (br d, *J* = 3.1 Hz, 1H), 8.77 (s, 1H), 8.31 (s, 1H), 8.07-7.98 (m, 2H), 6.87 (dd, *J* = 2.4, 1.2 Hz, 1H), 5.46 (ddd, *J* = 7.3, 6.1, 4.3 Hz, 1H), 3.90 (s, 3H), 3.79-3.67 (m, 1H), 3.45-3.35 (m, 1H), 3.29-3.09 (m, 4H).

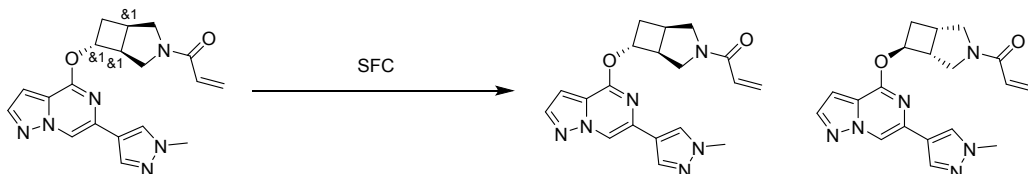
3. *Synthesis of rac-1-(((1R,5S,6R)-6-((6-(1-methyl-1H-pyrazol-4-yl)pyrazolo[1,5-a]pyrazin-4-yl)oxy)-3-azabicyclo[3.2.0]heptan-3-yl)prop-2-en-1-one*



To a solution of *rac-4-(((1R,5S,6R)-3-azabicyclo[3.2.0]heptan-6-yl)oxy)-6-(1-methyl-1H-pyrazol-4-yl)pyrazolo[1,5-a]pyrazine* (67 mg, 0.19 mmol, hydrochloride) and DIPEA (125 mg, 0.97 mmol, 168 μL) in CH₂Cl₂ (5 mL) was added acryloyl chloride (18 mg, 0.19 mmol, 16 μL) at -20 °C. After 10 min, the

reaction mixture was loaded onto silica and purified by column chromatography (12 g SiO₂, 0-90 % 3:1 EtOAc:EtOH in heptane) to afford *rac*-1-((1*R*,5*S*,6*R*)-6-((6-(1-methyl-1*H*-pyrazol-4-yl)pyrazolo[1,5-*a*]pyrazin-4-yl)oxy)-3-azabicyclo[3.2.0]heptan-3-yl)prop-2-en-1-one (64 mg, 91% yield) as a clear oil. LCMS (ESI⁺): *m/z* calcd. for C₁₉H₂₀N₆O₂ [M+H]⁺, 365.2; found, 365.2.

4. Isolation of 1-((1*R*,5*S*,6*R*)-6-((6-(1-methyl-1*H*-pyrazol-4-yl)pyrazolo[1,5-*a*]pyrazin-4-yl)oxy)-3-azabicyclo[3.2.0]heptan-3-yl)prop-2-en-1-one and 1-((1*S*,5*R*,6*S*)-6-((6-(1-methyl-1*H*-pyrazol-4-yl)pyrazolo[1,5-*a*]pyrazin-4-yl)oxy)-3-azabicyclo[3.2.0]heptan-3-yl)prop-2-en-1-one



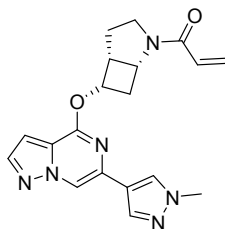
rac-1-((1*R*,5*S*,6*R*)-6-((6-(1-Methyl-1*H*-pyrazol-4-yl)pyrazolo[1,5-*a*]pyrazin-4-yl)oxy)-3-azabicyclo[3.2.0]heptan-3-yl)prop-2-en-1-one (64 mg, 0.18 mmol) was resolved by chiral SFC purification (CHIRALPAK AD-H 30 x 250mm, 5 μ m, 40% MeOH w/ No Modifier in CO₂ (flow rate: 100 mL/min, ABPR 120 bar, MBPR 40 psi, column temp 40 °C) to afford two compounds of arbitrarily assigned stereochemistry:

Peak 1: 1-((1*R*,5*S*,6*R*)-6-((6-(1-methyl-1*H*-pyrazol-4-yl)pyrazolo[1,5-*a*]pyrazin-4-yl)oxy)-3-azabicyclo[3.2.0]heptan-3-yl)prop-2-en-1-one (compound **14**, *R_f* = 2.83 min., 19 mg, 29% yield, 100% *ee*) HRMS (ESI⁺): *m/z* calcd. for C₁₉H₂₀N₆O₂ [M+H]⁺, 365.1721; found, 365.1729. ¹H NMR (500 MHz, dimethyl sulfoxide-*d*₆): δ (ppm) 8.77 (d, *J* = 7.3 Hz, 1H), 8.32-8.13 (s, 1H), 8.03-7.98 (m, 2H), 6.90-6.84 (m, 1H), 6.73 (dd, *J* = 16.5, 10.4 Hz, 1H), 6.28-6.15 (m, 1H), 5.78-5.70 (m, 1H), 5.27-5.14 (m, 1H), 4.50-4.15 (m, 1H), 3.90 (d, *J* = 7.9 Hz, 3H), 3.83-3.61 (m, 1H), 3.59-3.43 (m, 1H), 3.26-3.15 (m, 1H), 3.11-2.97 (m, 2H), 2.42-2.30 (m, 2H), and

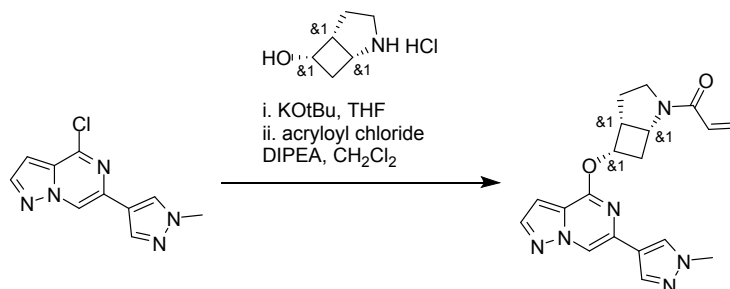
Peak 2: 1-((1*R*,5*S*,6*R*)-6-((6-(1-methyl-1*H*-pyrazol-4-yl)pyrazolo[1,5-*a*]pyrazin-4-yl)oxy)-3-azabicyclo[3.2.0]heptan-3-yl)prop-2-en-1-one (*R_f* = 3.37 min., 18 mg, 27% yield, 99.5% *ee*).

Compound 15:

1-((1*R*,5*R*,6*S*)-6-((6-(1-Methyl-1*H*-pyrazol-4-yl)pyrazolo[1,5-*a*]pyrazin-4-yl)oxy)-2-azabicyclo[3.2.0]heptan-2-yl)prop-2-en-1-one

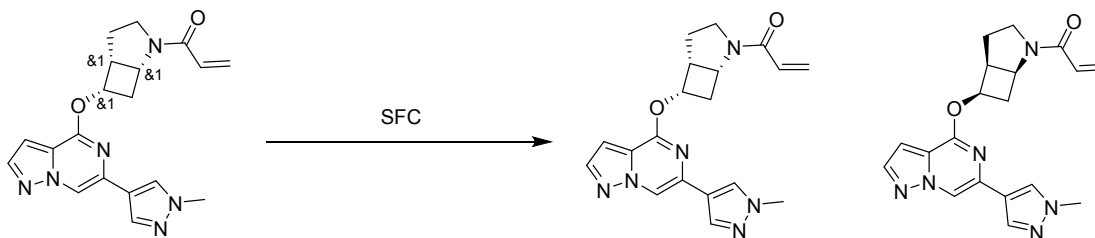


1. Synthesis of *rac*-1-((1*R*,5*R*,6*S*)-6-((6-(1-methyl-1*H*-pyrazol-4-yl)pyrazolo[1,5-*a*]pyrazin-4-yl)oxy)-3-azabicyclo[3.2.0]heptan-3-yl)prop-2-en-1-one



To a mixture of 4-chloro-6-(1-methyl-1*H*-pyrazol-4-yl)pyrazolo[1,5-*a*]pyrazine (178 mg, 0.76 mmol) and *rac*-(1*R*,5*R*,6*S*)-2-azabicyclo[3.2.0]heptan-6-ol hydrochloride (129 mg, 1.14 mmol) in THF (3 mL) was added KO*t*Bu (1.0 M in THF, 1.6 mL) at rt. The reaction mixture was concentrated after 15 min and the resulting residue was dissolved in CH₂Cl₂ (3 mL) and DIPEA (491 mg, 3.80 mmol, 662 μL) was added. The mixture was cooled to -78 °C, acryloyl chloride (83 mg, 0.91 mmol, 74 μL) was added and stirring was continued for 15 min. The reaction mixture was loaded onto a silica gel and purified *via* column chromatography (24 g SiO₂, 0-100% 3:1 EtOAc:EtOH in heptane) to afford *rac*-1-((1*R*,5*S*,6*S*)-6-((6-(1-methyl-1*H*-pyrazol-4-yl)pyrazolo[1,5-*a*]pyrazin-4-yl)oxy)-3-azabicyclo[3.2.0]heptan-3-yl)prop-2-en-1-one (239 mg, 86% yield). LCMS (ESI+): *m/z* calcd. for C₁₉H₂₀N₆O₂ [M+H]⁺, 365.2; found, 365.2.

2. Isolation of 1-((1*R*,5*R*,6*S*)-6-((6-(1-methyl-1*H*-pyrazol-4-yl)pyrazolo[1,5-*a*]pyrazin-4-yl)oxy)-3-azabicyclo[3.2.0]heptan-3-yl)prop-2-en-1-one and 1-((1*S*,5*S*,6*R*)-6-((6-(1-methyl-1*H*-pyrazol-4-yl)pyrazolo[1,5-*a*]pyrazin-4-yl)oxy)-3-azabicyclo[3.2.0]heptan-3-yl)prop-2-en-1-one



rac-1-((1*R*,5*S*,6*S*)-6-((6-(1-Methyl-1*H*-pyrazol-4-yl)pyrazolo[1,5-*a*]pyrazin-4-yl)oxy)-3-azabicyclo[3.2.0]heptan-3-yl)prop-2-en-1-one (239 mg, 0.66 mmol) was resolved by chiral SFC (CHIRALPAK AD-H 30 x 250mm, 5 μm, 40% MeOH w/ No Modifier in CO₂ (flow rate: 100 mL/min, ABPR 120 bar, MBPR 40 psi, column temp 40°C) to afford two compounds of arbitrarily assigned stereochemistry:

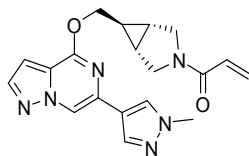
Peak 1: 1-((1*R*,5*R*,6*S*)-6-((6-(1-methyl-1*H*-pyrazol-4-yl)pyrazolo[1,5-*a*]pyrazin-4-yl)oxy)-3-azabicyclo[3.2.0]heptan-3-yl)prop-2-en-1-one (compound **15**, *R*_f = 4.04 min., 45 mg, 16% yield, 99.8%

ee) HRMS (ESI+): m/z calcd. for $C_{19}H_{20}N_6O_2$ $[M+H]^+$, 365.1721; found, 365.1724. 1H NMR (500 MHz, dimethyl sulfoxide- d_6): δ (ppm) 8.77 (s, 1H), 8.20 (d, $J = 3.7$ Hz, 1H), 8.02 (d, $J = 12.2$ Hz, 2H), 6.93-6.83 (m, 1H), 6.69-6.44 (m, 1H), 6.21-6.09 (m, 1H), 5.74-5.62 (m, 1H), 5.47-5.32 (m, 1H), 4.38 (br d, $J = 4.9$ Hz, 1H), 3.88 (s, 3H), 3.86-3.75 (m, 1H), 3.74-3.57 (m, 2H), 3.23-3.02 (m, 1H), 2.15-1.99 (m, 2H), 1.99-1.80 (m, 1H), and

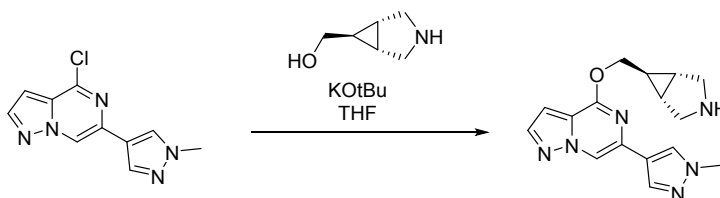
Peak 2: 1-((1*S*,5*S*,6*R*)-6-(((6-(1-methyl-1*H*-pyrazol-4-yl)pyrazolo[1,5-*a*]pyrazin-4-yl)oxy)-3-azabicyclo[3.2.0]heptan-3-yl)prop-2-en-1-one ($R_f = 4.46$ min., 55 mg, 20% yield, 92.1% *ee*).

Compound 16:

1-((1*R*,5*S*,6*r*)-6-(((6-(1-Methyl-1*H*-pyrazol-4-yl)pyrazolo[1,5-*a*]pyrazin-4-yl)oxy)methyl)-3-azabicyclo[3.1.0]hexan-3-yl)prop-2-en-1-one

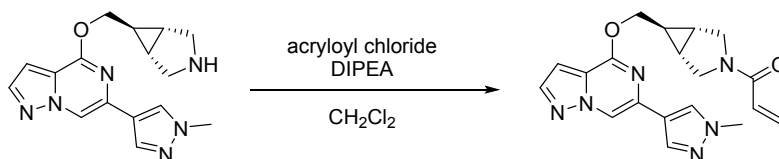


1. Synthesis of 4-(((1*R*,5*S*,6*r*)-3-azabicyclo[3.1.0]hexan-6-yl)methoxy)-6-(1-methyl-1*H*-pyrazol-4-yl)pyrazolo[1,5-*a*]pyrazine



To a solution of 4-chloro-6-(1-methyl-1*H*-pyrazol-4-yl)pyrazolo[1,5-*a*]pyrazine (100 mg, 0.43 mmol) and ((1*R*,5*S*,6*r*)-3-azabicyclo[3.1.0]hexan-6-yl)methanol (61 mg, 0.54 mmol) in THF (4 mL) was added KOtBu (120 mg, 1.07 mmol) at rt. After 30 min the reaction mixture was diluted with EtOAc (25 mL) and washed with sat. aq. NH_4Cl (10 mL), water (10 mL), and brine (10 mL). The combined organics were dried over Na_2SO_4 and concentrated *in vacuo* to afford 4-(((1*R*,5*S*,6*r*)-3-azabicyclo[3.1.0]hexan-6-yl)methoxy)-6-(1-methyl-1*H*-pyrazol-4-yl)pyrazolo[1,5-*a*]pyrazine which was used in the next step without further purification (assuming 100% yield). LCMS (ESI+): m/z calcd. for $C_{16}H_{18}N_6O$ $[M+H]^+$, 311.2; found, 311.2.

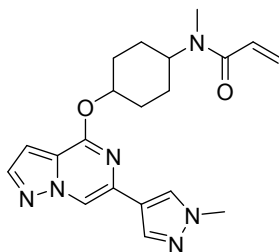
2. Synthesis of 1-((1*R*,5*S*,6*r*)-6-(((6-(1-methyl-1*H*-pyrazol-4-yl)pyrazolo[1,5-*a*]pyrazin-4-yl)oxy)methyl)-3-azabicyclo[3.1.0]hexan-3-yl)prop-2-en-1-one



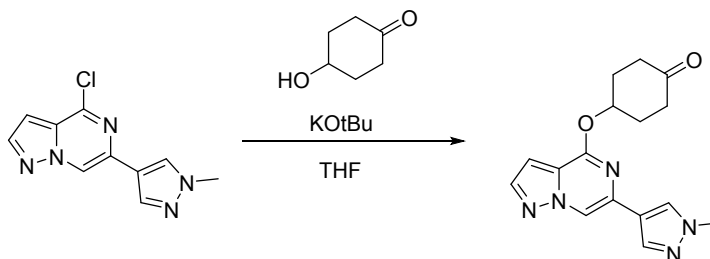
1-((1*R*,5*S*,6*r*)-6-(((6-(1-Methyl-1*H*-pyrazol-4-yl)pyrazolo[1,5-*a*]pyrazin-4-yl)oxy)methyl)-3-azabicyclo[3.1.0]hexan-3-yl)prop-2-en-1-one was synthesized in the same way as described for compound **14** (step 3) but starting from crude 4-(((1*R*,5*S*,6*r*)-3-azabicyclo[3.1.0]hexan-6-yl)methoxy)-6-(1-methyl-1*H*-pyrazol-4-yl)pyrazolo[1,5-*a*]pyrazine (132 mg, 0.43 mmol). The material was purified by column chromatography (24 g SiO₂, 0-100% EtOH:EtOAc (2% NH₄OH)1:3 in heptane) to afford the title compound (112 mg, 72% yield) as an off-white solid. HRMS (ESI⁺): *m/z* calcd. for C₁₉H₂₀N₆O₂ [M+H]⁺, 365.1721; found, 365.1729. ¹H NMR (500 MHz, acetonitrile-*d*₃): δ (ppm) 8.38 (s, 1H), 7.99 (s, 1H), 7.86-7.95 (m, 2H), 6.79 (d, *J* = 3.1 Hz, 1H), 6.55-6.43 (m, 1H), 6.23-6.11 (m, 1H), 5.63 (dd, *J* = 10.4, 2.4 Hz, 1H), 4.57-4.46 (m, 2H), 3.92 (s, 3H), 3.85-3.77 (m, 2H), 3.68 (dd, *J* = 10.4, 4.3 Hz, 1H), 3.45 (dd, *J* = 12.2, 4.9 Hz, 1H), 1.86-1.75 (m, 2H), 1.25 (tt, *J* = 7.0, 3.7 Hz, 1H).

Compound 17:

rac-*N*-methyl-*N*-((1*s*,4*s*)-4-(((6-(1-Methyl-1*H*-pyrazol-4-yl)pyrazolo[1,5-*a*]pyrazin-4-yl)oxy)cyclohexyl)acrylamide

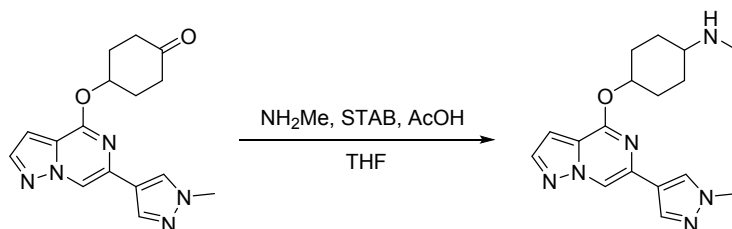


1. Synthesis of 4-(((6-(1-methyl-1*H*-pyrazol-4-yl)pyrazolo[1,5-*a*]pyrazin-4-yl)oxy)cyclohexan-1-one



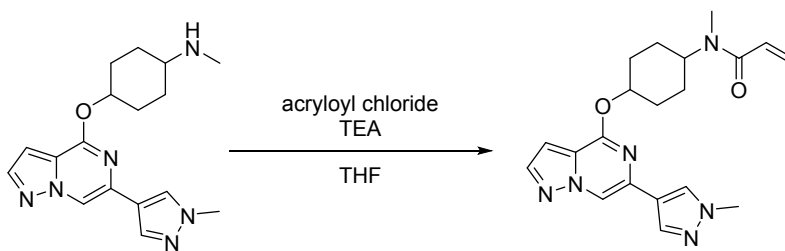
To a solution of 4-chloro-6-(1-methyl-1*H*-pyrazol-4-yl)pyrazolo[1,5-*a*]pyrazine (1.0 g, 4.28 mmol) and 4-hydroxycyclohexanone (537 mg, 4.71 mmol) in THF (15 mL) was dropwise added KOtBu (1.0 M in THF, 4.3 mL) at rt. After stirring overnight, the reaction mixture was loaded onto silica and purified by column chromatography (10 g SiO₂, 0-100% EtOAc in heptane) to afford the title compound (1.3 g, 98% yield). HRMS (ESI⁺): *m/z* calcd. for C₁₆H₁₇N₅O₂ [M+H]⁺, 312.1; found, 312.0.

2. *Synthesis of N-methyl-4-((6-(1-methyl-1H-pyrazol-4-yl)pyrazolo[1,5-a]pyrazin-4-yl)oxy)cyclohexan-1-amine*



Methylamine (2.0 M in THF, 642 μ L) and acetic acid (5.0 mg, 0.08 mmol, 5.0 μ L) were added to a flask containing 4-((6-(1-methyl-1H-pyrazol-4-yl)pyrazolo[1,5-a]pyrazin-4-yl)oxy)cyclohexan-1-one (80 mg, 0.26 mmol) at rt. After 15 min, STAB (109 mg, 0.51 mmol) was added to the resulting mixture and stirring was continued overnight. The volatiles were removed *in vacuo* to afford crude *N*-methyl-4-((6-(1-methyl-1H-pyrazol-4-yl)pyrazolo[1,5-a]pyrazin-4-yl)oxy)cyclohexan-1-amine (assumption 100% yield; 85 mg, 0.26 mmol) which was used without further purification in the next step. HRMS (ESI+): *m/z* calcd. for $C_{17}H_{22}N_6O$ $[M+H]^+$, 327.1; found, 327.0.

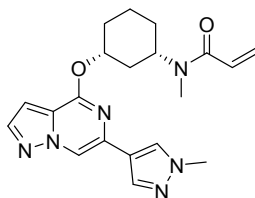
3. *Synthesis of N-methyl-N-(4-((6-(1-methyl-1H-pyrazol-4-yl)pyrazolo[1,5-a]pyrazin-4-yl)oxy)cyclohexyl)acrylamide*



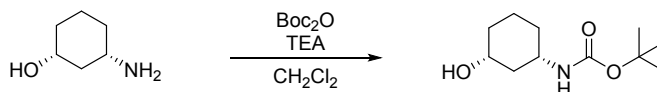
To a solution of *N*-methyl-4-((6-(1-methyl-1H-pyrazol-4-yl)pyrazolo[1,5-a]pyrazin-4-yl)oxy)cyclohexan-1-amine (60 mg, 0.18 mmol) in THF (2 mL) was added acryloyl chloride (33 mg, 0.37 mmol, 30 μ L) and TEA (93.0 mg, 0.92 mmol, 128 μ L) at rt. After 1 hr, the volatiles were removed *in vacuo* and the resulting residue was purified by HPLC (Waters XSelect CSH C18, 5 μ m, 19 mm \times 100 mm column with mobile phase H_2O (A) and MeCN (B) and a gradient of 5 – 50% B (0.2% NH_4OH final v/v % modifier) with flow rate at 30 mL/min) to afford *N*-methyl-*N*-(4-((6-(1-methyl-1H-pyrazol-4-yl)pyrazolo[1,5-a]pyrazin-4-yl)oxy)cyclohexyl)acrylamide (22 mg, 30% yield) as a white solid. HRMS (ESI+): *m/z* calcd. for $C_{20}H_{24}N_6O_2$ $[M+H]^+$, 381.2034; found, 381.2041. 1H NMR (500 MHz, chloroform-*d*): δ (ppm) 8.16–8.09 (m, 1H), 7.81 (m, 2H), 7.74–7.67 (m, 1H), 6.72–6.44 (m, 2H), 6.32–6.16 (m, 1H), 5.62 (br d, $J = 9.8$ Hz, 1H), 5.52 (br s, 1H), 5.22–5.08 (m, 0.4H), 4.72–4.55 (m, 0.6H), 3.98–3.87 (m, 3H), 2.94–2.83 (m, 3H), 2.28 (br t, $J = 15.6$ Hz, 2H), 1.96–1.58 (m, 6H).

Compound 18:

N-Methyl-*N*-((1*S*,3*R*)-3-((6-(1-methyl-1*H*-pyrazol-4-yl)pyrazolo[1,5-*a*]pyrazin-4-yl)oxy)cyclohexyl)acrylamide

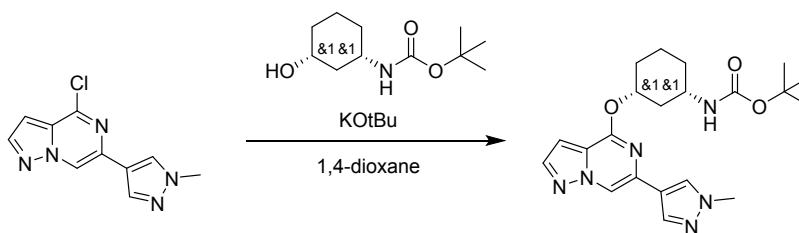


1. Synthesis of *rac*-*tert*-butyl ((1*S*,3*R*)-3-hydroxycyclohexyl)carbamate



To a solution of *rac*-(1*S*,3*R*)-aminocyclohexane-1-ol hydrochloride (1.0 g, 6.6 mmol) in CH₂Cl₂ (20 mL) and TEA (1.33 g, 13.19 mmol, 1.83 mL) was added a solution of (Boc)₂O (1.44 g, 6.59 mmol) in CH₂Cl₂ (5 mL) *via* syringe at 35°C and stirring was continued overnight. The reaction mixture was loaded onto silica and purified by column chromatography (24 g SiO₂, 0-100% 3:1 EtOAc:EtOH in heptane) to afford *rac*-*tert*-butyl ((1*S*,3*R*)-3-hydroxycyclohexyl)carbamate as a white solid (1.3 g, 93% yield). ¹H NMR (dimethyl sulfoxide-*d*₆): δ (ppm) 6.72 (br d, *J* = 7.9 Hz, 1H), 4.57 (d, *J* = 4.3 Hz, 1H), 3.35 (ddd, *J* = 15.0, 6.4, 4.3 Hz, 1H), 3.20 (br dd, *J* = 7.6, 3.4 Hz, 1H), 1.90 (br d, *J* = 11.6 Hz, 1H), 1.73 (br d, *J* = 11.6 Hz, 1H), 1.69-1.53 (m, 2H), 1.37 (s, 9H), 1.22-1.09 (m, 1H), 1.08-0.87 (m, 3H).

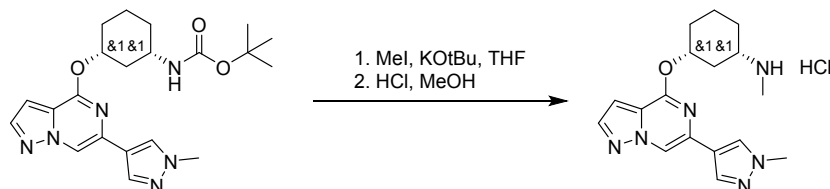
2. Synthesis of *rac*-*tert*-butyl ((1*R*,3*S*)-3-((6-(1-methyl-1*H*-pyrazol-4-yl)pyrazolo[1,5-*a*]pyrazin-4-yl)oxy)cyclohexyl)carbamate



To a solution of 4-chloro-6-(1-methyl-1*H*-pyrazol-4-yl)pyrazolo[1,5-*a*]pyrazine (250 mg, 1.07 mmol) and *rac*-*tert*-butyl ((1*R*,3*S*)-3-hydroxycyclohexyl)carbamate (250 mg, 1.16 mmol) in THF (2 mL) was added K_otBu (1.0 M in THF, 3.5 mL). After 5 min, sat aq. NaHCO₃ (5 mL) was added, and the biphasic mixture was extracted with EtOAc (3x 10 mL). The combined organic phase was concentrated *in vacuo* and purified by column chromatography (24 g SiO₂, 0-100% 3:1 EtOAc:EtOH in heptane) to afford *rac*-*tert*-butyl ((1*R*,3*S*)-3-((6-(1-methyl-1*H*-pyrazol-4-yl)pyrazolo[1,5-*a*]pyrazin-4-yl)oxy)cyclohexyl)carbamate (325 mg, 74% yield). LCMS (ESI⁺): *m/z* calcd. for C₂₁H₂₈N₆O₃ [M+H]⁺, 413.2; found, 413.2. ¹H NMR

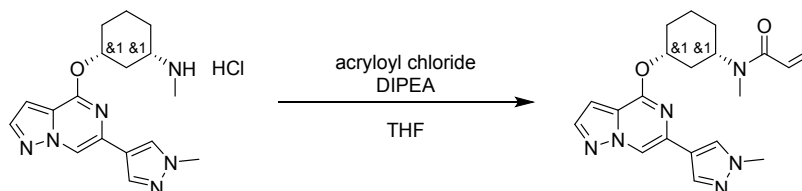
(dimethyl sulfoxide-*d*₆): δ (ppm) 8.73 (d, $J = 0.8$ Hz, 1H), 8.18 (s, 1H), 8.04-7.98 (m, 2H), 6.91-6.77 (m, 2H), 5.71 (br s, 1H), 3.88 (s, 3H), 3.79-3.64 (m, 1H), 2.11 (br d, $J = 14.3$ Hz, 1H), 1.96-1.86 (m, 1H), 1.85-1.56 (m, 6H), 1.44-1.22 (m, 9H).

3. *Synthesis of rac-(1S,3R)-N-methyl-3-((6-(1-methyl-1H-pyrazol-4-yl)pyrazolo[1,5-a]pyrazin-4-yl)oxy)cyclohexan-1-amine hydrochloride*



To a solution of *rac-tert-butyl* ((1*S*,3*R*)-3-((6-(1-methyl-1*H*-pyrazol-4-yl)pyrazolo[1,5-*a*]pyrazin-4-yl)oxy)cyclohexyl)carbamate (155 mg, 0.38 mmol) in THF (3 mL) was added KOtBu (1.0 M in THF, 1.6 mL) followed by iodomethane (213 mg, 1.50 mmol) at 40 °C. After 30min, sat. aq. NaHCO₃ (10 mL) was added to the reaction mixture and the resulting biphasic mixture was extracted with EtOAc (3 x 10 mL). The combined organic phase was concentrated *in vacuo* and the resulting residue was purified by column chromatography (24 g SiO₂, 0-100% 3:1 EtOAc:EtOH in heptane) to give a white solid which was dissolved in 1.25 M HCl in MeOH (10 mL) and heated at 40 °C for 16 hr. The reaction mixture was concentrated *in vacuo* to afford *rac*-(1*S*,3*R*)-*N*-methyl-3-((6-(1-methyl-1*H*-pyrazol-4-yl)pyrazolo[1,5-*a*]pyrazin-4-yl)oxy)cyclohexan-1-amine hydrochloride (85 mg, 63% yield) which was used without further purification in the next step. LCMS (ESI⁺): m/z calcd. for C₁₇H₂₂N₆O [M+H]⁺, 327.1; found, 327.1.

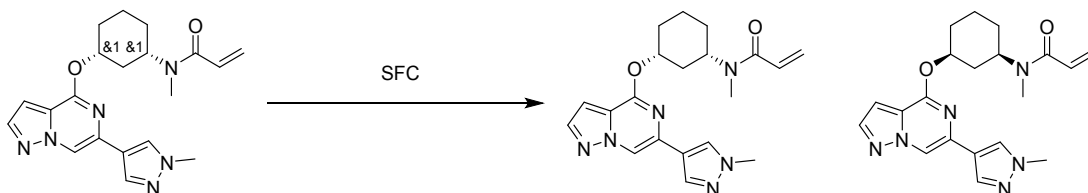
4. *Synthesis of rac-N-methyl-N-((1S,3R)-3-((6-(1-methyl-1H-pyrazol-4-yl)pyrazolo[1,5-a]pyrazin-4-yl)oxy)cyclohexyl)acrylamide*



To a solution of *rac*-(1*S*,3*R*)-*N*-Methyl-3-((6-(1-methyl-1*H*-pyrazol-4-yl)pyrazolo[1,5-*a*]pyrazin-4-yl)oxy)cyclohexan-1-amine hydrochloride (72 mg, 0.20 mmol) in THF (3 mL) were sequentially added TEA (101 mg, 1.00 mmol, 139 μ L) at rt and acryloyl chloride (18 mg, 0.20 mmol, 17 μ L) at -20 °C. After 5 min, sat. aq. NaHCO₃ (3 mL) was added, and the biphasic mixture was extracted with EtOAc (3 x 3 mL). The combined organic phase was concentrated *in vacuo* and the resulting residue was purified by HPLC (Waters Sunfire Prep C18, 5 μ m, 19 mm \times 100 mm column with mobile phase H₂O (A) and

MeCN (B) and a gradient of 5 – 60% B (0.2% TFA final v/v % modifier) with flow rate at 30 mL/min) to afford *rac*-*N*-methyl-*N*-((1*S*,3*R*)-3-((6-(1-methyl-1*H*-pyrazol-4-yl)pyrazolo[1,5-*a*]pyrazin-4-yl)oxy)cyclohexyl)acrylamide (76 mg, 99% yield) . LCMS (ESI+): *m/z* calcd. for C₂₀H₂₄N₆O₂ [M+H]⁺, 381.2; found, 381.2.

5. Isolation of *N*-methyl-*N*-((1*S*,3*R*)-3-((6-(1-methyl-1*H*-pyrazol-4-yl)pyrazolo[1,5-*a*]pyrazin-4-yl)oxy)cyclohexyl)acrylamide and *N*-methyl-*N*-((1*R*,3*S*)-3-((6-(1-methyl-1*H*-pyrazol-4-yl)pyrazolo[1,5-*a*]pyrazin-4-yl)oxy)cyclohexyl)acrylamide



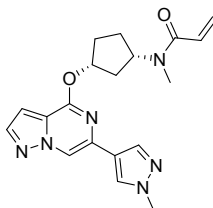
rac-*N*-Methyl-*N*-((1*S*,3*R*)-3-((6-(1-methyl-1*H*-pyrazol-4-yl)pyrazolo[1,5-*a*]pyrazin-4-yl)oxy)cyclohexyl)acrylamide (68 mg) was resolved by SFC (CHIRALPAK AD-H 30 x 250 mm, 5μm, 40% MeOH in CO₂, flow rate: 100 mL/min, ABPR 120 bar, MBPR 40 psi, column temp 40 °C) to afford two compounds of arbitrarily assigned stereochemistry:

Peak 1: *N*-methyl-*N*-((1*S*,3*R*)-3-((6-(1-methyl-1*H*-pyrazol-4-yl)pyrazolo[1,5-*a*]pyrazin-4-yl)oxy)cyclohexyl)acrylamide (compound **18**, R_f = 2.55 min., 13 mg, 18% yield, 99.3% *ee*) HRMS (ESI+): *m/z* calcd. for C₂₀H₂₄N₆O₂ [M+H]⁺, 381.2034; found, 381.2042. ¹H NMR (dimethyl sulfoxide-*d*₆): δ (ppm) 8.74 (s, 1H), 8.26 (s, 1H), 8.07-7.97 (m, 2H), 6.79 (s, 2H), 6.20-6.03 (m, 1H), 5.74-5.62 (m, 1H), 5.49-5.31 (m, 1H), 4.66-4.47 (m, 1H), 4.22-4.04 (m, 1H), 3.90 (d, *J* = 3.7 Hz, 3H), 2.32-2.11 (m, 3H), 2.00-1.13 (m, 7H), and

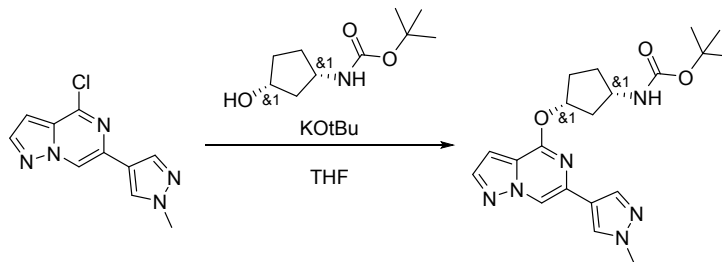
Peak 2: *N*-methyl-*N*-((1*R*,3*S*)-3-((6-(1-methyl-1*H*-pyrazol-4-yl)pyrazolo[1,5-*a*]pyrazin-4-yl)oxy)cyclohexyl)acrylamide (R_f = 3.52 min., 17 mg, 17% yield, 99.7% *ee*).

Compound 19:

N-Methyl-*N*-((1*S*,3*R*)-3-((6-(1-methyl-1*H*-pyrazol-4-yl)pyrazolo[1,5-*a*]pyrazin-4-yl)oxy)cyclopentyl)acrylamide

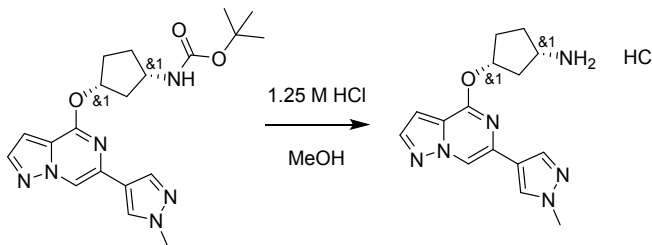


1. Synthesis of *rac-tert-butyl ((1R,3S)-3-((6-(1-methyl-1H-pyrazol-4-yl)pyrazolo[1,5-a]pyrazin-4-yl)oxy)cyclopentyl)carbamate*.



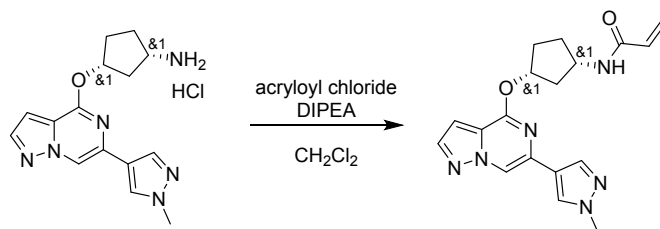
To a solution of *rac-tert-butyl ((1R,3S)-3-hydroxycyclopentyl)carbamate* (250 mg, 1.24 mmol) in THF (5 mL) was added KOtBu (123 mg, 1.10 mmol) at 0 °C. After 15 min, 4-chloro-6-(1-methyl-1H-pyrazol-4-yl)pyrazolo[1,5-a]pyrazine (250 mg, 1.07 mmol) was added, and the reaction mixture was brought to rt. After 30 min, sat. aq. NaHCO₃ (5 mL) was added, and the biphasic mixture was extracted with EtOAc (3 x 10 mL). The combined organic phase was dried over MgSO₄, filtered, and concentrated *in vacuo*. The resulting residue was purified by column chromatography (12 g SiO₂, 0-100% 3:1 EtOAc:EtOH in heptane) to afford *rac-tert-butyl ((1R,3S)-3-((6-(1-methyl-1H-pyrazol-4-yl)pyrazolo[1,5-a]pyrazin-4-yl)oxy)cyclopentyl)carbamate* (390 mg, 92% yield). LCMS (ESI+): *m/z* calcd. for C₂₀H₂₆N₆O₃ [M+H]⁺, 399.2; found, 399.2.

2. Synthesis of *rac-(1R,3S)-3-((6-(1-methyl-1H-pyrazol-4-yl)pyrazolo[1,5-a]pyrazin-4-yl)oxy)cyclopentan-1-amine*



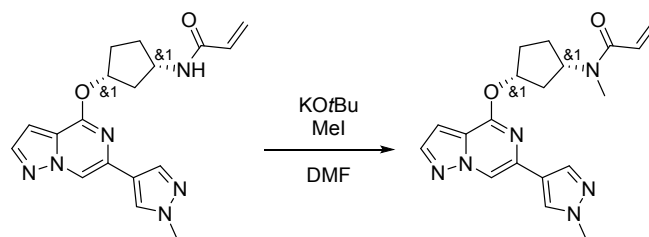
To a vial containing *tert-butyl ((cis)-3-((6-(1-methyl-1H-pyrazol-4-yl)pyrazolo[1,5-a]pyrazin-4-yl)oxy)cyclopentyl)carbamate* (390 mg, 0.98 mmol) was added 1.25 M HCl solution in MeOH (5 mL). The resulting reaction mixture was heated at 50 °C for 2 hr before the volatiles were removed *in vacuo* to afford *rac-(1R,3S)-3-((6-(1-methyl-1H-pyrazol-4-yl)pyrazolo[1,5-a]pyrazin-4-yl)oxy)cyclopentan-1-amine hydrochloride* (327 mg), which was used without further purification in the next step. LCMS (ESI+): *m/z* calcd. for C₁₅H₁₈N₆O [M+H]⁺, 299.2; found, 299.2.

3. Synthesis of *rac-N-((1R,3S)-3-((6-(1-methyl-1H-pyrazol-4-yl)pyrazolo[1,5-a]pyrazin-4-yl)oxy)cyclopentyl)acrylamide*



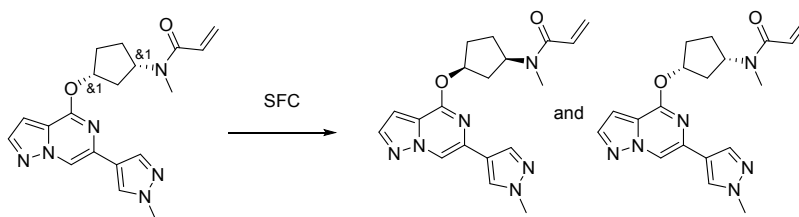
To a solution of *rac*-(1*R*,3*S*)-3-((6-(1-methyl-1*H*-pyrazol-4-yl)pyrazolo[1,5-*a*]pyrazin-4-yl)oxy)cyclopentan-1-amine hydrochloride (165 mg, 0.55 mmol) in CH₂Cl₂ (3 mL) was added DIPEA (215 mg, 1.66 mmol, 290 μ L) followed by dropwise addition of acryloyl chloride (50 mg, 0.55 mmol, 45 μ L) at -20 $^{\circ}$ C. After 5 min, the reaction mixture was loaded onto silica and purified by column chromatography (12 g SiO₂, 0-100% 3:1 EtOAc:EtOH in heptane) to afford *rac*-*N*-((1*R*,3*S*)-3-((6-(1-methyl-1*H*-pyrazol-4-yl)pyrazolo[1,5-*a*]pyrazin-4-yl)oxy)cyclopentyl)acrylamide (150 mg, 73% yield). LCMS (ESI⁺): *m/z* calcd. for C₁₈H₂₀N₆O₂ [M+H]⁺, 353.2; found, 353.2. ¹H NMR (500 MHz, dimethyl sulfoxide-*d*₆): δ (ppm) 8.74 (s, 1H), 8.21 (s, 2H), 8.02–7.99 (m, 2H), 6.83–6.79 (m, 1H), 6.25–6.16 (m, 1H), 6.10–6.02 (m, 1H), 5.63–5.52 (m, 2H), 4.20 (br d, *J* = 7.3 Hz, 1H), 3.89 (s, 3H), 2.68–2.59 (m, 1H), 2.12 (br d, *J* = 6.7 Hz, 1H), 2.05–1.95 (m, 2H), 1.77–1.64 (m, 2H).

4. *Synthesis of rac-N-methyl-N-((1R,3S)-3-((6-(1-methyl-1H-pyrazol-4-yl)pyrazolo[1,5-a]pyrazin-4-yl)oxy)cyclopentyl)acrylamide*



To a solution of *rac*-*N*-((1*R*,3*S*)-3-((6-(1-methyl-1*H*-pyrazol-4-yl)pyrazolo[1,5-*a*]pyrazin-4-yl)oxy)cyclopentyl)acrylamide (125 mg, 0.35 mmol) in DMF (1 mL) was added iodomethane (150 mg, 66 μ L, 0.35 mmol), followed by KO^tBu (1.0 M in THF, 1.0 mL) at rt. After 30 min, CH₂Cl₂ (5 mL) was added and the resulting mixture was loaded onto silica and purified by column chromatography (12 g SiO₂, 0-100% 3:1 EtOAc:EtOH in heptane) to afford *rac*-*N*-methyl-*N*-((1*R*,3*S*)-3-((6-(1-methyl-1*H*-pyrazol-4-yl)pyrazolo[1,5-*a*]pyrazin-4-yl)oxy)cyclopentyl)acrylamide (114 mg, 83% yield). LCMS (ESI⁺): *m/z* calcd. for C₁₉H₂₂N₆O₂ [M+H]⁺, 367.2; found, 367.2. ¹H NMR (500 MHz, dimethyl sulfoxide-*d*₆): δ (ppm) 8.74 (s, 1H), 8.21 (s, 1H), 8.03–7.99 (m, 2H), 6.95–6.69 (m, 2H), 6.17–6.03 (m, 1H), 5.70–5.63 (m, 2H), 5.18–4.55 (m, 1H), 3.88 (s, 3H), 2.99–2.72 (m, 4H), 2.50–2.39 (m, 2H), 2.03–1.97 (m, 1H), 1.91–1.81 (m, 2H).

5. Isolation of *N*-methyl-*N*-((1*R*,3*S*)-3-((6-(1-methyl-1*H*-pyrazol-4-yl)pyrazolo[1,5-*a*]pyrazin-4-yl)oxy)cyclopentyl)acrylamide and *N*-methyl-*N*-((1*S*,3*R*)-3-((6-(1-methyl-1*H*-pyrazol-4-yl)pyrazolo[1,5-*a*]pyrazin-4-yl)oxy)cyclopentyl)acrylamide



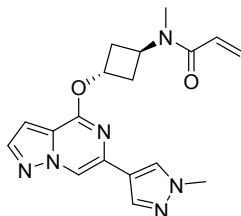
N-Methyl-*N*-((*cis*)-3-((6-(1-methyl-1*H*-pyrazol-4-yl)pyrazolo[1,5-*a*]pyrazin-4-yl)oxy)cyclopentyl)acrylamide (130 mg, 0.36 mmol) was resolved by chiral SFC purification (Chiralpak AD-H, 30 x 250 mm, 5mm column using 40% MeOH in CO₂. Flow rate: 100 mL/min; ABPR 120 bar; MBPR 40 psi, column temperature 40 °C) to afford two compounds of arbitrarily assigned stereochemistry:

Peak 1: *N*-methyl-*N*-((1*R*,3*S*)-3-((6-(1-methyl-1*H*-pyrazol-4-yl)pyrazolo[1,5-*a*]pyrazin-4-yl)oxy)cyclopentyl)acrylamide ($R_f = 2.88$ min., 35 mg, 28% yield, 100% *ee*), and

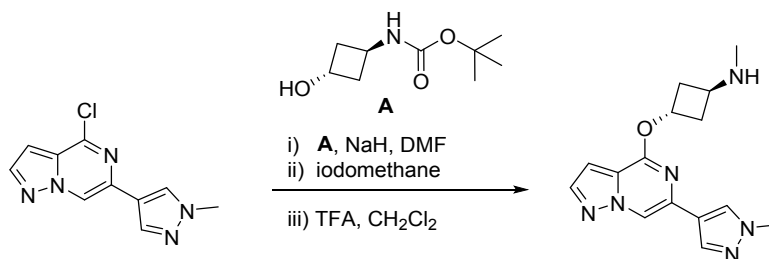
Peak 2: *N*-methyl-*N*-((1*R*,3*S*)-3-((6-(1-methyl-1*H*-pyrazol-4-yl)pyrazolo[1,5-*a*]pyrazin-4-yl)oxy)cyclopentyl)acrylamide (compound **19**, $R_f = 3.37$ min., 37 mg, 28% yield, 98.6% *ee*). HRMS (ESI⁺): *m/z* calcd. for C₁₉H₂₂N₆O₂ [M+H]⁺, 367.1877; found, 367.1883. ¹H NMR (500 MHz, dimethyl sulfoxide-*d*₆): δ (ppm) 8.75 (s, 1H), 8.21 (br s, 1H), 8.04-7.96 (m, 2H), 6.96-6.69 (m, 2H), 6.09 (br t, *J* = 16.5 Hz, 1H), 5.71-5.62 (m, 2H), 5.18-4.59 (m, 1H), 3.88 (s, 3H), 3.00-2.82 (m, 3H), 2.49-2.41 (m, 1H), 2.13-2.00 (m, 2H), 1.92-1.75 (m, 3H).

Compound 20:

N-Methyl-*N*-((1*r*,3*r*)-3-((6-(1-methyl-1*H*-pyrazol-4-yl)pyrazolo[1,5-*a*]pyrazin-4-yl)oxy)cyclobutyl)acrylamide

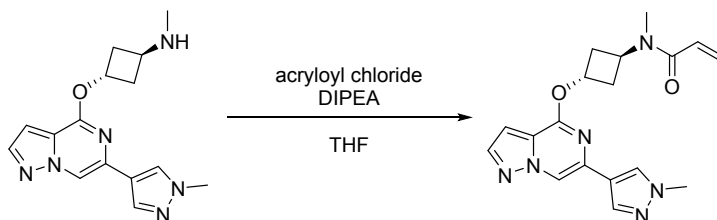


1. Synthesis of (*trans*)-*N*-methyl-3-((6-(1-methyl-1*H*-pyrazol-4-yl)pyrazolo[1,5-*a*]pyrazin-4-yl)oxy)cyclobutan-1-amine



- i) To a solution of 4-chloro-6-(1-methyl-1*H*-pyrazol-4-yl)pyrazolo[1,5-*a*]pyrazine (50 mg, 0.21 mmol) and *tert*-butyl ((1*r*,3*r*)-3-hydroxycyclobutyl)carbamate (44 mg, 0.24 mmol) in DMF (2.0 mL) was added NaH (26 mg, 0.64 mmol, 60% purity) at rt.
- ii) After 30 min, iodomethane (46 mg, 0.32 mmol, 20 μ L) was added and to the resulting reaction mixture and stirring was continued for 30 min. The reaction mixture was diluted with EtOAc (5 mL) and sat. aq. NaHCO₃ (5 mL) was added. The organic phase was separated and washed with water (5 mL) and brine (5 mL). The organic phase was dried over Na₂SO₄, filtered, and concentrated *in vacuo*.
- iii) The resulting residue was dissolved in CH₂Cl₂ (3 mL) and TFA (0.5 mL) was added. After stirring overnight, the volatiles were removed *in vacuo* to afford (1*r*,3*r*)-*N*-methyl-3-((6-(1-methyl-1*H*-pyrazol-4-yl)pyrazolo[1,5-*a*]pyrazin-4-yl)oxy)cyclobutan-1-amine which was used in the next step without further purification (assuming 100% yield). LCMS (ESI⁺): *m/z* calcd. for C₁₅H₁₈N₆O [M+H]⁺, 299.2; found, 299.0.

2. *Synthesis of N-methyl-N-((trans)-3-((6-(1-methyl-1H-pyrazol-4-yl)pyrazolo[1,5-a]pyrazin-4-yl)oxy)cyclobutyl)acrylamide*

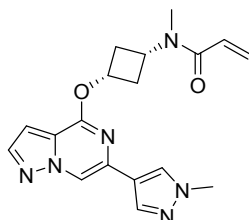


N-Methyl-*N*-((1*r*,3*r*)-3-((6-(1-methyl-1*H*-pyrazol-4-yl)pyrazolo[1,5-*a*]pyrazin-4-yl)oxy)cyclobutyl)acrylamide (26 mg, 72% yield over 2 steps) was synthesized analogous to the method described for compound **14** (step 3) but using (1*r*,3*r*)-*N*-methyl-3-((6-(1-methyl-1*H*-pyrazol-4-yl)pyrazolo[1,5-*a*]pyrazin-4-yl)oxy)cyclobutan-1-amine (31 mg, 0.10 mmol) and THF as solvent. Purification by column chromatography (12 g SiO₂, 0-100% 3:1 EtOAc:EtOH (2% NH₄OH) in heptane) afforded the title compound as off white solid. HRMS (ESI⁺): *m/z* calcd. for C₁₈H₂₀N₆O₂ [M+H]⁺, 353.1721; found, 353.1726. ¹H NMR (500 MHz, methanol-*d*₄): δ (ppm) 8.35 (br s, 1H), 7.99 (s, 1H), 7.94-

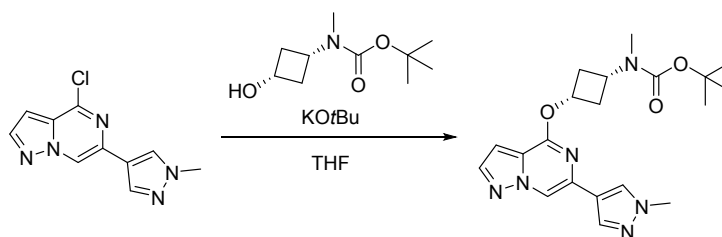
7.85 (m, 2H), 6.80 (d, $J = 1.8$ Hz, 1H), 6.72 (br s, 1H), 6.28-6.08 (m, 1H), 5.73 (br s, 1H), 5.54-5.43 (m, 1H), 5.29-4.93 (m, 1H), 3.91 (s, 3H), 3.21-3.04 (m, 3H), 2.95-2.74 (m, 2H), 2.60 (br s, 2H).

Compound 21:

N-Methyl-*N*-((1*s*,3*s*)-3-((6-(1-methyl-1*H*-pyrazol-4-yl)pyrazolo[1,5-*a*]pyrazin-4-yl)oxy)cyclobutyl)acrylamide

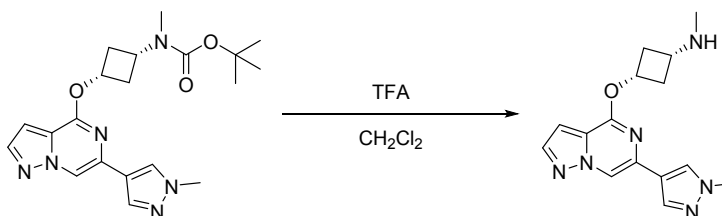


1. Synthesis of *tert*-butyl methyl((1*s*,3*s*)-3-((6-(1-methyl-1*H*-pyrazol-4-yl)pyrazolo[1,5-*a*]pyrazin-4-yl)oxy)cyclobutyl)carbamate



tert-Butyl methyl((1*s*,3*s*)-3-((6-(1-methyl-1*H*-pyrazol-4-yl)pyrazolo[1,5-*a*]pyrazin-4-yl)oxy)cyclobutyl)carbamate was synthesized analogous to the method described for compound **18** (step 2), but starting from *tert*-butyl ((*cis*)-3-hydroxycyclobutyl)(methyl)carbamate (750 mg, 3.70 mmol). The crude title compound was obtained as a pale orange residue (assuming 100% yield) which was used in the next reaction without further purification. LCMS (ESI+): m/z calcd. for $C_{20}H_{26}N_6O_3$ $[M+H]^+$, 399.2; found, 399.2.

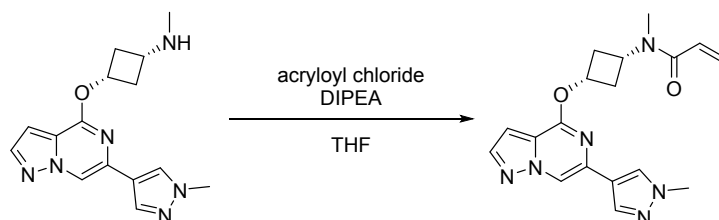
2. Synthesis of (1*s*,3*s*)-*N*-methyl-3-((6-(1-methyl-1*H*-pyrazol-4-yl)pyrazolo[1,5-*a*]pyrazin-4-yl)oxy)cyclobutan-1-amine



To a solution of crude *tert*-butyl methyl((1*s*,3*s*)-3-((6-(1-methyl-1*H*-pyrazol-4-yl)pyrazolo[1,5-*a*]pyrazin-4-yl)oxy)cyclobutyl)carbamate (1.35 g, 3.40 mmol) in CH_2Cl_2 (9 mL) was added TFA (3 mL) at rt. After

1 hr the reaction mixture was diluted with EtOAc (50 mL) followed by careful addition of sat. aq. NaHCO₃ (50 mL) under vigorous stirring. The resulting organic phase was separated and washed with water (10 mL), and brine (10 mL), separated, dried over Na₂SO₄, filtered, and concentrated *in vacuo* to afford (1*s*,3*s*)-*N*-methyl-3-((6-(1-methyl-1*H*-pyrazol-4-yl)pyrazolo[1,5-*a*]pyrazin-4-yl)oxy)cyclobutan-1-amine as an orange oil which was used without further purification in the next step (assumption 100% yield). LCMS (ESI+): *m/z* calcd. for C₁₅H₁₈N₆O [M+H]⁺, 299.2; found, 299.2.

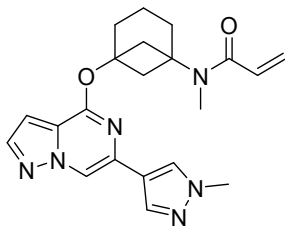
3. *Synthesis of N-methyl-N-((1*s*,3*s*)-3-((6-(1-methyl-1*H*-pyrazol-4-yl)pyrazolo[1,5-*a*]pyrazin-4-yl)oxy)cyclobutyl)acrylamide*



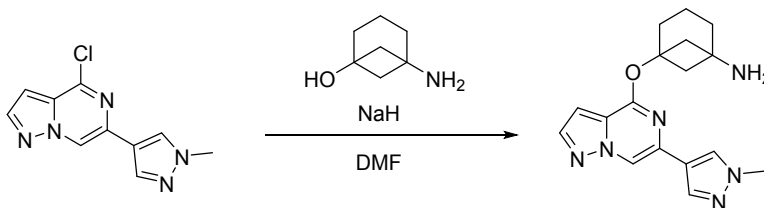
To a solution (1*s*,3*s*)-*N*-methyl-3-((6-(1-methyl-1*H*-pyrazol-4-yl)pyrazolo[1,5-*a*]pyrazin-4-yl)oxy)cyclobutan-1-amine and DIPEA (277 mg, 2.14 mmol, 370 μL) in THF (2 mL) was added acryloyl chloride (39 mg, 0.43 mmol, 35 μL) at rt. After 30 min, the reaction mixture was diluted with EtOAc (5 mL) and sat. aq. NaHCO₃ (5 mL) was added. The organic phase was separated and washed with water (5 mL) and brine (5 mL). The organic phase was dried over Na₂SO₄, filtered, and concentrated *in vacuo*. Column chromatography (24 g SiO₂, 10-100% 3:1 EtOAc:EtOH in heptane) of the resulting residue afforded *N*-methyl-*N*-((1*s*,3*s*)-3-((6-(1-methyl-1*H*-pyrazol-4-yl)pyrazolo[1,5-*a*]pyrazin-4-yl)oxy)cyclobutyl)acrylamide (41 mg, 54% yield). HRMS (ESI+): *m/z* calcd. for C₁₈H₂₀N₆O₂ [M+H]⁺, 353.1721; found, 353.1724. ¹H NMR (500 MHz, acetonitrile-*d*₃): δ (ppm) 8.34 (d, *J* = 1.2 Hz, 1H), 7.97 (s, 1H), 7.90 (d, *J* = 2.4 Hz, 1H), 7.88 (s, 1H), 6.76-6.65 (m, 2H), 6.178 (br d, *J* = 14.7 Hz, 1H), 5.68 (dd, *J* = 10.4, 2.4 Hz, 1H), 5.16 (br s, 1H), 4.76-4.37 (m, 1H), 3.90 (s, 3H), 3.04-2.92 (m, 5H), 2.49-2.39 (m, 2H).

Compound 22:

***N*-Methyl-*N*-((5-((6-(1-methyl-1*H*-pyrazol-4-yl)pyrazolo[1,5-*a*]pyrazin-4-yl)oxy)bicyclo[3.1.1]heptan-1-yl)acrylamide**

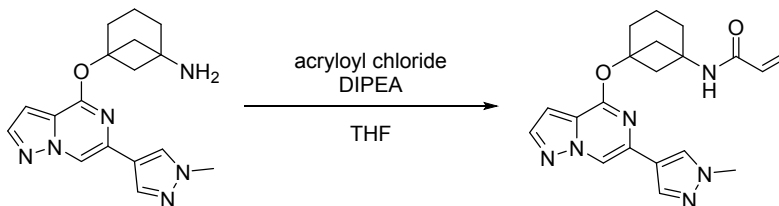


1. *Synthesis of 5-((6-(1-methyl-1H-pyrazol-4-yl)pyrazolo[1,5-a]pyrazin-4-yl)oxy)bicyclo[3.1.1]heptan-1-amine*



To a solution of 4-chloro-6-(1-methyl-1H-pyrazol-4-yl)pyrazolo[1,5-a]pyrazine (50 mg, 0.21 mmol) and 5-aminobicyclo[3.1.1]heptan-1-ol (30 mg, 0.24 mmol) in DMF (2.5 mL) was added NaH (26 mg, 0.64 mmol, 60% purity) in one portion at rt. The resulting reaction mixture was heated at 50 °C for 30 min. 3:1 EtOAc:EtOH (3 mL) was added to the reaction mixture and it was loaded onto silica and purified by column chromatography (12 g SiO₂, 0-100% 3:1 EtOAc:EtOH (2% NH₄OH) in heptane) to afford 5-((6-(1-methyl-1H-pyrazol-4-yl)pyrazolo[1,5-a]pyrazin-4-yl)oxy)bicyclo[3.1.1]heptan-1-amine (36 mg, 52% yield) as an off-white solid. LCMS (ESI⁺): *m/z* calcd. for C₁₇H₂₀N₆O [M+H]⁺, 325.1; found, 325.1.

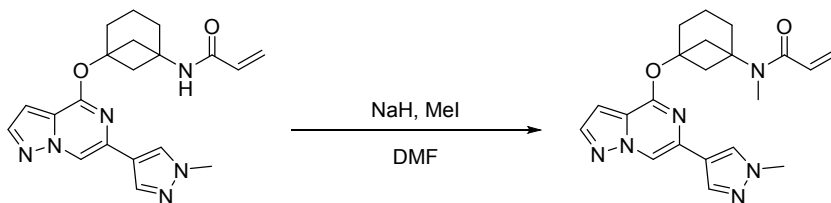
2. *Synthesis of N-(5-((6-(1-methyl-1H-pyrazol-4-yl)pyrazolo[1,5-a]pyrazin-4-yl)oxy)bicyclo[3.1.1]heptan-1-yl)acrylamide*



N-Methyl-*N*-(5-((6-(1-methyl-1H-pyrazol-4-yl)pyrazolo[1,5-a]pyrazin-4-yl)oxy)bicyclo[3.1.1]heptan-1-yl)acrylamide was synthesized using an analogous method to that described for compound **14** (step 3) but starting from 5-((6-(1-methyl-1H-pyrazol-4-yl)pyrazolo[1,5-a]pyrazin-4-yl)oxy)bicyclo[3.1.1]heptan-1-amine (35 mg, 0.11 mmol) and using THF as solvent. The material was purified by column chromatography (12 g SiO₂, 10-100% 3:1 EtOAc:EtOH (2% NH₄OH) in heptane) to afford the title compound (31 mg, 76% yield) as an off-white solid. LCMS (ESI⁺): *m/z* calcd. for C₂₀H₂₂N₆O₂ [M+Na]⁺, 401.1; found, 401.1. ¹H NMR (500 MHz, methanol-*d*₄): δ (ppm) 8.41 (d, *J*=1.2 Hz, 1H), 8.05 (s, 1H),

7.93 (s, 1H), 7.90 (d, $J=2.4$ Hz, 1H), 6.75 (dd, $J=1.2, 2.4$ Hz, 1H), 6.23-6.18 (m, 2H), 5.62 (dd, $J=7.3, 4.3$ Hz, 1H), 3.96 (s, 3H), 2.78-2.71 (m, 2H), 2.50-2.43 (m, 2H), 2.33 (t, $J=6.4$ Hz, 2H), 2.08-1.96 (m, 4H).

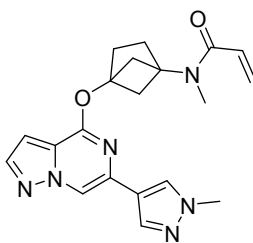
3. *Synthesis of N-methyl-N-(5-((6-(1-methyl-1H-pyrazol-4-yl)pyrazolo[1,5-a]pyrazin-4-yl)oxy)bicyclo[3.1.1]heptan-1-yl)acrylamide*



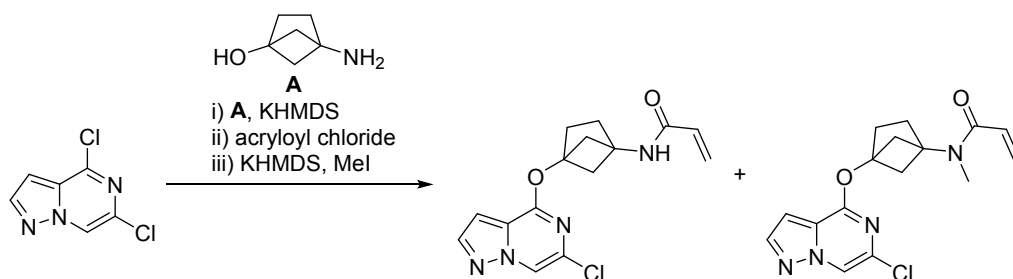
To a solution of *N*-(5-((6-(1-methyl-1H-pyrazol-4-yl)pyrazolo[1,5-a]pyrazin-4-yl)oxy)bicyclo[3.1.1]heptan-1-yl)acrylamide (24 mg, 0.06 mmol) and iodomethane (14 mg, 0.10 mmol) in DMF (2 mL) was added NaH (8 mg, 0.19 mmol, 60% purity) at rt. After 30min, MeOH (100 μ L) was added to the reaction mixture and it was loaded onto silica and purified by column chromatography (12 g SiO₂, 10-100% 3:1 EtOAc:EtOH (2% NH₄OH) in heptane) to afford *N*-methyl-*N*-(5-((6-(1-methyl-1H-pyrazol-4-yl)pyrazolo[1,5-a]pyrazin-4-yl)oxy)bicyclo[3.1.1]heptan-1-yl)acrylamide (8.6 mg, 35% yield) as an off-white solid. HRMS (ESI⁺): m/z calcd. for C₂₁H₂₄N₆O₂ [M+H]⁺, 393.2034; found, 393.2042. ¹H NMR (500 MHz, methanol-*d*₄): δ (ppm) 8.45-8.37 (m, 1H), 8.06 (s, 1H), 7.94 (s, 1H), 7.90 (d, $J = 2.4$ Hz, 1H), 6.75 (d, $J = 1.8$ Hz, 1H), 6.73-6.56 (m, 1H), 6.19 (dd, $J = 16.5, 1.8$ Hz, 1H), 5.76-5.67 (m, 1H), 3.96 (s, 3H), 3.05-2.92 (m, 3H), 2.87 (br dd, $J = 7.0, 2.1$ Hz, 2H), 2.61-2.27 (m, 4H), 2.14-1.95 (m, 4H).

Compound 23:

N-Methyl-*N*-(4-((6-(1-methyl-1H-pyrazol-4-yl)pyrazolo[1,5-a]pyrazin-4-yl)oxy)bicyclo[2.1.1]hexan-1-yl)acrylamide

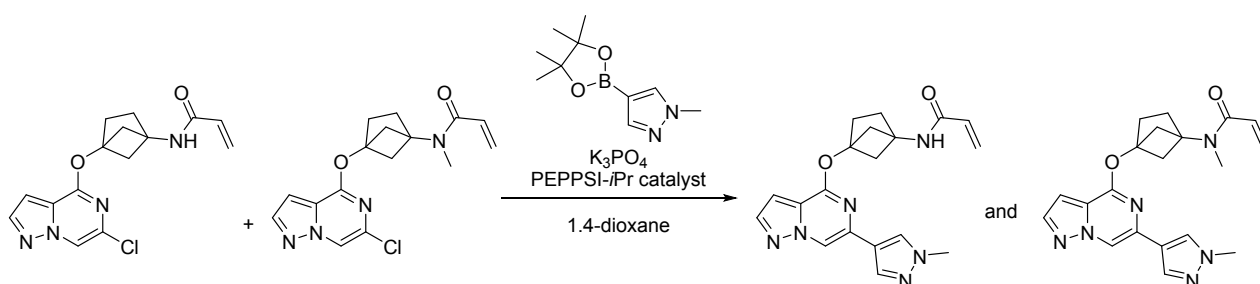


1. *Synthesis of N-(4-((6-chloropyrazolo[1,5-a]pyrazin-4-yl)oxy)bicyclo[2.1.1]hexan-1-yl)acrylamide and N-(4-((6-chloropyrazolo[1,5-a]pyrazin-4-yl)oxy)bicyclo[2.1.1]hexan-1-yl)-N-methylacrylamide*



- i) To a solution of 4-aminobicyclo[2.1.1]hexan-1-ol hydrochloride (**A**, 300 mg, 2.01 mmol) in THF (10 mL) was added KHMDS (1M THF, 3.65 mL) at rt within 5 min. After 10 min, a solution of 4,6-dichloropyrazolo[1,5-*a*]pyrazine (343 mg, 1.82 mmol) in THF (4 mL) was added dropwise within 5 min.
- ii) After 15 min, acryloyl chloride (165 mg, 1.82 mmol, 150 μ L) was added dropwise to the dark brown reaction mixture at rt and stirring was continued for another 30 min.
- iii) Additional KHMDS (1M THF, 3.65 mL) was added to the reaction mixture followed by the dropwise addition of iodomethane (140 μ L, 2.28 mmol) at rt. After 1 hr, EtOAc (10 mL) and sat aq. NaHCO₃ (10 mL) were added to the reaction mixture. The biphasic mixture was vigorously stirred for 15 min, the organic phase was separated and washed with water (10 mL), brine (10 mL), dried over Na₂SO₄, filtered, and concentrated *in vacuo*. The resulting residue was purified by column chromatography (24 g SiO₂, 0-100% 3:1 EtOAc:EtOH (2% NH₄OH) in heptane) to afford an inseparable 4:1 mixture of *N*-(4-((6-chloropyrazolo[1,5-*a*]pyrazin-4-yl)oxy)bicyclo[2.1.1]hexan-1-yl)-*N*-methylacrylamide and *N*-(4-((6-chloropyrazolo[1,5-*a*]pyrazin-4-yl)oxy)bicyclo[2.1.1]hexan-1-yl)acrylamide as an orange oil (353 mg) which was used without further purification in the next step. LCMS (ESI+): *m/z* calcd. for C₁₅H₁₅ClN₄O₂ [M+H]⁺, 319.0; found, 319.0. LCMS (ESI+): *m/z* calcd. for C₁₆H₁₇ClN₄O₂ [M+H]⁺, 333.1; found, 333.1.

2. *Synthesis of N*-(4-((6-(1-methyl-1H-pyrazol-4-yl)pyrazolo[1,5-*a*]pyrazin-4-yl)oxy)bicyclo[2.1.1]hexan-1-yl)acrylamide and *N*-methyl-*N*-(4-((6-(1-methyl-1H-pyrazol-4-yl)pyrazolo[1,5-*a*]pyrazin-4-yl)oxy)bicyclo[2.1.1]hexan-1-yl)acrylamide



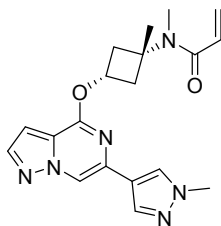
A 4:1 mixture of *N*-(4-((6-chloropyrazolo[1,5-*a*]pyrazin-4-yl)oxy)bicyclo[2.1.1]hexan-1-yl)-*N*-methylacrylamide, *N*-(4-((6-chloropyrazolo[1,5-*a*]pyrazin-4-yl)oxy)bicyclo[2.1.1]hexan-1-yl)acrylamide

(353 mg, 1.06 mmol), 1-methyl-4-(4,4,5,5-tetramethyl-1,3,2-dioxaborolan-2-yl)-1*H*-pyrazole (441, 2.12 mmol), K₃PO₄ (675 mg, 3.18 mmol), and PEPPSI-*i*Pr catalyst (145 mg, 0.21 mmol) in 1,4-dioxane (10 mL) and water (1 mL) was degassed by purging with N₂ for 30 min. The resulting mixture was heated at reflux for 1 hr, cooled to rt and diluted with EtOAc (25 mL). The organic phase was separated and washed with water (20 mL) and brine (20 mL), dried over Na₂SO₄, filtered and concentrated *in vacuo*. The resulting residue was purified by column chromatography (24 g SiO₂, 20-100% 3:1 EtOAc:EtOH (2% NH₄OH) in heptane), followed by HPLC (XSelect CSH Prep C18 OBD 5 μm 30 x 100mm; Method: (A) 95% [H₂O] // (B) 5% [Acetonitrile] w/ 0.2% NH₄OH (initial conditions hold for 0.5min) then a linear gradient to 5% (A) / 75% (B) over 12 min (flow rate: 50 mL/min) to afford:

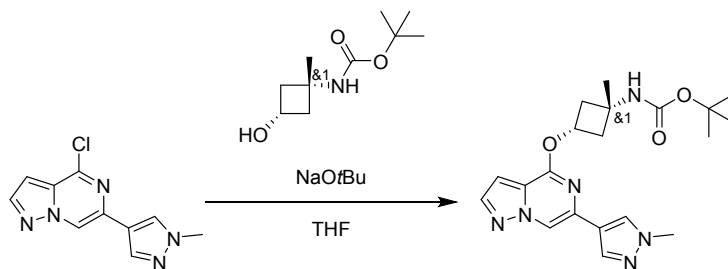
N-(4-((6-(1-Methyl-1*H*-pyrazol-4-yl)pyrazolo[1,5-*a*]pyrazin-4-yl)oxy)bicyclo[2.1.1]hexan-1-yl)acrylamide (13 mg, 3% yield). LCMS (ESI+): *m/z* calcd. for C₁₉H₂₀N₆O₂ [M+H]⁺, 365.1; found, 365.1. ¹H NMR (500 MHz, methanol-*d*₄): δ (ppm) 8.44 (s, 1H), 8.12 (s, 1H), 8.01-7.87 (m, 2H), 6.77 (d, *J* = 1.8 Hz, 1H), 6.31-6.18 (m, 2H), 5.65 (dd, *J* = 7.6, 4.6 Hz, 1H), 3.96 (s, 3H), 2.47 (br s, 2H), 2.44-2.33 (m, 2H), 2.32-2.19 (m, 2H), 2.13-2.03 (m, 2H), and *N*-Methyl-*N*-(4-((6-(1-methyl-1*H*-pyrazol-4-yl)pyrazolo[1,5-*a*]pyrazin-4-yl)oxy)bicyclo[2.1.1]hexan-1-yl)acrylamide (compound **23**, 71 mg, 18% yield). HRMS (ESI+): *m/z* calcd. For C₂₀H₂₂N₆O₂ [M+H]⁺, 379.1877; found, 379.1883. ¹H NMR (500 MHz, methanol-*d*₄): δ (ppm) 8.37 (s, 1H), 8.00 (s, 1H), 7.95-7.79 (m, 2H), 6.72 (d, *J* = 1.8 Hz, 2H), 6.21 (dd, *J* = 17.1, 1.8 Hz, 1H), 5.72 (dd, *J* = 10.7, 2.1 Hz, 1H), 3.93 (s, 3H), 3.07 (br s, 3H), 2.64 (br s, 2H), 2.37-1.98 (m, 6H).

Compound 24:

N-Methyl-*N*-((1*S*,3*S*)-1-methyl-3-((6-(1-methyl-1*H*-pyrazol-4-yl)pyrazolo[1,5-*a*]pyrazin-4-yl)oxy)cyclobutyl)acrylamide

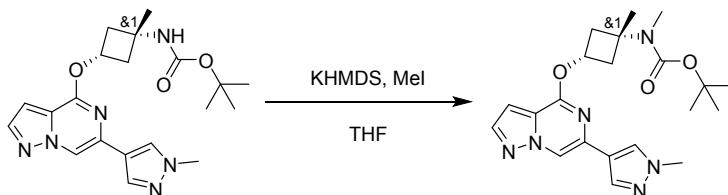


1. Synthesis of *tert*-butyl ((1*S*,3*r*)-1-methyl-3-((6-(1-methyl-1*H*-pyrazol-4-yl)pyrazolo[1,5-*a*]pyrazin-4-yl)oxy)cyclobutyl)carbamate



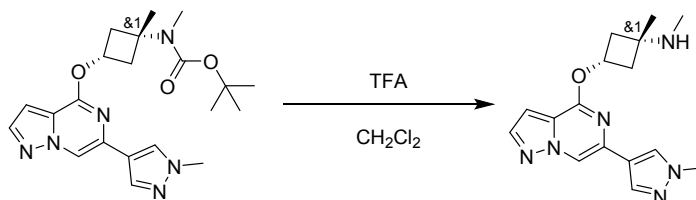
To a solution of *tert*-butyl ((1*SR*,3*r*)-3-hydroxy-1-methylcyclobutyl)carbamate (355 mg, 1.76 mmol) in THF (3 mL) was added NaOtBu (311 mg, 3.24 mmol) at 0 °C. After 10 min, 4-chloro-6-(1-methyl-1*H*-pyrazol-4-yl)pyrazolo[1,5-*a*]pyrazine (341 mg, 1.46 mmol) was added as a solid and the reaction mixture was brought to rt and stirred for 1.5 hr. EtOAc (5 mL) and sat. aq. NaHCO₃ (5 mL) were added, and the resulting biphasic mixture was extracted with EtOAc (3 x 5 mL). The combined organic phase was separated and washed with water (5 mL) and brine (5 mL), dried over Na₂SO₄, filtered, and concentrated *in vacuo*. Column chromatography (24 g SiO₂, 30-85 % EtOAc in heptane) of the resulting residue afforded *tert*-butyl ((1*SR*,3*r*)-1-methyl-3-((6-(1-methyl-1*H*-pyrazol-4-yl)pyrazolo[1,5-*a*]pyrazin-4-yl)oxy)cyclobutyl)carbamate (467 mg, 80% yield) as a white solid. LCMS (ESI+): *m/z* calcd. for C₂₀H₂₆N₆O₃ [M+H]⁺, 399.2; found, 399.2.

2. *Synthesis of tert-butyl methyl((1SR,3r)-1-methyl-3-((6-(1-methyl-1H-pyrazol-4-yl)pyrazolo[1,5-a]pyrazin-4-yl)oxy)cyclobutyl)carbamate*



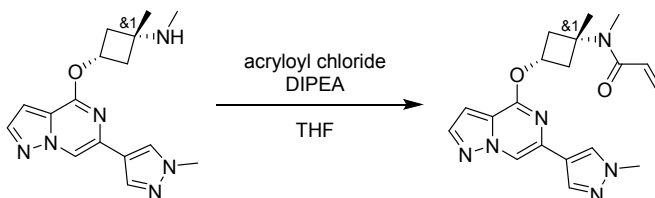
To a solution of *tert*-butyl ((1*SR*,3*r*)-1-methyl-3-((6-(1-methyl-1*H*-pyrazol-4-yl)pyrazolo[1,5-*a*]pyrazin-4-yl)oxy)cyclobutyl)carbamate (236 mg, 0.59 mmol) in THF (4 mL) was added KHMDS (1.0 M in THF, 1.8 mL) at -25 °C. After 10 min, iodomethane (80 μL, 1.29 mmol) was added dropwise and the resulting mixture was brought to rt. After 2 hr, EtOAc (5 mL) and sat. aq. NaHCO₃ (5 mL) were added, and the resulting biphasic mixture was extracted with EtOAc (3 x 5 mL). The combined organic phase was separated and washed with water (5 mL) and brine (5 mL), dried over Na₂SO₄, filtered, and concentrated *in vacuo*. The resulting residue was purified by column chromatography (24 g SiO₂, 20-70 % EtOAc in heptane) to afford *tert*-butyl methyl((1*SR*,3*r*)-1-methyl-3-((6-(1-methyl-1*H*-pyrazol-4-yl)pyrazolo[1,5-*a*]pyrazin-4-yl)oxy)cyclobutyl)carbamate (215 mg, 88% yield). LCMS (ESI+): *m/z* calcd. for C₂₁H₂₈N₆O₃ [M+H]⁺, 413.2; found, 413.2.

3. *Synthesis of (1SR,3r)-N,1-dimethyl-3-((6-(1-methyl-1H-pyrazol-4-yl)pyrazolo[1,5-a]pyrazin-4-yl)oxy)cyclobutan-1-amine*



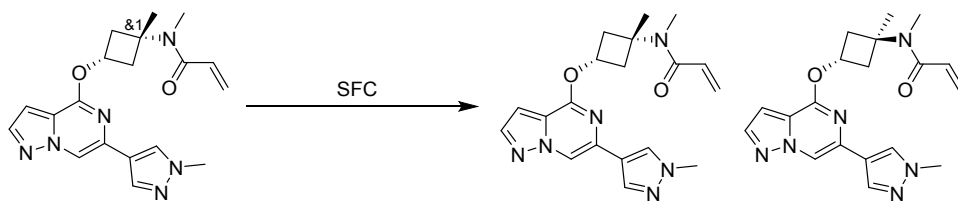
To a solution of *tert*-butyl methyl((1*SR*,3*r*)-1-methyl-3-((6-(1-methyl-1*H*-pyrazol-4-yl)pyrazolo[1,5-*a*]pyrazin-4-yl)oxy)cyclobutyl)carbamate (215 mg, 0.52 mmol) in CH₂Cl₂ (2 mL) was added TFA (350 μL, 4.60 mmol) at 0 °C. The reaction was brought to rt and stirred for 2 hr after which the volatiles were removed *in vacuo* to afford (1*SR*,3*r*)-*N*,1-dimethyl-3-((6-(1-methyl-1*H*-pyrazol-4-yl)pyrazolo[1,5-*a*]pyrazin-4-yl)oxy)cyclobutan-1-amine trifluoroacetate (221 mg, assumption 100% yield) which was used without purification in the next step. LCMS (ESI+): *m/z* calcd. for C₁₆H₂₀N₆O [M+H]⁺, 313.1; found, 313.1.

4. *Synthesis of N-methyl-N-((1SR,3r)-1-methyl-3-((6-(1-methyl-1H-pyrazol-4-yl)pyrazolo[1,5-a]pyrazin-4-yl)oxy)cyclobutyl)acrylamide*



N-Methyl-*N*-((1*SR*,3*r*)-1-methyl-3-((6-(1-methyl-1*H*-pyrazol-4-yl)pyrazolo[1,5-*a*]pyrazin-4-yl)oxy)cyclobutyl)acrylamide (124 mg, 48% yield) was synthesized analogous to the method described for compound **14** (step 3) but using *N*,1-dimethyl-3-[(6-(1-methylpyrazol-4-yl)pyrazolo[1,5-*a*]pyrazin-4-yl]oxy-cyclobutanamine trifluoroacetate (297 mg, 0.73 mmol) and THF as solvent. The crude material was purified by column chromatography (24 g SiO₂, 10-100% 3:1 EtOAc:EtOH (2% NH₄OH) in heptane). LCMS (ESI+): *m/z* calcd. for C₁₉H₂₂N₆O₂ [M+H]⁺, 367.1; found, 367.1. ¹H NMR (500MHz, dimethyl sulfoxide-*d*₆) δ (ppm) 8.76 (d, *J* = 3.7 Hz, 1H), 8.22-8.15 (m, 1H), 8.06-7.97 (m, 2H), 6.91-6.80 (m, 1H), 6.73-6.35 (m, 1H), 6.09 (br t, *J* = 14.0 Hz, 1H), 5.70-5.60 (m, 1H), 5.45-5.20 (m, 1H), 3.89 (d, *J* = 14.0 Hz, 3H), 2.98-2.79 (m, 5H), 2.49-2.22 (m, 2H), 1.57-1.38 (m, 3H).

5. *Isolation of N-methyl-N-((1s,3s)-1-methyl-3-((6-(1-methyl-1H-pyrazol-4-yl)pyrazolo[1,5-a]pyrazin-4-yl)oxy)cyclobutyl)acrylamide and N-methyl-N-((1s,3r)-1-methyl-3-((6-(1-methyl-1H-pyrazol-4-yl)pyrazolo[1,5-a]pyrazin-4-yl)oxy)cyclobutyl)acrylamide*



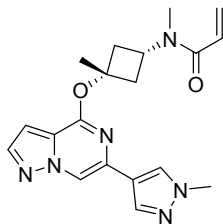
N-Methyl-*N*-((1*S*,3*r*)-1-methyl-3-((6-(1-methyl-1*H*-pyrazol-4-yl)pyrazolo[1,5-*a*]pyrazin-4-yl)oxy)cyclobutyl)acrylamide (124 mg, 0.34 mmol) was purified by chiral SFC purification (Chiralpak IA 30 x 250 mm, 5mm column using 30% MeOH in CO₂. Flow rate: 100 mL/min; ABPR 120 bar; MBPR 40 psi, column temperature 40 °C) to afford two compounds of arbitrarily assigned stereochemistry:

Peak 1: *N*-methyl-*N*-((1*s*,3*s*)-1-methyl-3-((6-(1-methyl-1*H*-pyrazol-4-yl)pyrazolo[1,5-*a*]pyrazin-4-yl)oxy)cyclobutyl)acrylamide (compound **24**, $R_f = 3.87$ min 44 mg, 34% yield, 100% *ee*) as a white solid. HRMS (ESI+): m/z calcd. for C₁₉H₂₂N₆O₂ [M+H]⁺, 367.1877; found, 367.1884. ¹H NMR (500MHz, dimethyl sulfoxide-*d*₆): δ (ppm) 8.75 (s, 1H), 8.20 (s, 1H), 8.01 (d, $J = 2.4$ Hz, 2H), 6.82 (s, 1H), 6.71-6.41 (m, 1H), 6.07 (br d, $J = 16.5$ Hz, 1H), 5.63 (dd, $J = 10.4, 2.4$ Hz, 1H), 5.32-5.19 (m, 1H), 3.91 (s, 3H), 2.96-2.79 (m, 5H), 2.53-2.51 (m, 1H), 2.36 (br d, $J = 1.8$ Hz, 1H), 1.57-1.40 (m, 3H), and

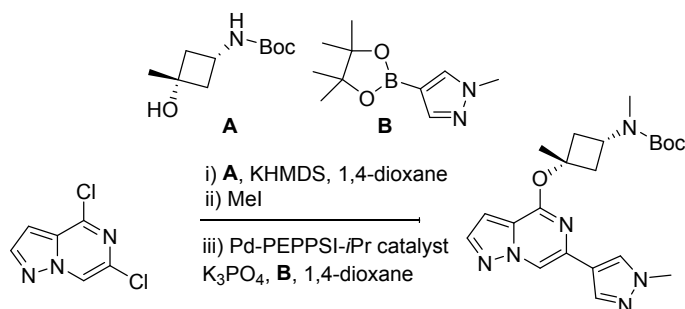
Peak 2: *N*-methyl-*N*-((1*s*,3*r*)-1-methyl-3-((6-(1-methyl-1*H*-pyrazol-4-yl)pyrazolo[1,5-*a*]pyrazin-4-yl)oxy)cyclobutyl)acrylamide as a colorless film ($R_f = 3.99$ min, 44 mg, 34% yield, 99.0% *ee*). LCMS (ESI+): m/z calcd. for C₁₉H₂₂N₆O₂ [M+H]⁺, 367.1; found, 367.1. ¹H NMR (500MHz, dimethyl sulfoxide-*d*₆): δ (ppm) 8.77 (s, 1H), 8.17 (s, 1H), 8.04 (d, $J = 2.4$ Hz, 1H), 7.99 (s, 1H), 6.89 (d, $J = 1.2$ Hz, 1H), 6.69 (br s, 1H), 6.11 (br d, $J = 16.5$ Hz, 1H), 5.65 (br d, $J = 10.4$ Hz, 1H), 5.41 (br s, 1H), 3.93-3.83 (m, 3H), 3.05-2.82 (m, 5H), 2.38-2.24 (m, 2H), 1.50 (br s, 3H).

Compound 25:

N-Methyl-*N*-((1*s*,3*s*)-3-methyl-3-((6-(1-methyl-1*H*-pyrazol-4-yl)pyrazolo[1,5-*a*]pyrazin-4-yl)oxy)cyclobutyl)acrylamide

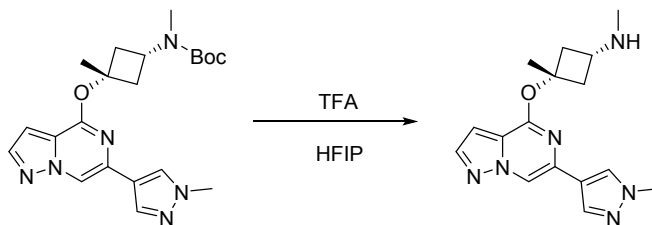


1. Synthesis of *tert*-butyl methyl((1*s*,3*s*)-3-methyl-3-((6-(1-methyl-1*H*-pyrazol-4-yl)pyrazolo[1,5-*a*]pyrazin-4-yl)oxy)cyclobutyl)carbamate



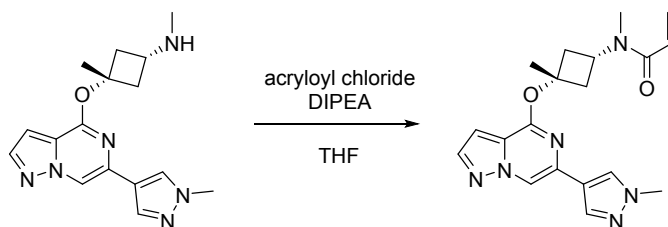
In a 100-mL one-necked round bottom flask equipped with a condenser under a N₂-atmosphere, KHMDS (1 M in THF, 2.2 mL) was added to a solution of *tert*-butyl ((1*s*,3*s*)-3-hydroxy-3-methylcyclobutyl)carbamate (150 mg, 0.75 mmol) in 1,4-dioxane (7.5 mL) at rt. After 5 min, a solution of 4,6-dichloropyrazolo[1,5-*a*]pyrazine (128 mg, 0.68 mmol) in 1,4-dioxane (2.5 mL) was added dropwise to the thick white suspension. Iodomethane (240 mg, 1.70 mmol, 105 μ L) was added to the resulting orange suspension at rt and stirring was continued for an additional 30 min. The resulting reaction mixture was degassed by purging with N₂ for 30 min, after which a degassed solution of K₃PO₄ (531 mg, 2.50 mmol) in water (2.5 mL) was added at rt. After an additional 10 min of purging of the clear orange reaction mixture with N₂, a previously degassed solution of 1-methyl-4-(4,4,5,5-tetramethyl-1,3,2-dioxaborolan-2-yl)pyrazole (212 mg, 1.02 mmol) in 1,4-dioxane (2.0 mL) was added followed by solid Pd-PEPPSI™-IPr catalyst (93 mg, 0.14 mmol). After purging of the reaction mixture with N₂ for an additional 15 min, the reaction mixture was heated at reflux for 3 hr. To the vigorously stirred reaction mixture was added EtOAc (20 mL) followed by water (20 mL). After 30 min, the organic phase was separated, and the volatiles were removed under reduced pressure. The resulting residue was purified by column chromatography (40 g SiO₂, 0-80% 3:1 EtOAc:EtOH with 2% NH₄OH modifier in heptane) to afford the title compound as a pale-yellow oil (130 mg, 47% yield). LCMS (ESI⁺): *m/z* calcd. for C₂₁H₂₈N₆O₃ [M+H]⁺, 413.2; found, 413.2. ¹H NMR (500 MHz, methanol-*d*₄): δ (ppm) 8.42 (s, 1H), 8.05 (s, 1H), 7.93 (s, 1H), 7.91 (d, *J* = 2.4 Hz, 1H), 6.77 (d, *J* = 1.2 Hz, 1H), 4.45-4.10 (m, 1H), 3.95 (s, 3H), 2.82 (s, 3H), 2.81-2.74 (m, 2H), 2.67 (br s, 2H), 1.81 (s, 3H), 1.46 (s, 9H).

2. *Synthesis of (1*s*,3*s*)-N,3-dimethyl-3-((6-(1-methyl-1*H*-pyrazol-4-yl)pyrazolo[1,5-*a*]pyrazin-4-yl)oxy)cyclobutan-1-amine*



To a solution of *tert*-butyl methyl((1*S*,3*S*)-3-methyl-3-((6-(1-methyl-1*H*-pyrazol-4-yl)pyrazolo[1,5-*a*]pyrazin-4-yl)oxy)cyclobutyl)carbamate (4.05 g, 9.82 mmol) in HFIP (45 mL) was added TFA (2.24 g, 19.60 mmol, 1.5 mL) at rt. The resulting reaction mixture was stirred overnight. EtOAc (50 mL) was added followed by a sat. aq. NaHCO₃ solution (25 mL) and brine (10 mL). After vigorous stirring for 30 min, the organic phase was separated, dried over sodium sulfate, filtered, and concentrated *in vacuo*. The resulting residue was purified by column chromatography (24 g SiO₂, 80-100% 3:1 EtOAc:EtOH with 2% NH₄OH modifier in heptane) to afford the title compound as a pale-yellow gum (2.53 g, 82% yield). LCMS (ESI+): *m/z* calcd. for C₁₆H₂₀N₆O [M+H]⁺, 313.1; found, 313.1.

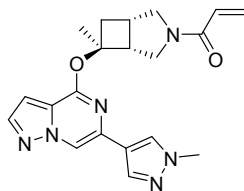
3. *Synthesis of N-methyl-N-((1*S*,3*S*)-3-methyl-3-((6-(1-methyl-1*H*-pyrazol-4-yl)pyrazolo[1,5-*a*]pyrazin-4-yl)oxy)cyclobutyl)acrylamide*



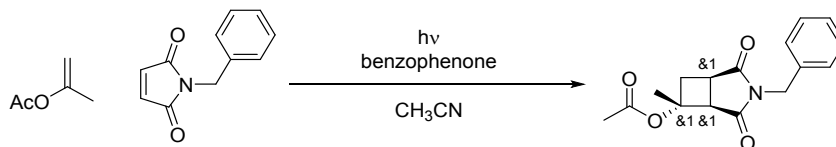
To a solution of *N*-methyl-*N*-((1*S*,3*S*)-3-methyl-3-((6-(1-methyl-1*H*-pyrazol-4-yl)pyrazolo[1,5-*a*]pyrazin-4-yl)oxy)cyclobutyl)acrylamide (4.05 g, 9.82 mmol) and DIPEA (2.8 g, 21.7 mmol, 3.8 mL) in THF (50 mL) was added acryloyl chloride (819 mg, 9.04 mmol, 740 μL) at 0 °C. After 30 min, the reaction mixture was diluted with EtOAc (50 mL) and a sat. aq. NaHCO₃ solution (50 mL) was added. The vigorously stirred biphasic mixture was brought to rt and stirring was continued for another 30 min. The organic phase was separated, washed with water (25 mL) and brine (25 mL), dried over Na₂SO₄, filtered, and concentrated *in vacuo*. The resulting residue was purified by column chromatography (80 g SiO₂, 0-100% 3:1 EtOAc:EtOH with 2% NH₄OH modifier in heptane). The colorless solid was recrystallized from EtOAc/heptane (1/3, 45 mL) to afford the title compound as a free flowing crystalline solid (1.8 g, 68% yield). Melting point = 137.5 °C. HRMS (ESI+): *m/z* calcd. for C₁₉H₂₂N₆O₂ [M+H]⁺, 367.1877; found, 367.1885. ¹H NMR (500 MHz, methanol-*d*₄): δ (ppm) 8.44 (s, 1H), 8.06 (s, 1H), 7.98-7.85 (m, 2H), 6.85-6.67 (m, 2H), 6.26-6.12 (m, 1H), 5.74 (br d, *J* = 9.2 Hz, 1H), 4.77-4.45 (m, 1H), 3.95 (s, 3H), 3.12-2.94 (m, 3H), 2.94-2.62 (m, 4H), 1.86 (s, 3H).

Compound 26:

1-((1*S*,5*R*,6*S*)-6-Methyl-6-((6-(1-methyl-1*H*-pyrazol-4-yl)pyrazolo[1,5-*a*]pyrazin-4-yl)oxy)-3-azabicyclo[3.2.0]heptan-3-yl)prop-2-en-1-one

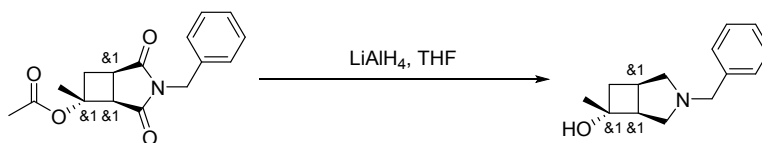


1. Synthesis of *rac*-(1*R*,5*R*,6*R*)-3-benzyl-6-methyl-2,4-dioxo-3-azabicyclo[3.2.0]heptan-6-yl acetate



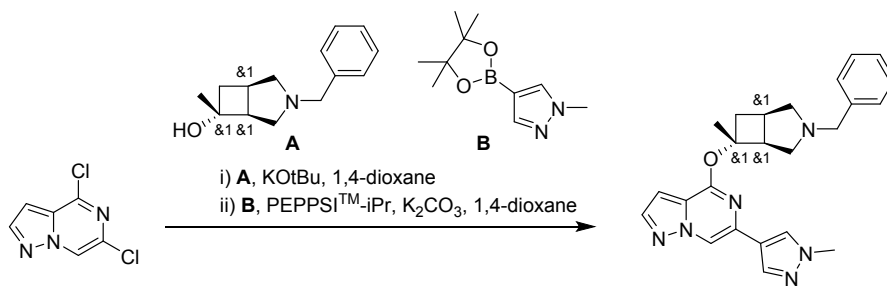
A solution of 1-benzyl-1*H*-pyrrole-2,5-dione (2.00 g, 10.68 mmol), prop-1-en-2-yl acetate (1.07 g, 10.68 mmol) and benzophenone (390 mg, 2.14 mmol) in MeCN (30 mL) was irradiated with UV light (Sylvania Ecologic F25T8/350BL RG2 25 W fluorescent lamps, $\lambda_{\text{max}} = 360$ nm) under a N_2 atmosphere at rt for 3 days. The reaction mixture was concentrated *in vacuo* and the resulting residue was purified by column chromatography (24 g SiO_2 , 0-50% EtOAc in heptane) to afford *rac*-(1*R*,5*R*,6*R*)-3-benzyl-6-methyl-2,4-dioxo-3-azabicyclo[3.2.0]heptan-6-yl acetate (2.0 g, 65% yield). LCMS (ESI⁺): *m/z* calcd. for $\text{C}_{16}\text{H}_{17}\text{NO}_4$ [M+H]⁺, 288.1; found, 288.1.

2. Synthesis of *rac*-(1*R*,5*S*,6*R*)-3-benzyl-6-methyl-3-azabicyclo[3.2.0]heptan-6-ol



To a solution of *rac*-(1*R*,5*R*,6*R*)-3-benzyl-6-methyl-2,4-dioxo-3-azabicyclo[3.2.0]heptan-6-yl acetate (200 mg, 0.70 mmol) in THF (3 mL) was added LiAlH_4 (2.0 M in THF, 1.3 mL) at 0 °C. After 30 min, the reaction mixture heated at 50 °C overnight. The reaction was cooled to 0 °C and diluted by the slow addition of water (2 mL) and 30% NaOH (1 mL). The organic phase was decanted off and the remaining emulsion was rinsed with THF (3 x 10 mL). The combined organics were concentrated *in vacuo* to give a clear oil which was purified by column chromatography (24 g SiO_2 , 0-50% 3:1 EtOAc:EtOH (2% diethylamine) in heptane) to afford *rac*-(1*R*,5*S*,6*R*)-3-benzyl-6-methyl-3-azabicyclo[3.2.0]heptan-6-ol (95 mg, 63% yield) as a clear oil. LCMS (ESI⁺): *m/z* calcd. for $\text{C}_{14}\text{H}_{19}\text{NO}$ [M+H]⁺, 218.1; found, 218.1.

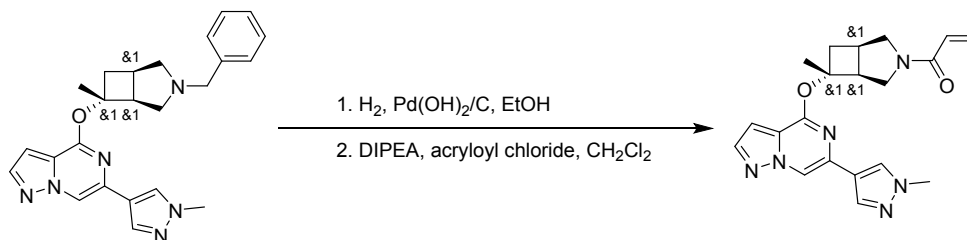
3. Synthesis of *rac*-4-(((1*R*,5*S*,6*R*)-3-benzyl-6-methyl-3-azabicyclo[3.2.0]heptan-6-yl)oxy)-6-(1-methyl-1*H*-pyrazol-4-yl)pyrazolo[1,5-*a*]pyrazine



i) To a solution of *rac*-(1*R*,5*S*,6*R*)-3-benzyl-6-methyl-3-azabicyclo[3.2.0]heptan-6-ol (95 mg, 0.44 mmol) in THF (3 mL) was added KOtBu (1 M THF, 437 μ L) at rt. After 30 min, the resulting mixture was concentrated *in vacuo*. The resulting residue was dissolved in THF (3 mL) and 4,6-dichloropyrazolo[1,5-*a*]pyrazine (85 mg, 0.45 mmol) was added. The mixture was stirred for 15 min before being concentrated *in vacuo*.

ii) A mixture of the resulting residue, 1-methyl-4-(4,4,5,5-tetramethyl-1,3,2-dioxaborolan-2-yl)pyrazole (225 mg, 1.08 mmol), K₂CO₃ (200 mg, 1.45 mmol) and PEPPSI™-Ipr (15 mg, 0.02 mmol) in 1,4-dioxane (3 mL), and water (1 mL) was degassed by purging with N₂ for 15 min followed by heating at reflux for 30 min. The reaction mixture was brought to rt and water (10 mL) was added. The phases were separated, and the aq. layer was extracted with EtOAc (3 x 10 mL). The combined organic phase was evaporated to dryness and purified by column chromatography (12 g SiO₂, 0-100% EtOAc in heptane) to afford *rac*-4-(((1*R*,5*S*,6*R*)-3-benzyl-6-methyl-3-azabicyclo[3.2.0]heptan-6-yl)oxy)-6-(1-methyl-1*H*-pyrazol-4-yl)pyrazolo[1,5-*a*]pyrazine (160 mg, 88% yield). LCMS (ESI⁺): *m/z* calcd. for C₂₄H₂₆N₆O [M+H]⁺, 415.2; found, 415.2.

4. Synthesis of *rac*-1-((1*S*,5*R*,6*S*)-6-methyl-6-((6-(1-methyl-1*H*-pyrazol-4-yl)pyrazolo[1,5-*a*]pyrazin-4-yl)oxy)-3-azabicyclo[3.2.0]heptan-3-yl)prop-2-en-1-one

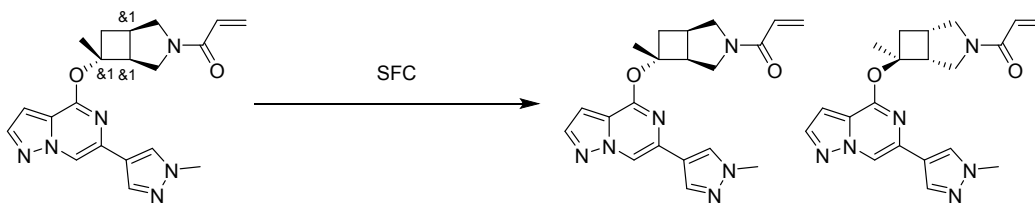


Step 1: Pd(OH)₂/C (150 mg, 0.21 mmol, 20% purity) was added to a solution of *rac*-4-(((1*R*,5*S*,6*R*)-3-benzyl-6-methyl-3-azabicyclo[3.2.0]heptan-6-yl)oxy)-6-(1-methyl-1*H*-pyrazol-4-yl)pyrazolo[1,5-*a*]pyrazine (160 mg, 0.39 mmol) in EtOH (5 mL). The mixture was purged with H₂ for 5 min and stirred under H₂-atmosphere (1atm) at rt overnight. The reaction mixture was filtered through a pad of Celite®, the pad was washed with 3:1 EtOAc:EtOH (50 mL) and the combined organic phase was concentrated *in*

vacuo. The resulting residue was purified by column chromatography (12 g SiO₂, 3:1 EtOAc:EtOH (2% diethylamine) in heptane) to afford *rac*-6-(1-methyl-1*H*-pyrazol-4-yl)-4-(((1*R*,5*S*,6*R*)-6-methyl-3-azabicyclo[3.2.0]heptan-6-yl)oxy)pyrazolo[1,5-*a*]pyrazine (40 mg, 32% yield). LCMS (ESI+): *m/z* calcd. for C₁₇H₂₀N₆O [M+H]⁺, 325.1; found, 325.1.

Step 2: To a solution of *rac*-6-(1-methyl-1*H*-pyrazol-4-yl)-4-(((1*R*,5*S*,6*R*)-6-methyl-3-azabicyclo[3.2.0]heptan-6-yl)oxy)pyrazolo[1,5-*a*]pyrazine (40 mg, 0.12 mmol) in CH₂Cl₂ (5 mL) was added DIPEA (48 mg, 0.37 mmol, 65 μL) and acryloyl chloride (11 mg, 0.12 mmol, 10 μL) at -20 °C. After 10 min, the reaction mixture was loaded onto silica and purified by chromatography (12 g SiO₂, 0-100% 3:1 EtOAc:EtOH in heptane) to afford *rac*-1-((1*S*,5*R*,6*S*)-6-methyl-6-((6-(1-methyl-1*H*-pyrazol-4-yl)pyrazolo[1,5-*a*]pyrazin-4-yl)oxy)-3-azabicyclo[3.2.0]heptan-3-yl)prop-2-en-1-one (35 mg, 75% yield) as a colorless oil. LCMS (ESI+): *m/z* calcd. for C₂₀H₂₂N₆O₂ [M+H]⁺, 379.2; found, 379.2.

5. *Isolation of 1-((1*R*,5*S*,6*R*)-6-methyl-6-((6-(1-methyl-1*H*-pyrazol-4-yl)pyrazolo[1,5-*a*]pyrazin-4-yl)oxy)-3-azabicyclo[3.2.0]heptan-3-yl)prop-2-en-1-one and 1-((1*S*,5*R*,6*S*)-6-methyl-6-((6-(1-methyl-1*H*-pyrazol-4-yl)pyrazolo[1,5-*a*]pyrazin-4-yl)oxy)-3-azabicyclo[3.2.0]heptan-3-yl)prop-2-en-1-one*



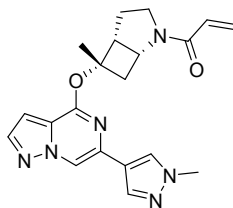
rac-1-((1*S*,5*R*,6*S*)-6-Methyl-6-((6-(1-methyl-1*H*-pyrazol-4-yl)pyrazolo[1,5-*a*]pyrazin-4-yl)oxy)-3-azabicyclo[3.2.0]heptan-3-yl)prop-2-en-1-one (35 mg) was separated by chiral SFC purification (LUX Cellulose-2 LC 30 x 250 mm, 5 μm, 40% MeOH in CO₂, flow rate: 100 mL/min, ABPR 120 bar, MBPR 40 psi, column temp 40 °C) to afford two compounds of arbitrarily assigned stereochemistry:

Peak 1: 1-((1*R*,5*S*,6*R*)-6-methyl-6-((6-(1-methyl-1*H*-pyrazol-4-yl)pyrazolo[1,5-*a*]pyrazin-4-yl)oxy)-3-azabicyclo[3.2.0]heptan-3-yl)prop-2-en-1-one (*R_f* = 3.33 min., 9 mg, 25% yield, 95.6 % *ee*), and

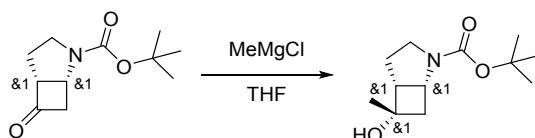
Peak 2: 1-((1*S*,5*R*,6*S*)-6-methyl-6-((6-(1-methyl-1*H*-pyrazol-4-yl)pyrazolo[1,5-*a*]pyrazin-4-yl)oxy)-3-azabicyclo[3.2.0]heptan-3-yl)prop-2-en-1-one (compound **26**, *R_f* = 3.93 min., 9 mg, 25% yield, 3.93 min, 96.0% *ee*). HRMS (ESI+): *m/z* calcd. for C₂₀H₂₂N₆O₂ [M+H]⁺, 379.1877; found, 379.1888. ¹H NMR (600 MHz, dimethyl sulfoxide-*d*₆): δ (ppm) = 8.72 (s, 1H), 8.12 (d, *J* = 8.0 Hz, 1H), 8.01 (d, *J* = 1.9 Hz, 1H), 7.98-7.90 (m, 1H), 6.87-6.76 (m, 1H), 6.70 (dd, *J* = 16.8, 10.3 Hz, 1H), 6.20 (br d, *J* = 16.8 Hz, 1H), 5.80 - 5.65 (m, 1H), 4.35 - 4.19 (m, 1H), 3.89 (s, 3H), 3.85 - 3.72 (m, 1H), 3.63 - 3.51 (m, 1H), 3.38 (br d, *J* = 8.4 Hz, 1H), 3.32 (s, 1H), 3.14-2.93 (m, 1H), 2.88-2.74 (m, 1H), 2.14-2.03 (m, 1H), 1.67-1.53 (m, 3H).

Compound 27:

1-((1*R*,5*R*,6*S*)-6-Methyl-6-((6-(1-methyl-1*H*-pyrazol-4-yl)pyrazolo[1,5-*a*]pyrazin-4-yl)oxy)-2-azabicyclo[3.2.0]heptan-2-yl)prop-2-en-1-one

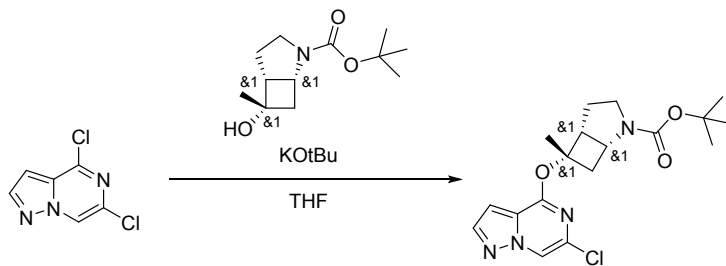


1. Synthesis of *rac*-*tert*-butyl (1*R*,5*R*,6*S*)-6-hydroxy-6-methyl-2-azabicyclo[3.2.0]heptane-2-carboxylate



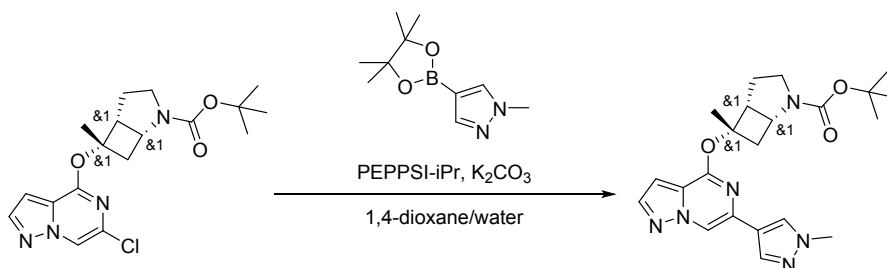
To a solution of methyl magnesium chloride (3 M in THF, 75 mL) in THF (150 mL) was slowly added a solution of *rac*-*tert*-butyl (1*R*,5*R*)-6-oxo-2-azabicyclo[3.2.0]heptane-2-carboxylate (32.5 g, 153.8 mmol) in THF (100 mL) at -78 °C over 1 hr. The reaction was allowed to warm to rt overnight. Sat. aq. NH₄Cl (50 mL) was added dropwise followed by water (400 mL) and heptane (200 mL) at 0 °C. The aqueous layer was separated and extracted with EtOAc (300 mL) and the combined organic phase was washed with brine (200 mL), dried over Na₂SO₄, filtered and concentrated *in vacuo* to afford *rac*-*tert*-butyl (1*R*,5*R*,6*S*)-6-hydroxy-6-methyl-2-azabicyclo[3.2.0]heptane-2-carboxylate (33.7 g, 96% yield). ESI-MS (M-*t*Bu+H)⁺: 172.0. ¹H NMR (500 MHz, dimethyl sulfoxide-*d*₆): δ (ppm) 4.85-4.68 (m, 1H), 3.95-3.74 (m, 1H), 3.51-3.35 (m, 2H), 2.77-2.63 (m, 1H), 2.32-2.20 (m, 1H), 2.16-2.05 (m, 1H), 1.79-1.60 (m, 2H), 1.43-1.32 (m, 9H), 1.28-1.21 (m, 3H).

2. Synthesis of *rac*-*tert*-butyl (1*R*,5*R*,6*S*)-6-((6-chloropyrazolo[1,5-*a*]pyrazin-4-yl)oxy)-6-methyl-2-azabicyclo[3.2.0]heptane-2-carboxylate



To a solution of *rac-tert*-butyl (1*R*,5*R*,6*S*)-6-hydroxy-6-methyl-2-azabicyclo[3.2.0]heptane-2-carboxylate (33.65 g, 148.00 mmol) in 1,4-dioxane (200 mL) was added KO*t*Bu (1 M in THF, 225 mL) at rt. After 30 min, the volatiles were removed, and the resulting residue was redissolved in THF (150 mL). A solution of 4,6-dichloropyrazolo[1,5-*a*]pyrazine (35 g, 186 mmol) in THF (150 mL) was added dropwise at 0 °C over 30 min. After stirring for 15 min, 4,6-dichloropyrazolo[1,5-*a*]pyrazine (8 g, 42.60 mmol) was added batchwise at rt. After 15 min, the reaction mixture was concentrated *in vacuo*, EtOAc (100 mL) and water (400 mL) were added, and the resulting biphasic mixture was extracted with EtOAc (2 x 300 mL). The combined organic phase was concentrated *in vacuo* and the resulting residue was purified by column chromatography (80 g SiO₂, 0-50% EtOAc in heptane) to afford *rac-tert*-butyl (1*R*,5*R*,6*S*)-6-(6-chloropyrazolo[1,5-*a*]pyrazin-4-yl)oxy-6-methyl-2-azabicyclo[3.2.0]heptane-2-carboxylate (57.7 g, 95% yield). LCMS (ESI+): *m/z* calcd. for C₁₈H₂₃ClN₄O₃ [M+H]⁺, 379.1; found, 379.1. ¹H NMR (500 MHz, dimethyl sulfoxide-*d*₆): δ (ppm) 8.71-8.68 (m, 1H), 8.13-8.07 (m, 1H), 6.98-6.92 (m, 1H), 4.12-3.96 (m, 1H), 3.49-3.36 (m, 2H), 3.27-3.13 (m, 1H), 2.72-2.64 (m, 1H), 2.29-2.19 (m, 1H), 2.18-2.07 (m, 1H), 1.96-1.84 (m, 1H), 1.77-1.71 (m, 3H), 1.39-1.33 (m, 9H).

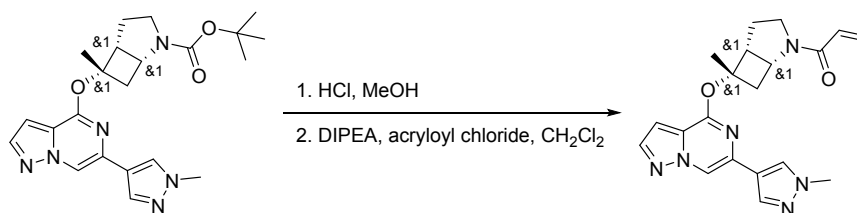
3. *Synthesis of rac-tert-butyl (1R,5R,6S)-6-methyl-6-((6-(1-methyl-1H-pyrazol-4-yl)pyrazolo[1,5-a]pyrazin-4-yl)oxy)-2-azabicyclo[3.2.0]heptane-2-carboxylate*



A mixture of *rac-tert*-butyl (1*R*,5*R*,6*S*)-6-(6-chloropyrazolo[1,5-*a*]pyrazin-4-yl)oxy-6-methyl-2-azabicyclo[3.2.0]heptane-2-carboxylate (55 g, 133.6 mmol), 1-methyl-4-(4,4,5,5-tetramethyl-1,3,2-dioxaborolan-2-yl)pyrazole (42.0 g, 201.9 mmol) and K₂CO₃ (35.0 g, 253.3 mmol) in 1,4-dioxane (300 mL) and water (100 mL) was with purged with N₂ for 30 min. PEPPSI™-IPr catalyst (500 mg, 0.73 mmol) was added as a solid, and the resulting reaction mixture was heated under N₂-atmosphere at reflux for 45 min. The mixture was brought to rt, and water (300 mL) and EtOAc (200 mL) were added. After stirring vigorously for 30 min, the layers were separated and the aq. layer was extracted with EtOAc (300 mL). The combined organic phase was concentrated *in vacuo* and the resulting residue was purified by column chromatography (80 g SiO₂, 0-25% EtOAc in heptane) to afford *rac-tert*-butyl (1*R*,5*R*,6*S*)-6-methyl-6-((6-(1-methyl-1*H*-pyrazol-4-yl)pyrazolo[1,5-*a*]pyrazin-4-yl)oxy)-2-azabicyclo[3.2.0]heptane-2-carboxylate (55.6 g, 98% yield). LCMS (ESI+): *m/z* calcd. for C₂₂H₂₈N₆O₃ [M+H]⁺, 425.2; found,

425.2. ¹H NMR (500 MHz, dimethyl sulfoxide-*d*₆): δ (ppm) 8.77-8.72 (m, 1H), 8.17-8.13 (m, 1H), 8.03-8.00 (m, 1H), 8.00-7.96 (m, 1H), 6.89-6.78 (m, 1H), 4.16-4.00 (m, 1H), 3.92-3.86 (m, 3H), 3.48-3.27 (m, 3H), 2.83-2.72 (m, 1H), 2.27-2.19 (m, 1H), 2.19-2.05 (m, 1H), 1.95-1.85 (m, 1H), 1.79 (s, 3H), 1.40-1.33 (m, 9H).

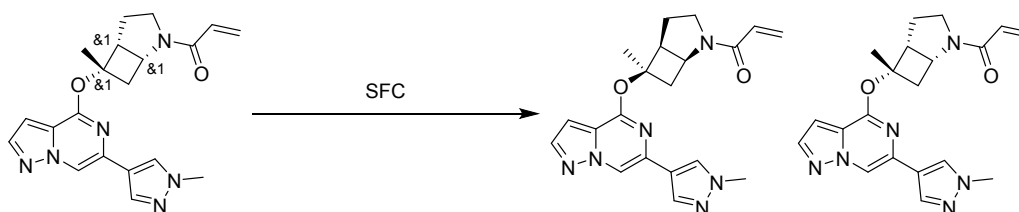
4. *Synthesis of rac-1-((1R,5R,6S)-6-methyl-6-((6-(1-methyl-1H-pyrazol-4-yl)pyrazolo[1,5-a]pyrazin-4-yl)oxy)-2-azabicyclo[3.2.0]heptan-2-yl)prop-2-en-1-one*



Step 1: To solution of *rac-tert-butyl (1R,5R,6S)-6-methyl-6-((6-(1-methyl-1H-pyrazol-4-yl)pyrazolo[1,5-a]pyrazin-4-yl)oxy)-2-azabicyclo[3.2.0]heptane-2-carboxylate* (55 g, 129.60 mmol) in MeOH (300 mL) was added 4 M HCl in 1,4-dioxane (100 mL) at 0 °C over 15 min. The reaction mixture was brought to rt and stirred for 90 min. The reaction mixture was concentrated and the resulting crude material was recrystallized from 3:1 EtOAc:EtOH (300 mL) to afford *rac-4-(((1R,5R,6S)-6-methyl-2-azabicyclo[3.2.0]heptan-6-yl)oxy)-6-(1-methylpyrazol-4-yl)pyrazolo[1,5-a]pyrazine hydrochloride* (42.5 g, 86% yield) which was used without further purification in the next step. LCMS (ESI⁺): *m/z* calcd. for C₁₇H₂₀N₆O [M+H]⁺, 325.1; found, 325.1.

Step 2: To a solution of this solid (42 g, 116.00 mmol) and DIPEA (48.2 g, 373.2 mmol, 65.0 mL) in CH₂Cl₂ (400 mL) was added acryloyl chloride (11.14 g, 123.10 mmol, 9.95 mL) at -42 °C over 15 min. After stirring for an additional 10 min, the reaction mixture was concentrated *in vacuo* to half its volume, loaded onto silica and purified by column chromatography (80 g SiO₂, 0-100% EtOAc in heptane) to give *rac-1-((1R,5R,6S)-6-methyl-6-(6-(1-methylpyrazol-4-yl)pyrazolo[1,5-a]pyrazin-4-yl)oxy)-2-azabicyclo[3.2.0]heptan-2-yl)prop-2-en-1-one* (34.2 g, 72% yield). LCMS (ESI⁺): *m/z* calcd. for C₂₀H₂₂N₆O₂ [M+H]⁺, 379.2; found, 379.2.

5. *Isolation of 1-((1R,5R,6S)-6-methyl-6-((6-(1-methyl-1H-pyrazol-4-yl)pyrazolo[1,5-a]pyrazin-4-yl)oxy)-2-azabicyclo[3.2.0]heptan-2-yl)prop-2-en-1-one and 1-((1S,5S,6R)-6-methyl-6-((6-(1-methyl-1H-pyrazol-4-yl)pyrazolo[1,5-a]pyrazin-4-yl)oxy)-2-azabicyclo[3.2.0]heptan-2-yl)prop-2-en-1-one*



rac-1-((1*R*,5*R*,6*S*)-6-Methyl-6-(6-(1-methylpyrazol-4-yl)pyrazolo[1,5-*a*]pyrazin-4-yl)oxy)-2-azabicyclo[3.2.0]heptan-2-yl)prop-2-en-1-one (34.20 g, 90.43 mmol) was resolved by chiral SFC purification ((*S,S*) Whelk O-1 [Regis Technologies] 2.1 x 25 cm, 45% EtOH with 0.25% Et₃N in CO₂, flow rate: 80 g/min, System pressure 100 bar, column temp 25 °C) to afford two compounds of arbitrarily assigned stereochemistry

Peak 1: 1-((1*R*,5*R*,6*S*)-6-methyl-6-((6-(1-methyl-1*H*-pyrazol-4-yl)pyrazolo[1,5-*a*]pyrazin-4-yl)oxy)-2-azabicyclo[3.2.0]heptan-2-yl)prop-2-en-1-one ($R_f = 2.6$ min, 14.3 g, 98.3% *ee*), and

Peak 2: 1-((1*S*,5*S*,6*R*)-6-methyl-6-((6-(1-methyl-1*H*-pyrazol-4-yl)pyrazolo[1,5-*a*]pyrazin-4-yl)oxy)-2-azabicyclo[3.2.0]heptan-2-yl)prop-2-en-1-one (compound **27**, $R_f = 2.9$ min, 10.7 g, 98.8% *ee*). HRMS (ESI⁺): *m/z* calcd. for C₂₀H₂₂N₆O₂ [M+H]⁺, 379.1877; found, 379.1886. ¹H NMR (500 MHz, dimethyl sulfoxide-*d*₆): δ (ppm) 8.75-8.72 (m, 1H), 8.18-8.11 (m, 1H), 8.02-7.99 (m, 1H), 7.99-7.95 (m, 1H), 6.85-6.79 (m, 1H), 6.59-6.44 (m, 1H), 6.16-6.05 (m, 1H), 5.70-5.59 (m, 1H), 4.43-4.31 (m, 1H), 3.89 (s, 3H), 3.78-3.61 (m, 1H), 3.56-3.43 (m, 1H), 3.37-3.28 (m, 1H), 2.97-2.82 (m, 1H), 2.35-2.08 (m, 2H), 2.06-1.89 (m, 1H), 1.84-1.79 (m, 3H).

Assays

BTK Biochemical Activity Assay (BTK IC₅₀)

BTK kinase activity and inhibitor efficacy were assessed by monitoring the degree of phosphorylation of a fluorescein-labeled polyGAT peptide substrate (Invitrogen PV3611). This was done in the presence of active BTK enzyme (Upstate 14-552), ATP, and the compound of interest. For a standard assay, 24 μL of an ATP/peptide master mix (final concentration; ATP 10 μM , polyGAT 100 nM) in kinase buffer (10 mM Tris-HCl, pH 7.5, 10 mM MgCl₂, 200 μM Na₃PO₄, 5 mM DTT, 0.01% Triton X-100, and 0.2 mg/mL casein) was aliquoted into each well of a black 96-well plate (Costar 3694). Subsequently, we added 1 μL of a 4-fold, 40 \times compound titration in 100% DMSO and 15 μL of the BTK enzyme mix in 1 \times kinase buffer, resulting in a final BTK enzyme concentration of 0.25 nM. After 30 min, the reaction was quenched with 28 μL of 50 mM EDTA. Following this, 5 μL aliquots of the reaction mixture were transferred to a low volume, white 384-well plate (Corning 3674), and 5 μL of a 2 \times detection buffer (Invitrogen PV3574, with 4 nM Tb-PY20 antibody, Invitrogen PV3552) was added before a 45 min incubation at room temperature in the dark for time-resolved fluorescence (TRF) measurement on a Molecular Devices M5 (332 nm excitation; 488 nm emission; 518 nm fluorescein emission) instrument. To calculate IC₅₀ values, a four-parameter fit was applied, with 100% enzyme activity determined from the DMSO control and 0% activity from the EDTA control.

Continuous-read Kinetic Enzyme Assay (log k_{inact}/K_i)

To precisely assess the biochemical effectiveness of the inhibitors, we calculated the ratio of their inactivation rate constant to their equilibrium inhibition constant (k_{inact}/K_i) using continuous-read kinetic enzyme assays. The k_{inact}/K_i ratio represents the second-order rate constant that reflects the overall efficiency of covalent bond formation resulting from the initial reversible binding affinity (K_i) and the maximal inactivation rate (k_{inact}). In each assay reaction mixture, we included full-length recombinant BTK at a concentration of 5 nM, various concentrations of the inhibitors, and substrates such as ATP (1 mM) and SOX-peptide (AQT0101, AssayQuant Technologies) maintained at a concentration below its K_m . Phosphorylation of the SOX-peptide substrate by BTK was continuously monitored by chelation enhanced fluorescence. The k_{inact}/K_i ratios were determined by globally fitting full progress curves from reactions containing several different BIIB129 concentrations using the software package DynaFit.

CD69 Whole Blood Assay

Concentrations of the compound were incrementally added to heparinized venous blood obtained from healthy donors, ensuring that the final concentration of dimethyl sulfoxide (DMSO) in all samples reached 0.1%. The cells were then incubated at 37 °C for 60 min. Subsequently, the drug-treated samples and positive control samples (treated with DMSO) were stimulated using either 0.1 µg/mL mouse anti-human IgD-dextran (1A62) or 20 µg/mL polyclonal rabbit F(ab')₂ anti-human IgD. In contrast, the negative control unstimulated sample received phosphate-buffered saline (PBS). Following this, the plate was incubated overnight (for 18 to 22 hr) at 37 °C. The cells were stained with fluorochrome-conjugated anti-CD19 and anti-CD69 antibodies. To eliminate red blood cells and fix the remaining cells, a lyse/fix solution was employed through hypotonic lysis. The fixed cells were then subjected to flow cytometry analysis. Specifically, CD19⁺ B cells were gated and examined for CD69 expression. The percentage of B cells expressing CD69 relative to the DMSO control was plotted against the logarithm (base 10) of the inhibitor concentrations. The resulting data was fitted to a 4-parameter logistic curve model to ascertain the IC₅₀ value, as illustrated in a representative experiment.

Immortalized TMD8 Cell Assay

TMD8 B cells were treated with titrating concentrations of inhibitors so that the final concentration of dimethyl sulfoxide (DMSO) was 0.1% and incubated for 72 hr or 35 hr at 37°C. ATP levels were measured as an indirect quantification of cell numbers using the CellTiter-Glo® Luminescent Cell Viability Assay. The luminescence signal was plotted versus the log₁₀ of the concentration of inhibitors and the data was fit to the 4-parameter logistic curve model to determine the IC₅₀ value as shown in one representative experiment. 1e⁵ TMD8 cells were pulsed with 110 µM EdU and incubated for 2 hr prior to staining for flow cytometry. Cells were stained with fluorochrome-conjugated anti-CD36 and anti-CD19 antibodies, fixed, and analyzed by flow cytometry for expression of cell surface markers. EdU⁺ TMD8 cells were quantified by using the Click-It Plus EdU Flow Cytometry Assay Kit. TMD8 B cells were gated and analyzed for the inhibition of CD36 and CD19 expression, and frequency of EdU⁺ cells. The percentage of EdU⁺ TMD8 cells (normalized against DMSO control) and the percent inhibition of CD19 and CD36 surface cell marker geometric MFI (normalized against DMSO control) were plotted versus the log₁₀ of the inhibitor concentration. The best-fit curve (variable Hill slope) was generated to obtain the IC₅₀ values as shown in one representative experiment.

Protein Crystallography

Protein expression, purification, crystallography, and structure solution were performed as previously published (45) with additional refinement in Phenix. (46) Crystals were generated, diffraction data was collected and processed, and models were built and refined as described previously.^{1,2} Briefly, the kinase domain of human BTK 372–659 at 5 mg/mL was incubated with each compound to a final concentration of 0.5 mM at 4 °C overnight. The complex was crystallized in 0.1 M BisTRIS pH 6.5, 0.2 M ammonium acetate, 0.1 M guanidine HCl, and 20% PEG2200 MME in sitting drops at 4 °C over 3–5 days. The crystals were cryoprotected in 0.1 M BisTRIS pH 6.5, 0.2 M ammonium acetate, 0.1 M guanidine HCl, 20% PEG2200 MME, and 10% PEG200, and diffraction data were collected at SLS beamline X06SA. The structure was solved using molecular replacement in Phenix followed by multiple rounds of refinement in Phenix and model building in Coot. Crystal structure information for BTK bound to **10**, **25** or **27** has been deposited in the RCSB PDB with accession codes 8TU3, 8TU4 and 8TU5, respectively, with data and model coordinates available upon publication.

Table S1. Data collection and refinement statistics

	<i>10</i>	<i>25</i>	<i>27</i>
Accession Code	8TU3	8TU4	8TU5
Data collection^a			
Space group	P2 ₁ 2 ₁ 2	P2 ₁ 2 ₁ 2	P2 ₁ 2 ₁ 2
Cell dimensions			
<i>a</i> , <i>b</i> , <i>c</i> (Å)	70.43, 104.61, 38.08	70.17, 104.69, 37.96	64.78, 102.04, 38.28
α , β , γ (°)	90, 90, 90	90, 90, 90	90, 90, 90
Resolution (Å)	50-1.7 (1.8-1.7)	50-1.6 (1.7-1.6)	50-2.1 (2.23-2.1)
R_{merge}^b	0.175 (2.007)	0.118 (1.154)	0.167 (1.30)
$I / \sigma I^c$	8.19 (0.91)	6.48 (1.07)	5.15 (1.06)
Completeness (%)	99.9 (99.8)	97.6 (96.2)	99.1 (99.0)
Redundancy	6.45 (6.27)	2.81 (2.43)	3.15 (3.17)
Refinement			
Resolution (Å)	35.78-1.7 (1.761-1.7)	41.96-1.6 (1.657-1.6)	38.28-2.1 (2.175-2.1)
No. reflections	31752 (3121)	37555 (3678)	15364 (1488)
Used in R_{free}	1589 (156)	1878 (184)	770 (75)
$R_{\text{work}} / R_{\text{free}}^d$	0.2277/0.2769	0.2205/0.2592	0.2585/0.2727
No. atoms			
Protein	2084	2093	1979
Ligand/ion	27	27	28
Water	79	90	35
<i>B</i> -factors			
Protein	27.46	25.41	39.98
Ligand/ion	29.16	25.14	35.72
Water	26.61	26.82	37.09
r.m.s. deviations			
Bond lengths (Å)	0.274	0.217	0.229
Bond angles (°)	4.72	3.74	4.95
Ramachandran plot (%) ^e			
Favored regions	98.02	97.62	98.02
Allowed regions	1.98	2.38	1.98
Outliers	0.00	0.00	0.00

^a Values in parentheses are for highest-resolution shell.

^b Percent difference among intensities of equivalent reflections.

^c Ratio of reflection intensity to estimated error, averaged.

^d R_{work} and R_{free} are defined as $\frac{\sum ||F_{\text{obs}}| - |F_{\text{calc}}||}{\sum |F_{\text{obs}}|}$ for the reflections in the working and the test set, respectively, where F_{obs} refers to experimental reflection amplitudes and F_{calc} refers to amplitudes calculated from the model.

^e As determined using MolProbity (molprobity.biochem.duke.edu)³

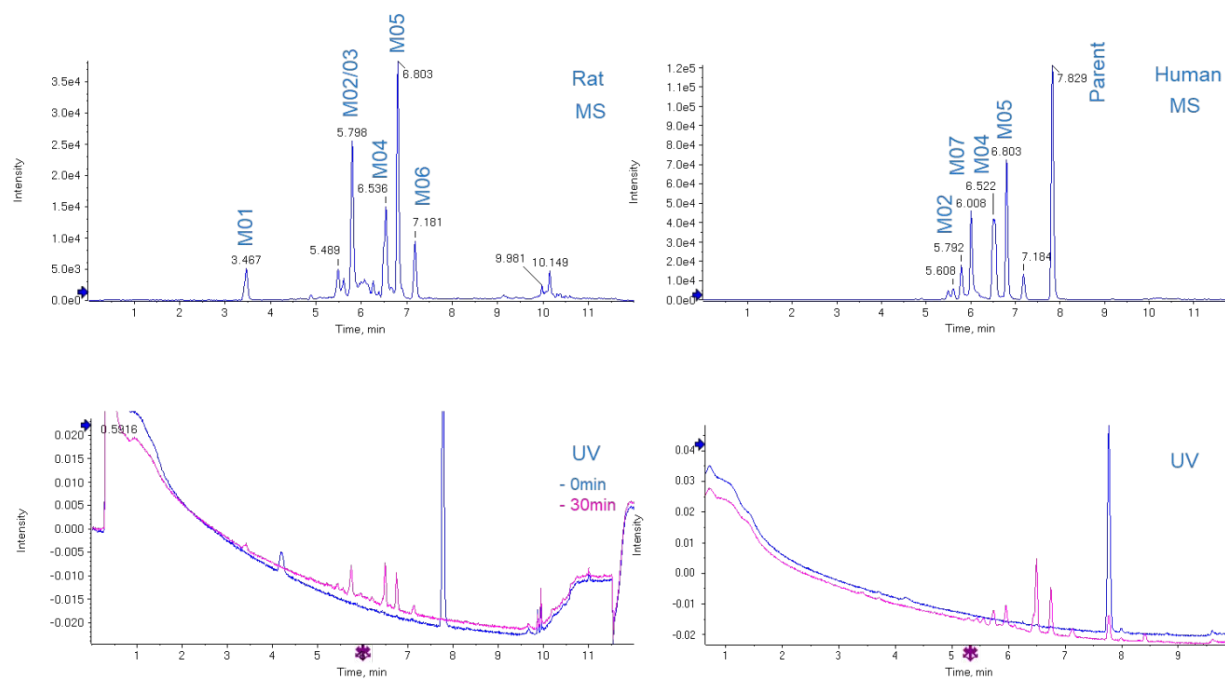
Metabolite ID of compound 10

***In vitro* metabolism of compound 10 in rat and human liver microsomes.**

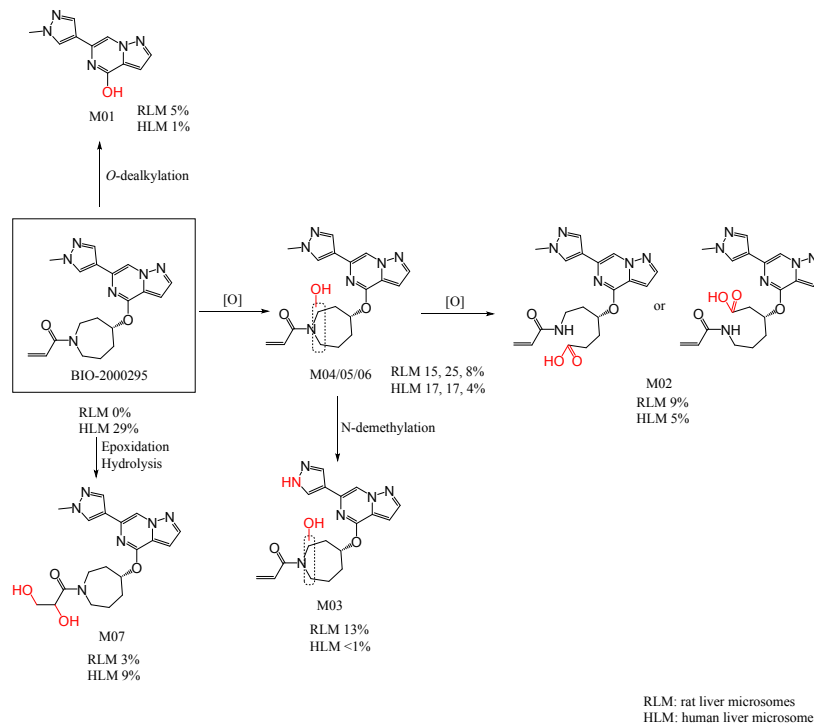
Methods

- Drug concentration: 10 μ M
- Human (mix gender, Pool 200) and rat (male, SD, pooled) liver microsomes (Xenotech); 1 mg/mL protein
- Potassium phosphate buffer 100 mM pH 7.4, Magnesium chloride 5 mM
- NADPH, 2 mM
- Incubation time for the data shown: 30 min @ 37°C
- Incubation volume: 1,200 μ L (300 μ L aliquots removed at T = 0, 30 and 60 minutes)
- Reaction stopped using 300 μ L ice cold acetonitrile, centrifuged for 10 min @ 3220 g and 100 μ L of supernatant was transferred and 10 μ L was injected for LC-MSMS analysis.
- Samples analyzed on Sciex API6600 TripleTOF
- Data analyzed using Peak View and Metabolite Pilot

Figure S 1. LC-HRMS extracted ion chromatogram and UV (300 nm) chromatogram of cpd 10 and its major metabolites (>5% drug-related LC-MS peak areas) following 30 min *in vitro* incubation in rat and human liver microsomes



Scheme S1. Proposed major metabolic pathways of compound **10** following 30 min *in vitro* incubation in rat and human liver microsomes.



***In-vitro* metabolism of compound 10 in rat, dog, monkey and human hepatocytes.**

Methods

- drug concentration: 10 μM
- Hepatocytes (Xenotech); 1×10^6 cells/mL; viability 70.2% (rat), 71.0% (dog), 75.3% (monkey) and 64.0% (human)
- DMEM (1x) –Dulbecco's Modified Eagle Medium
- Incubation time for the data shown: 2 hr @ 37°C, 5% CO₂
- Incubation volume: 300 μL /time point (time points taken 0, 0.5, 1, 2, and 4 hr)
- Reaction stopped using 300 μL ice cold acetonitrile, centrifuged for 10 min @ 3220g and 100 μL of supernatant was transferred and 10 μL was injected for LC-MSMS analysis.
- Samples analyzed on Sciex API6600 TripleTOF
- Data analyzed using Peak View and Metabolite Pilot

Table S2. Percent of LC-MS peak areas of compound 10 and its metabolites following 2 hrs *in vitro* incubation in rat, dog, monkey and human hepatocytes, respectively

Peak ID	Rat	Dog	Monkey	Human
M01	7.5	<2	<2	<2
M02	5.5	<2	<2	<2
M03	5.4	12	<2	ND
M04	4.8	ND	ND	ND
M05	13.8	<2	<2	<2
M06	5.2	ND	<2	ND
M07	2.5	<2	<2	ND
M08	17.9	25.2	16	19.5
M09	8.9	2.2	<2	<2
M10	5.7	12.5	11.7	2
M11	6.6	<2	2	<2
M12	ND	<2	ND	ND
M13	<2	2.2	24.1	23.5
M14	<2	4.7	ND	ND
M15	<2	<2	2.6	2.5
M16	ND	ND	<2	ND
M17	ND	<2	2.1	<2
M18	ND	<2	7.6	<2
M19	ND	<2	2.2	<2
M20	<2	<2	2.3	7
M21	<2	<2	<2	2.1
Parent	0	1.4	0	4.9

Color codes:

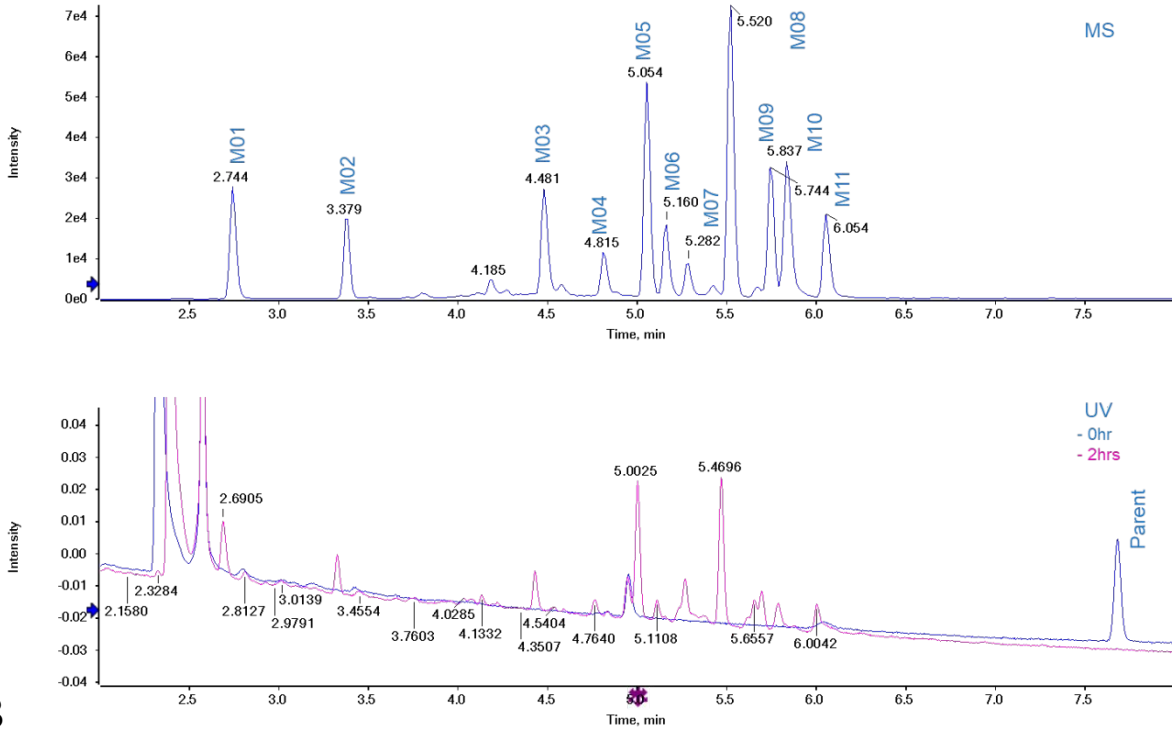
Azepane as metabolism site, incl. mix of N-des-methyl

Acrylamide as metabolism site

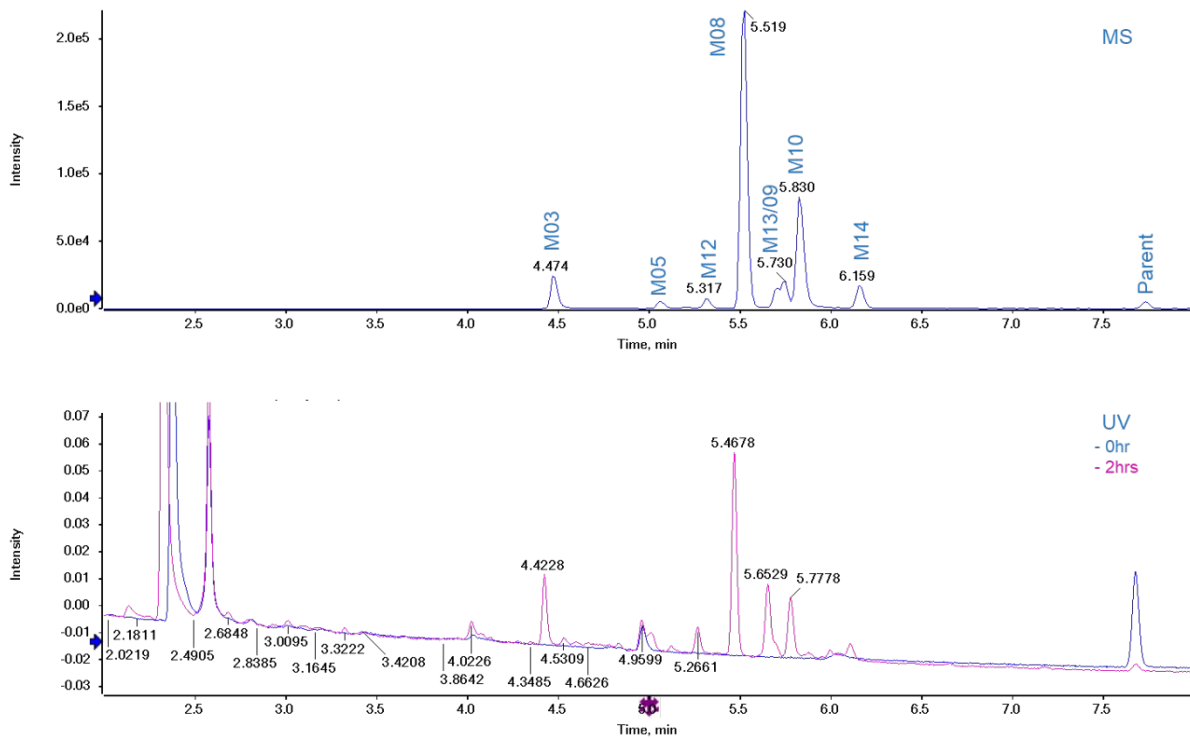
Mix of azepane and acrylamide sites

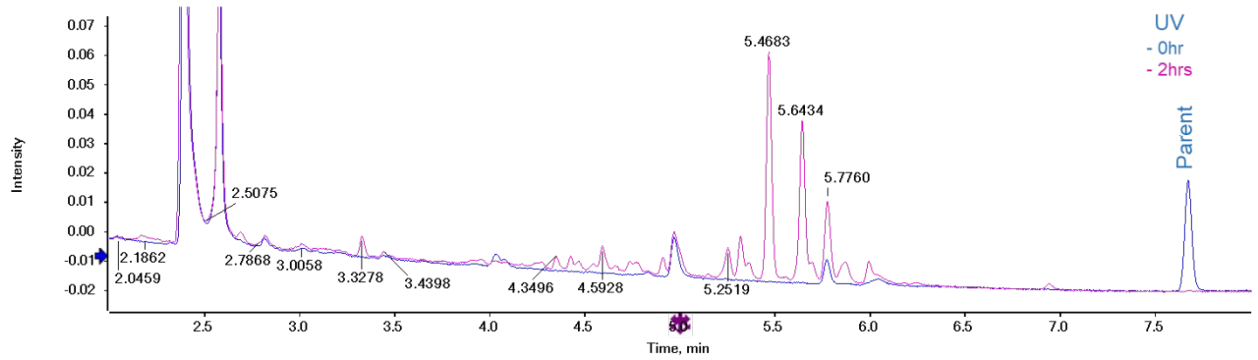
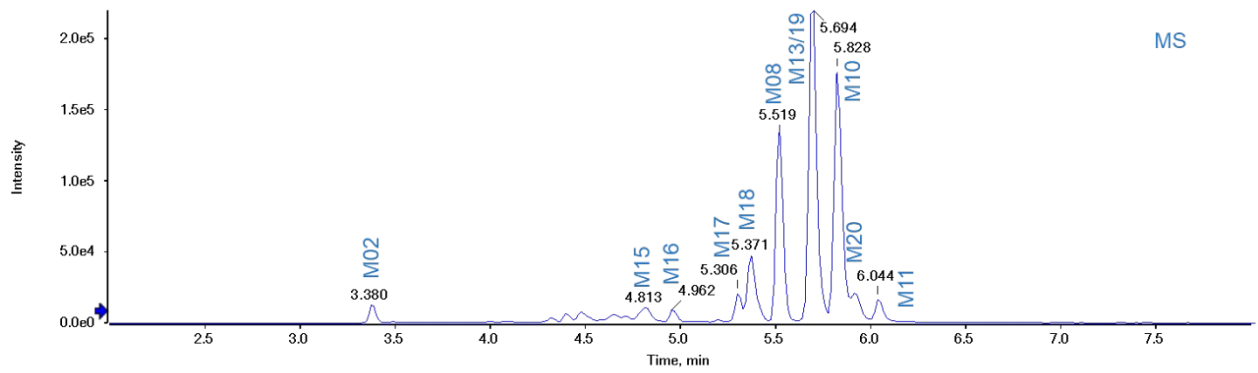
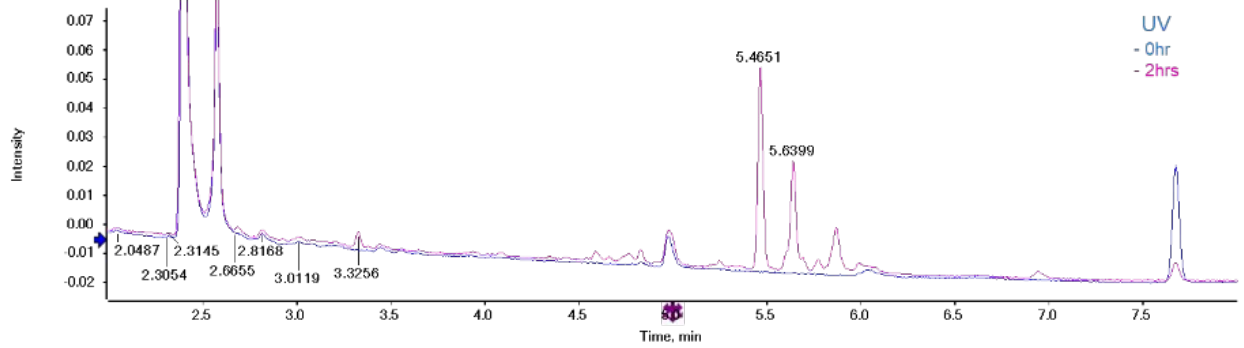
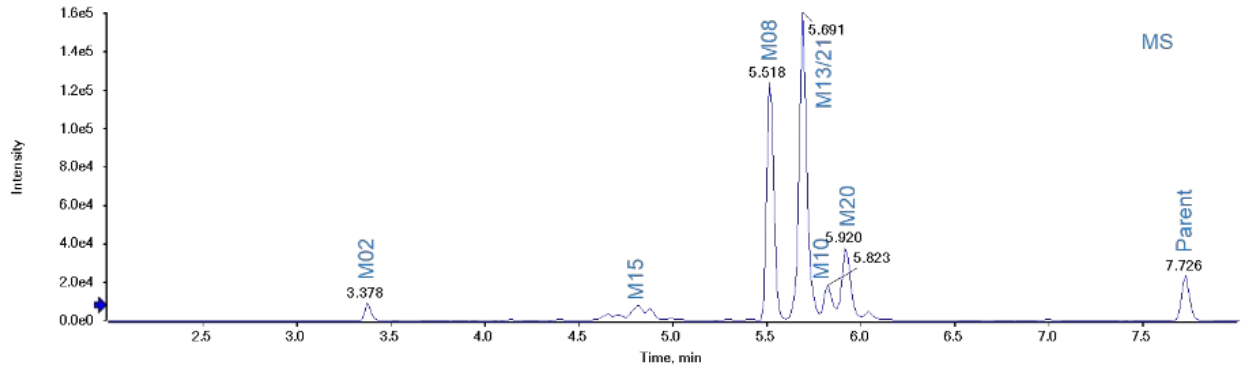
Figure S2. LC-HRMS extracted ion chromatogram and UV (300 nm) chromatogram of compound **10** and its major metabolites (>2% drug-related LC-MS peak areas) following 2 hr *in vitro* incubation in rat (A), dog (B), monkey (C) and human (D) hepatocytes.

A

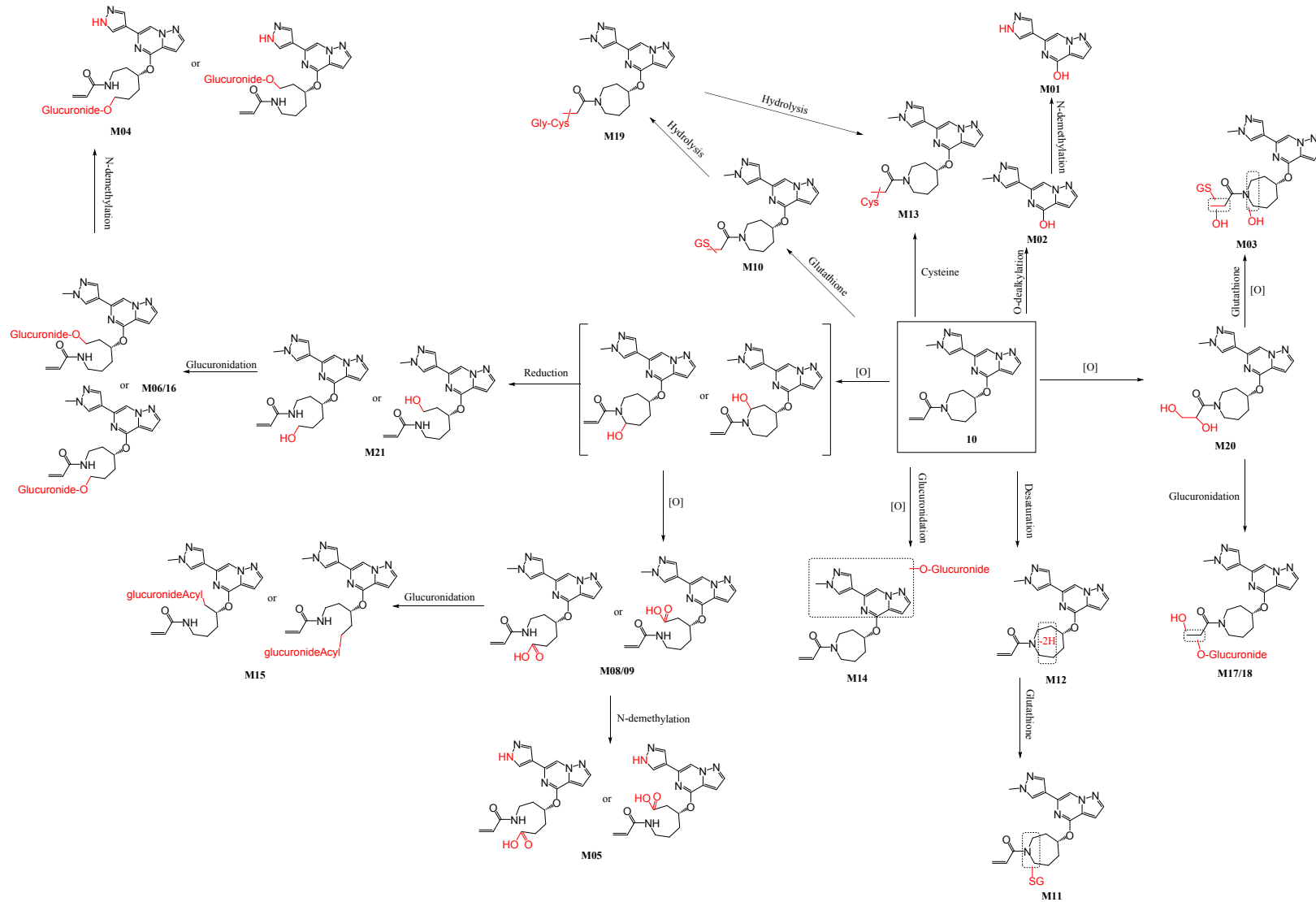


B



C**D**

Scheme S2. Proposed metabolic pathways of cpd **10** following 2 hr *in vitro* incubation in rat, dog, monkey and human hepatocytes.

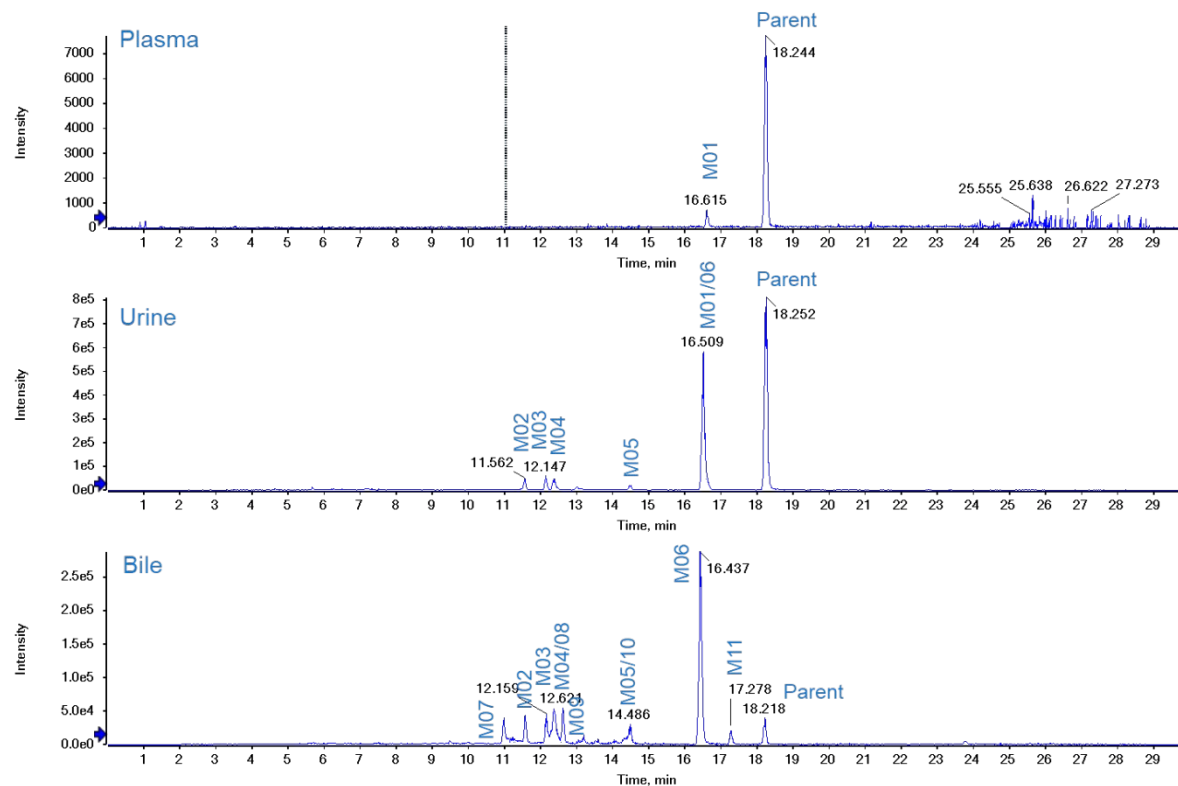


***In-vivo* metabolism of compound 10 in rat plasma, urine and bile.**

Methods

- The boxes contain rat plasma, urine and bile (n = 3) for each time point were kept in the freezer at -80 °C.
- Prior to extraction, samples were thawed at room temperature no longer than 1 hr.
- Urine or bile samples collected from the bile duct cannulated (BDC) rats were pooled proportionally to original sample collection weights of individual time intervals, resulting in one pooled urine or bile sample representing the accumulative excretion over 24 hr postdose.
- Plasma samples collected from the rats were pooled based on Hamilton method^{4,5}, resulting in one pooled plasma sample representing the average concentration of area under the curve from 0 to 24 hr postdose.
- 5 x volume CH₃CN/MeOH was added into 100 μL of pooled sample for protein precipitation.
- Crashed samples were centrifuged at 13,000rpm for 10 min. The resulting supernatant was dried down under nitrogen gas at ambient temperature until around 90 μL.
- 10 μL of CH₃CN was added into concentrated samples and sonicated to get clear solution.
- Samples were injected on the 5600 QTOF and data was analyzed using Peak View and Metabolite Pilot.

Figure S3. LC-HRMS extracted chromatogram of compound **10** and its major metabolites (>1% drug-related LC-MS peak areas) in pooled rat plasma, urine and bile over 24 hr post an IV dose.



Scheme S3. Proposed metabolic pathways of compound **10** in rat plasma, urine, and bile following an IV dose.

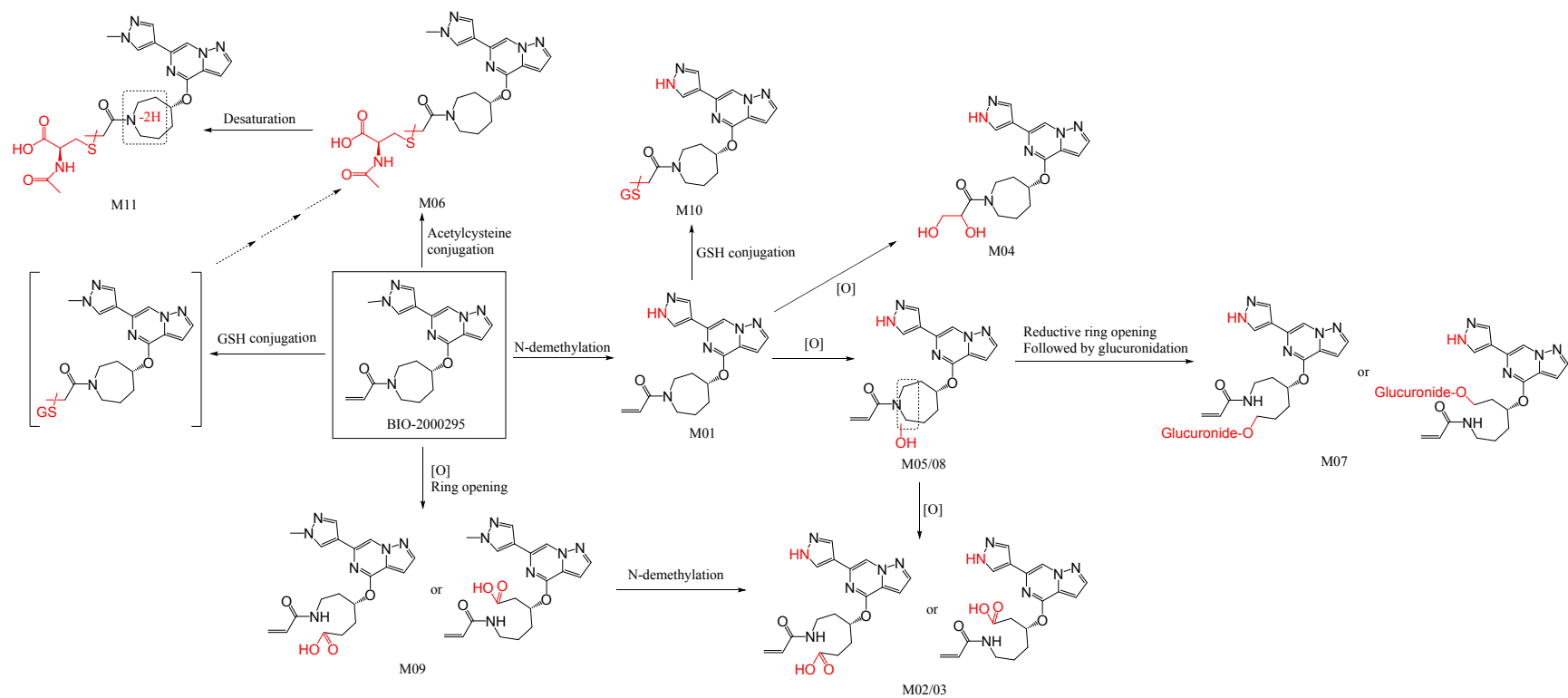


Table S3. Percent of LC-MS peak areas of compounds 10 and *in vivo* metabolites in rat urine and bile over 24 hr post an IV dose.

Peak ID	Urine	Bile
M01	1.7%	<1%
M02	2.3%	4.8%
M03	2.8%	4.4%
M04	3.2%	5.4%
M05	1.3%	4.4%
M06	34.0%	42.4%
M07	<1%	4.1%
M08	ND	8.3%
M09	<1%	5.2%
M10	ND	1.1%
M11	ND	2.5%
Parent	49.7%	4.6%

Color codes:

Azepane as metabolism site, , incl. mix of N-des-methyl

Acrylamide as metabolism site

Mix of azepane and acrylamide sites

Metabolism of BIIB129 (25)

Cross-Species *In Vitro* Metabolic Stability in Liver Microsomes and Hepatocytes

In vitro metabolic stability of BIIB129 (25) was assessed in liver microsomes and hepatocytes of 4 species (rat, dog, monkey, and human), and the *in vitro* metabolites were identified in hepatocytes of 5 species (mouse, rat, dog, monkey, and human). The results are summarized in the following sections.

The calculated *in vitro* CL_{int} values of BIIB129 (25) were determined from *in vitro* metabolic stability assays using pooled microsomes or hepatocytes from rat, beagle dog, cynomolgus monkey, or human liver. Incubations in liver microsomes (0.5 mg/mL) and hepatocytes (1 million cells/mL) were performed at a BIIB129 concentration of 1 μ M. The CL_{int} and the calculated *in vivo* CL_h corrected for $f_{u,p}$ and $f_{u,mics}$ are summarized in **Table S4**. BIIB129 had moderate to high cross-species *in vitro* CL_{int} . Calculated hepatic clearance generally under-predicted *in vivo* plasma clearance by 4 to 8-fold also shown in **Table S4**

Table S4. Intrinsic Clearance and Calculated Hepatic Clearance of BIIB129 in Rat, Dog, Monkey, and Human Liver Microsomes and Hepatocytes

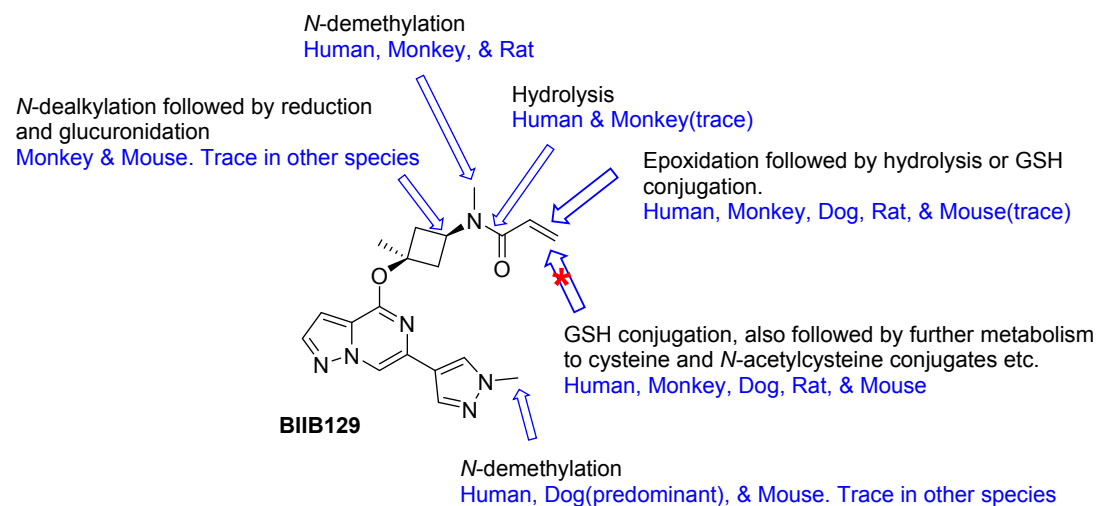
Species	Liver Microsomes		Hepatocytes		In vivo		
	CL_{int} (mL/min/kg)	Predicted in vivo CL_h (mL/min/kg)	CL_{int} (mL/min/kg)	Predicted in vivo CL_h (mL/min/kg)	Observed CL (mL/min/kg)	Fold under- prediction (microso- mes)	Fold under- prediction (hepatocy- tes)
Rat	112 \pm 3	12.3	91.8 \pm 1.9	9.7	87	7.1	8.9
Dog	77.3 \pm 1.4	7.4	188.1 \pm 6.1	12.1	74.2	10	6.1
Monkey	174 \pm 3	16.4	99.5 \pm 4.9	10.2	54-68	3.3-4.1	5.3-6.7
Human	36.4 \pm 1.7	3.8	25.8 \pm 1.3	2.8	NA	NA	NA

$Q_h = 55, 31, 44$ and 20 mL/min/kg for rat, dog, monkey and human, respectively, were used in the calculation for this table.

Metabolic Profile of BIIB129 (25) in Vitro:

The *in vitro* metabolism of BIIB129 (25) was investigated in human, monkey, dog, rat, and mouse hepatocytes. Following a 4-hr incubation with 10 μ M initial concentration, BIIB129 was extensively metabolized in mouse, rat, dog, and monkey hepatocytes, and relatively stable in human hepatocytes. Metabolites were detected and identified using LC-HRMS and MS/MS. The sites of drug metabolism of BIIB129 in hepatocytes across species are summarized in **Figure S4**. The *in vitro* biotransformation scheme proposed for a total of 16 metabolites identified in hepatocytes across species can be found in **Scheme S5**. Many metabolites shown in the biotransformation scheme have undergone sequential metabolic steps involving more than 1 site of drug metabolism, as summarized in **Figure S4**. No unique human metabolite was observed in hepatocytes. The most prominent site of *in vitro* metabolism observed across species was the acrylamide warhead, e.g., presumably epoxidation followed by hydrolysis of the epoxide to form a diol metabolite M03, or the direct glutathione conjugate M02 and its subsequent metabolites. Other sites of metabolism include *N*-dealkylation, including two *N*-demethylation metabolites M8 and M10. Overall, the hepatocyte metabolite profiles of BIIB129 in the rat and monkey resemble the human profile more closely than the profiles for the mouse and dog, supporting the selection of rat and monkey as nonclinical toxicology species.

Figure S4. Sites of BIIB129 (25) Drug Metabolism in Human, Monkey, Dog, Rat, and Mouse Hepatocytes



* This pathway also occurs extrahepatically, e.g., in whole blood *in vitro*

Note: GSH conjugation of the acrylamide warhead also occurs extrahepatically. This was confirmed by the *in vitro* formation of GSH, Cys-Gly, and Cys conjugates of BIIB129 in human and monkey whole blood after an incubation at 37°C.

Scheme S4. Proposed metabolic pathways (> 1% drug-related LC-MS peak area) of BIIB129 (**25**) following a 4-hr incubation in human, monkey, dog, rat, and mouse hepatocytes.

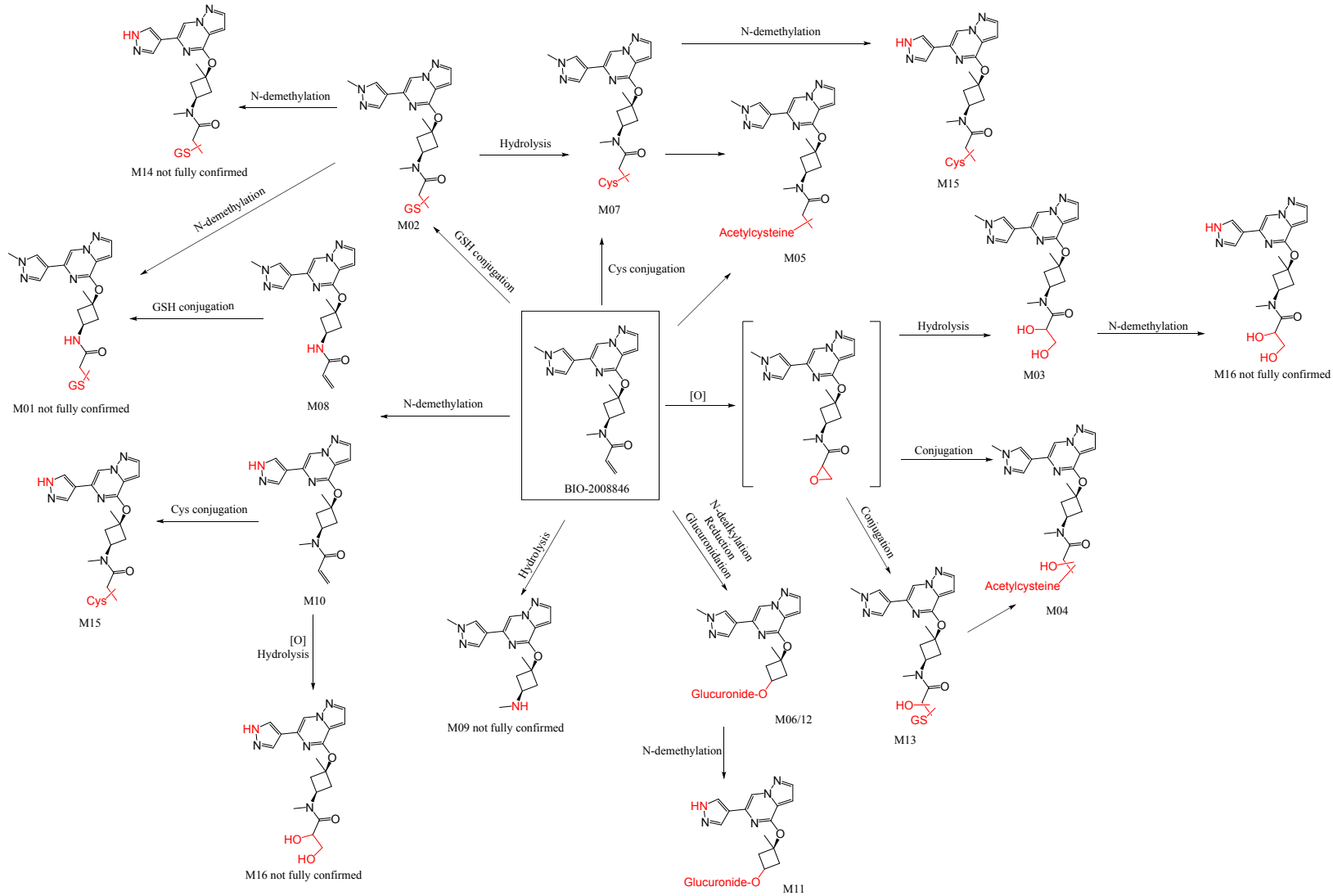


Table S5. Drug-related LC-MS areas (%) of BIIB129 and metabolites following 4-hr incubation in human, monkey, dog, rat, and mouse hepatocytes, respectively.

Peak ID	Human	Monkey	Dog	Rat	Mouse
M01	ND	<1	ND	3.7	ND
M02	<1	7.9	30.6	42.3	88.1
M03	9.1	7.6	3.1	9.4	<1
M04	<1	<1	ND	6.9	ND
M05	<1	4.2	<1	33.8	ND
M06	<1	4	ND	<1	2.3
M07	5.3	39.5	3.1	<1	ND
M08	1.6	8.8	ND	<1	ND
M09	1.4	<1	ND	ND	ND
M10	2.5	<1	34.2	<1	ND
M11	<1	<1	ND	<1	2.1
M12	<1	<1	<1	<1	1.3
M13	ND	<1	2.4	<1	<1
M14	ND	<1	21.9	<1	<1
M15	<1	<1	21.5	<1	ND
M16	<1	<1	10	<1	ND
Parent	80.2	16.6	0	3.9	0

Note: LC-MS peak area (%) may not be proportional to relative level of individual metabolites, since MS signal response can vary among metabolites, sometimes significantly

Color codes:

Acrylamide as the only site of metabolism

N-des-methyl active metabolites

In-vivo metabolism of BIIB129 (25) in rat plasma, urine and bile

Metabolite profiling and identification of Wistar rat plasma, bile, and urine was conducted after administration of a single oral dose of BIIB129 (30 mg/kg) to BDC rats. Rat plasma samples were pooled using the Hamilton method. Bile or bile samples were pooled proportionally to the original sample collection weights of individual time intervals. Two pooled samples were obtained for each of three samples matrices, representing 0-5 hr and 5-24 hr post-dose. In pooled plasma, BIIB129 was identified and accounted for around 60% of the total drug-related LC-MS peak area. In pooled 0-5 hr bile, BIIB129 accounted for 3% of the total drug-related peak area. In pooled 0-5 hr urine, BIIB129 was not detected. Major metabolites (> 10% drug-related peak area) of BIIB129 include direct glutathione conjugation and downstream products (M02, M05), oxidation followed by glutathione conjugation and downstream products (M13, M21, M23), and oxidation followed by hydrolysis (M03).

Scheme S5. Proposed biotransformation scheme of BIIB129 (25) observed in rat plasma, bile and urine following an oral dose

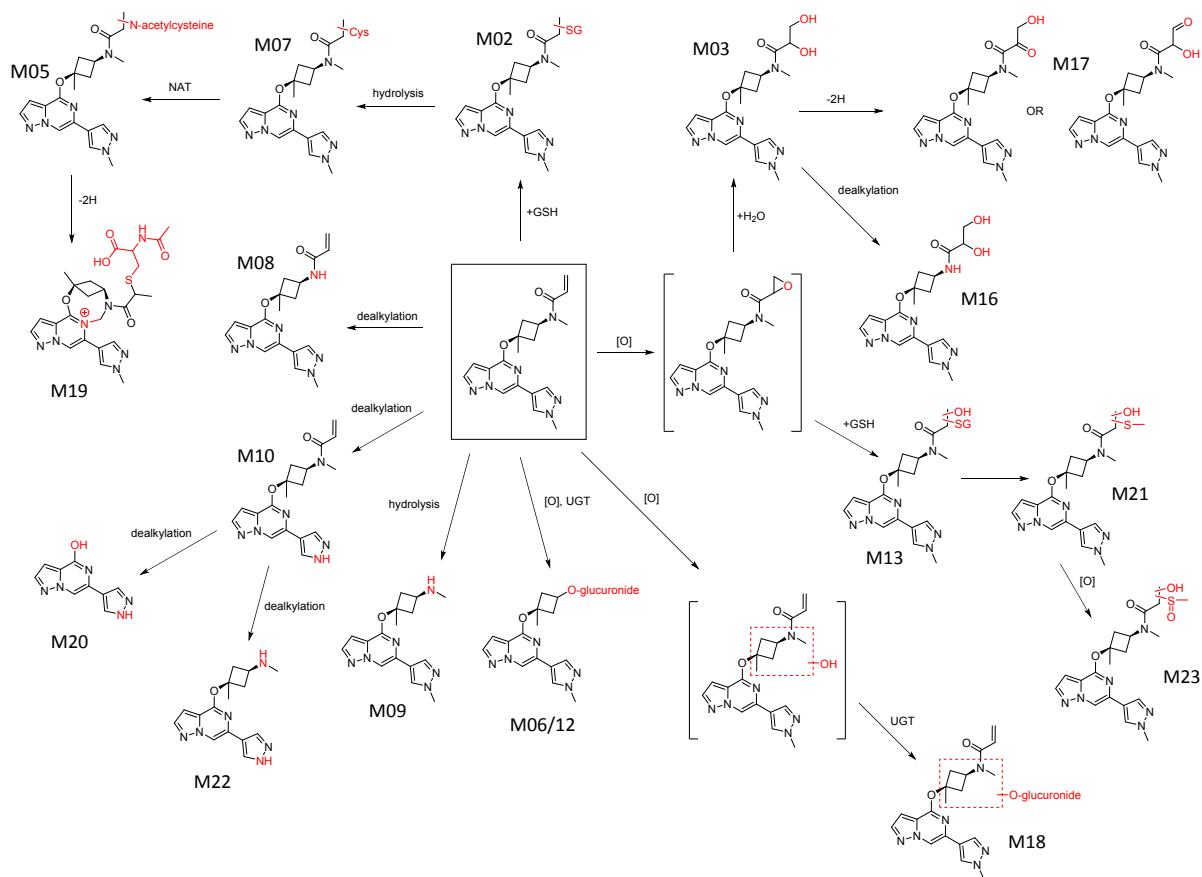


Table S6. Parent and metabolite levels in rat plasma, bile and urine after an oral dose of BIIB129 (percent of all drug-related LC-MS extracted ion chromatographic peak areas)

ID	Metabolism	Plasma		Bile	Urine
		0-5 h	5-24 h	0-5 h	0-5 h
BIIB129	Parent drug	66	58	3	
M02	GSH addition			12	
M03	Oxidation to epoxide → hydrolysis	10	2		12
M05	GSH addition → hydrolysis	< 1	< 1	75	40
M06	Oxidation → glucuronidation			< 1	
M07	GSH addition → hydrolysis	9	3		
M08	N-dealkylation	4	4		
M09	Hydrolysis	< 1	1		4
M10	N-dealkylation	7	4		
M12	Oxidation → glucuronidation			< 1	
M13	Oxidation to epoxide → GSH addition			6	27
M16	Oxidation to epoxide → hydrolysis → N-dealkylation				2
M17	Oxidation to epoxide → hydrolysis → desaturation			2	
M18	Oxidation → glucuronidation			2	
M19	GSH addition → hydrolysis → desaturation				3
M20	di-N-dealkylation	< 1			3
M21	Oxidation to epoxide → GSH addition → mercapturic acid pathway	6	18		7
M22	di-N-dealkylation				2
M23	Oxidation to epoxide → GSH addition → mercapturic acid pathway → oxidation to sulfoxide		23		

PK/PD modeling

PK/PD modeling in mice was performed to describe the time course of BTK target occupancy in various tissues. The time course of BTK inactivation was modeled using the following equation:

$$\frac{d(BTK_{free})}{dt} = K_{syn} - BTK_{free} * K_{deg} - BTK_{free} * k_{inact} * \frac{C_{free}}{K_i + C_{free}}$$

In the above equation, BTK_{free} represents unbound target; K_{syn} and K_{deg} represent the zero order and first order target synthesis rate and degradation rate constant, respectively; C_{free} represents the unbound drug concentration; and k_{inact} and K_i represent the inactivation rate constant and inhibition constant for covalent inhibition, respectively. Both k_{inact} and K_i were estimated by the model.

The PK/PD relationship for BTK target occupancy in various tissues following PO dosing of BIIB129 was established in mice. The potency for BTK inactivation (k_{inact}/K_i) was estimated as approximately $2.50 \frac{1}{ng/mL * h}$ ($250,000 M^{-1} \cdot s^{-1}$) and the BTK half-life in mice was estimated as approximately 35 hr (consistent with the range of BTK half-life reported in literature in rodents. (Haselmayer, Camps, et al. 2019)).⁶

Prediction of Human PK Parameters of BIIB129 (25)

A summary of nonclinical (in vitro and in vivo) data and the human PK prediction method(s) and results for various parameters of interest is provided in this section.

1. Volume of distribution (V_{ss}): The human V_{ss} value was predicted from monkey V_{ss} using single-species scaling with a correction for unbound fraction. The results were in close alignment with the in-silico predictions (1.12 L/kg) from the Oie-Tozer method (**Table S7**).
2. Bioavailability (F): Human oral bioavailability was predicted by averaging the oral bioavailability observed in rat, dog, and monkey following PO dosing of BIIB129 (**Table S7**).
3. Unbound brain to plasma concentration ratio ($K_{p,uu}$): Human brain $K_{p,uu}$ was predicted from the nonclinical in vitro efflux ratios and then adjusted using observed in vivo brain $K_{p,uu}$ vs. predicted $K_{p,uu}$ in rats and monkeys (**Table S7**).
4. Plasma clearance (CL): A range of human plasma clearance was predicted using in vitro- in vivo extrapolation (microsomes) and allometric scaling techniques. **Table S8** provides a summary of the clearance prediction results from both methods. The human CL value was averaged from two methods and estimated as 44.5 mL/min/kg.

Table S7. Summary of Relevant Nonclinical (in vitro, in vivo) Data and Human Pharmacokinetics Prediction Method and Results for V_{ss} , K_{puu} and F .

Parameter	Method	Nonclinical values/data	Predicted human value
V_{ss}	Single species (monkey) scaling with unbound fraction correction	Monkey V_{ss} : 1.18 (L/kg) Monkey f_{up} : 10.9% Human f_{up} : 12.2%	Human V_{ss} : 1.18 (L/kg)
K_{puu}	In vitro- in vivo extrapolation of transporter activity	BCRP efflux ratio: 1.38 P-gp efflux ratio: 11 Rat brain K_{puu} : 0.11 Monkey brain K_{puu} : 0.27	Human brain K_{puu} : 0.3
F	Averaging nonclinical F across species	Rat F : 27% Dog F : 4.5% Monkey F : 21%	Human F : 18%

Table S8. Summary of Relevant Nonclinical (in vitro, in vivo) Data and Human Pharmacokinetics Prediction Method(s) and Results for Clearance

Method: In vitro- in vivo Extrapolation (Well Stirred Model)				
Species	Intrinsic microsome CL (mL/min/kg)	Predicted plasma CL (mL/min/kg)	Observed plasma CL (mL/min/kg)	Ratio (observed/predicted) (Correction factor)
Rat	112	9.33	87	9.3
Dog	77.3	5.62	74	13
Monkey	174	15.5	53	3.4
Human	36.4	3.82	NA	8.6 (average)
Predicted human CL from microsomes (correction factor*predicted plasma CL) = 33 mL/min/kg				
Method: Allometry				
Species	Body Weight (kg)	Observed plasma CL (mL/min/kg)	Total clearance vs. body weight-based allometry	
Mouse	0.02	93	Equation: $CL = a \cdot W^b$ Results: $\log(a) = 1.87$ $b = 0.94$ $R^2 = 0.99$	
Rat	0.25	87		
Dog	10	74		
Monkey	5	53		
Human	70			
Predicted human CL from allometry = 56 mL/min/kg				

Activity of BIIB129 (25) in the BioMAP Human Cell-Based Assay









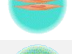



BIIB129 (**25**, **BIO-2008864**) was tested at 4 concentrations (0.37, 1.1, 3.3, 10 μ M) for its potential inhibitory activity using the BioMAP system, developed by BioSeek/DiscoverX, which is comprised of a series of 12 validated culture systems in which human primary cells derived from different tissue sources are stimulated with relevant agonists (Figure 5, Panel A). Quantification of an array of biomarker readouts from each culture system allowed assessment of BIIB129 effects on a variety of tissue cell types and the generation of an overall biological activity profile (**Figure S5, Panel A**).

The only culture system significantly impacted by BIIB129 at the therapeutically relevant concentration of 370 nM (with a threshold effect size criterion of 30% relative to biomarker values observed in vehicle-treated conditions) was the BT culture system. The BT culture system is comprised of primary B cells and PBMCs stimulated with anti-IgM antibody and a suboptimal concentration of TCR ligands allowing for expression of B-cell costimulatory molecules by T cells. In this system, BIIB129 inhibited most biomarker readouts, among which were B-cell proliferation, cytokine secretion (IL-2, IL-6, TNF α) and antibody production (IgG). By contrast, at this same concentration, BIIB129 had no or minimal effects in the SAg system in which PBMCs are stimulated by TCR ligands. At higher concentrations in the μ M range and above, additional effects were observed in other systems outside of the BT system such as the T-cell system (SAg system). Additional cellular pathways were also affected at these μ M concentrations such as TLR2 and TLR4 pathway in endothelium/PBMCs (LPS system and /Mphg system), IL1/IFN γ /TNF α in epithelial cells (BE3C system) and smooth muscle cells (CASM3C system), IL1/IFN γ /TNF α /EGF/FGF/PDGF in fibroblasts (HDF3CGF system), and TGF β /TNF in lung fibroblasts (MyoF system).

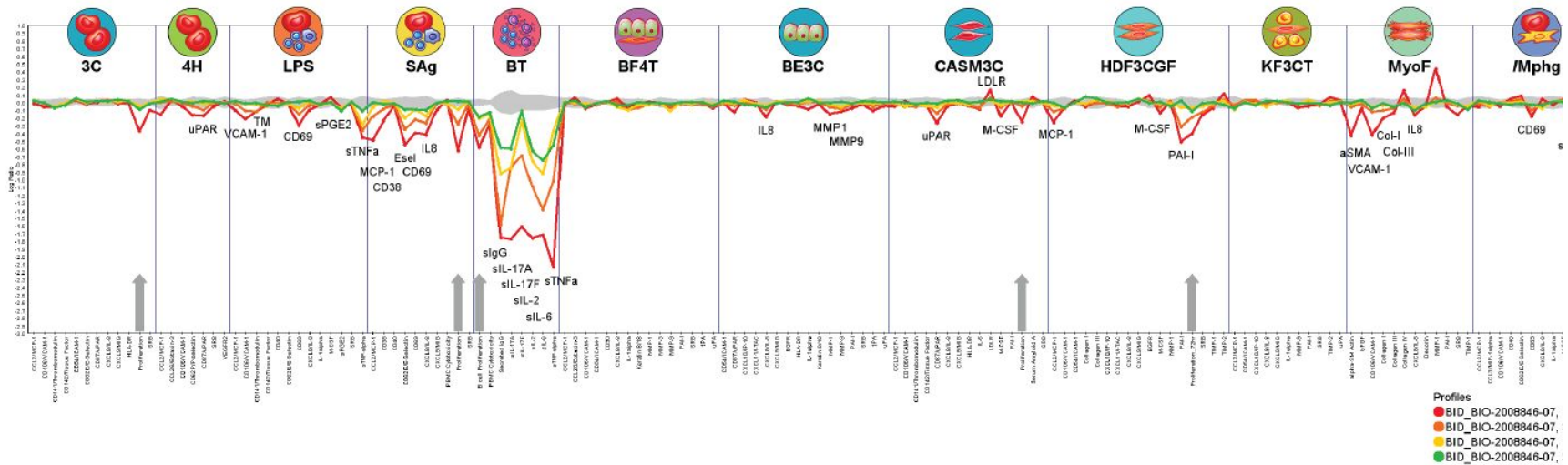
Note that at the therapeutically relevant dose of 20 mg BID predicted to achieve 90% BTK target occupancy in the CNS at the trough of the dosing interval, the C_{\max} concentration of BIIB129 is expected to be approximately 50 nM. Altogether, these results confirm biochemical and in-cell selectivity results by establishing the selective functional effects of BIIB129 on B-cell activation and effector functions at the concentration of 370 nM. At this concentration which is approximately 7 times higher than the concentration predicted to be achieved at C_{\max} of the therapeutically efficacious dose, there was no or minimal effect on any of the cellular systems tested in this assay, as expected based on the selectivity profile of BIIB129.

Figure S5. BIIB129 Shows Highly Selective Inhibitory Activity Restricted to the BT Co-Culture System in the BioMAP Human Cell-Based Assay

(A)

System + Symbol	Human Primary Cells	Disease / Tissue Relevance	Biomarker Readouts
3C 	Venular endothelial cells	Cardiovascular Disease, Chronic Inflammation	MCP-1, VCAM-1, TM, TF, ICAM-1, E-selectin, uPAR, IL-8, MIG, HLA-DR, Proliferation, SRB
4H 	Venular endothelial cells	Asthma, Allergy, Autoimmunity	MCP-1, Eotaxin-3, VCAM-1, P-selectin, uPAR, SRB, VEGFR11
LPS 	Peripheral blood mononuclear cells + Venular endothelial cells	Cardiovascular Disease, Chronic Inflammation	MCP-1, VCAM-1, TM, TF, CD40, E-selectin, CD69, IL-8, IL1 α , M-CSF, sPGE2, SRB, sTNF α
SAg 	Peripheral blood mononuclear cells + Venular endothelial cells	Autoimmune Disease, Chronic Inflammation	MCP-1, CD38, CD40, E-selectin, CD69, IL-8, MIG, PBMC Cytotoxicity, Proliferation, SRB
BT 	Peripheral blood mononuclear cells + B cells	Asthma, Allergy, Oncology, Autoimmunity	B cell Proliferation, PBMC Cytotoxicity, Secreted IgG, sIL17A, sIL17F, sIL-2, sIL-6, sTNF α
BF4T 	Bronchial epithelial cells + Dermal fibroblasts	Asthma, Allergy, Fibrosis, Lung Inflammation	MCP-1, Eotaxin-3, VCAM-1, ICAM-1, CD90, IL-8, IL1 α , Keratin 8/18, MMP-1, MMP-3, MMP-9, PAI-1, SRB, tPA, uPA
BE3C 	Bronchial epithelial cells	Lung Inflammation, COPD	ICAM-1, uPAR, IP-10, I-TAC, IL-8, MIG, EGFR, HLA-DR, IL1 α , Keratin 8/18, MMP-1, MMP-9, PAI-1, SRB, tPA, uPA
CASM3C 	Coronary artery smooth muscle cells	Cardiovascular Inflammation, Restenosis	MCP-1, VCAM-1, TM, TF, uPAR, IL-8, MIG, HLA-DR, IL-6, LDLR, M-CSF, PAI-1, Proliferation, SAA, SRB
HDF3CGF 	Dermal fibroblasts	Fibrosis, Chronic Inflammation	MCP-1, VCAM-1, ICAM-1, Collagen I, Collagen III, IP-10, I-TAC, IL-8, MIG, EGFR, M-CSF, MMP-1, PAI-1, Proliferation_72hr, SRB, TIMP-1, TIMP-2
KF3CT 	Keratinocytes + Dermal fibroblasts	Psoriasis, Dermatitis, Skin Biology	MCP-1, ICAM-1, IP-10, IL-8, MIG, IL1 α , MMP-9, PAI-1, SRB, TIMP-2, uPA
MyoF 	Lung fibroblasts	Fibrosis, Chronic Inflammation, Wound Healing, Matrix Remodeling	α -SM Actin, bFGF, VCAM-1, Collagen-I, Collagen-III, Collagen-IV, IL-8, Decorin, MMP-1, PAI-1, TIMP-1, SRB
/ Mphg 	Venular endothelial cells + Macrophages	Cardiovascular Inflammation, Restenosis, Chronic Inflammation	MCP-1, MIP-1 α , VCAM-1, CD40, E-selectin, CD69, IL-8, IL1 α , M-CSF, sIL10, SRB, SRB-Mphg

(B)



(A) Twelve culture systems are used in the BioMAP assay for screening compounds. The primary human cell types and biomarker readouts are shown. (B) Effects of the indicated concentrations of BIIB129 on each biomarker within each culture system are shown. The gray area shows the 95% confidence area of each biomarker response in the absence of drug. Data points that fall outside of the gray area significantly inhibit (below) or increase (above) the biomarker response at the indicated concentration of BIIB129.

Kinome Selectivity:

Determining Kinome Selectivity using *scanMAX*TM

Kinome selectivity for compounds **10**, **25** (BIIB129) and **27** was assessed against a panel of 409 kinases using Eurofins *KINOMEscan*TM *scanMAX*TM Profiling Service⁷ at 1 and 10 μ M compound concentration. Results and raw data from this screen are available in a separate document with binding interactions reported as “Percent Control”. See additional information.

Results for BIIB129 (25): was screened at 1 μ M (**Table S9.**), and results for primary screen binding interactions were reported as “% Control remaining”, where lower numbers indicate stronger hits in the matrix (i.e., kinases exhibiting higher affinity for BIIB129). From this initial phase, 22 kinases (ARK5, AURKA, AURKC, BIKE, BLK, CDCL1, CDK9, CSFR1, EPHB6, ERK4, ERK5, FLT3, GRK4, JAK2, JAK3, PCTK2, PIP5K1A, PLK4, SNARK, TEC, TXK, and YSK4) were identified as exhibiting less than 30% remaining bound kinase relative to control conditions in the presence of 1 μ M BIIB129. A dissociation constant (K_d) for BIIB129 was determined against each of the 22 kinases. Based on the K_d values it was determined that, with the exception of TEC and TXK, BIIB129 exhibits > 100-fold selectivity for BTK versus all other kinases tested. The binding selectivity of BIIB129 for BTK versus TEC and TXK was 2.6- and 1.9-fold (**Table S10.**).

Assay conditions for the *KINOMEscan*TM *scanMAX*TM: For most assays, kinase-tagged T7 phage strains were grown in an E. coli host derived from the BL21 strain. The lysates were centrifuged and filtered to remove cell debris. The remaining kinases were produced in HEK-293 cells and subsequently tagged with DNA for quantitative PCR detection. Streptavidin-coated magnetic beads were treated with biotinylated small molecule ligands for 30 minutes at room temperature to generate affinity resins for kinase assays, blocked with excess biotin, and washed. Binding reactions were assembled by combining kinases, liganded affinity beads, and test compounds in buffer. Reactions were performed in 384-well plates incubated at room temperature with shaking for 1 hour, washed, resuspended in elution buffer and incubated at room temperature with shaking for 30 minutes. The kinase concentration in the eluates was measured by quantitative PCR.

Determining Kinome Selectivity using *KdELECT*TM

Compounds **2** (evobrutinib), **4** (tolebrutinib), **10**, **25** (BIIB129) and **27** were assessed using dissociation constant measurement (K_d) in Eurofins *KINOMEscan*TM *KdELECT*TM profiling service against nine kinases containing a reactive cysteine in the active site which is required for covalent binding with the acrylamide. Results and raw data from this screen are available in a separate document with dissociation constants K_d given in nM concentration. See manuscript and additional information.

Table S9. Kinome selectivity of BIO-2134406 in Eurofins KINOMEScan™ scanMAX™ at 1 μM concentration

Kinase	% Control remaining	Kinase	% Control remaining	Kinase	% Control remaining	Kinase	% Control remaining	Kinase	% Control remaining	Kinase	% Control remaining	Kinase	% Control remaining
AAK1	46	CHEK1	100	FGFR4	100	MAPKAPK2	100	PDGFRA	72	RSK2	80	WNK4	100
ABL1	77	CHEK2	71	FGR	100	MAPKAPK5	93	PDGFRB	70	RSK2	76	YANK1	100
ABL1	99	CIT	100	FLT1	100	MARK1	100	PDPK1	100	RSK3	100	YANK2	100
ABL2	100	CLK1	100	FLT3	21	MARK2	76	PFCDPK1	78	RSK3	100	YANK3	100
ACVR1	93	CLK2	94	FLT3	76	MARK3	100	PFK5	100	RSK4	80	YES	100
ACVR1B	100	CLK3	100	FLT4	100	MARK4	100	PFTAIRE2	100	RSK4	100	YSK1	100
ACVR2A	100	CLK4	100	FRK	100	MAST1	93	PFTK1	100	S6K1	77	YSK4	24
ACVR2B	100	CSF1R	26	FYN	100	MEK1	96	PHKG1	100	SBK1	89	ZAK	100
ACVRL1	100	CSF1R	9.2	GAK	75	MEK2	83	PHKG2	100	SGK	79	ZAP70	100
ADCK3	100	CSK	100	GCN2	100	MEK3	30	PIK3C2B	100	SgK110	100		
ADCK4	100	CSNK1A1	100	GRK1	75	MEK4	92	PIK3C2G	100	SGK2	60		
AKT1	100	CSNK1A1L	100	GRK2	79	MEK5	76	PIK3CA	100	SGK3	77		
AKT2	100	CSNK1D	100	GRK3	59	MEK6	100	PIK3CB	59	SIK	100		
AKT3	93	CSNK1E	100	GRK4	14	MELK	100	PIK3CD	100	SIK2	88		
ALK	61	CSNK1G1	85	GRK7	100	MERTK	100	PIK3CG	91	SLK	100		
AMPK	100	CSNK1G2	100	GSK3A	100	MET	63	PIK4CB	55	SNARK	5.9		
AMPK	100	CSNK1G3	100	GSK3B	90	MINK	95	PIKFYVE	49	SNRK	100		
ANKK1	100	CSNK2A1	83	HASPIN	75	MKK7	70	PIM1	100	SRC	60		
ARK5	15	CSNK2A2	99	HCK	100	MKNK1	76	PIM2	100	SRMS	80		
ASK1	100	CTK	65	HIPK1	100	MKNK2	87	PIM3	100	SRPK1	88		
ASK2	89	DAPK1	100	HIPK2	100	MLCK	100	PIP5K1A	29	SRPK2	77		
AURKA	20	DAPK2	100	HIPK3	79	MLK1	100	PIP5K1C	70	SRPK3	82		
AURKB	46	DAPK3	100	HIPK4	100	MLK2	100	PIP5K2B	31	STK16	39		
AURKC	14	DCAMK1L	80	HPK1	55	MLK3	100	PIP5K2C	57	STK33	100		
AXL	51	DCAMK2L	100	HUNK	100	MIRCKA	100	PKAC-alpha	100	STK35	100		
BIKE	27	DCAMK3L	100	ICK	74	MIRCKB	100	PKAC-beta	100	STK36	100		
BLK	21	DDR1	100	IGF1R	100	MST1	86	PKMYT1	100	STK39	50		
BMPR1A	100	DDR2	91	IKK-alpha	89	MST1R	100	PKN1	100	SYK	100		
BMPR1B	73	DLK	62	IKK-beta	79	MST2	100	PKN2	89	TAK1	100		
BMPR2	73	DMPK	86	IKK-epsil	100	MST3	100	PKNB	93	TAOK1	86		
BMX	49	DMPK2	100	INSR	100	MST4	96	PLK1	86	TAOK2	79		
BRAF	96	DRAK1	100	INSRR	100	MTOR	77	PLK2	82	TAOK3	76		
BRAF	94	DRAK2	100	IRAK1	74	MUSK	100	PLK3	90	TBK1	99		
BRK	100	DYRK1A	97	IRAK3	78	MYLK	76	PLK4	26	TEC	7.5		
BRSK1	100	DYRK1B	100	IRAK4	86	MYLK2	100	PRKCD	100	TESK1	100		
BRSK2	100	DYRK2	78	ITK	47	MYLK4	100	PRKCE	100	TGFBR1	100		
BTK	0	EGFR	98	JAK1	100	MYO3A	82	PRKCH	100	TGFBR2	100		
BUB1	100	EIF2AK1	100	JAK1	90	MYO3B	55	PRKCI	100	TIE1	100		
CAMK1	100	EPHA1	100	JAK2	23	NDR1	87	PRKCQ	88	TIE2	100		
CAMK1B	90	EPHA2	100	JAK3	6.3	NDR2	100	PRKD1	100	TLK1	100		
CAMK1D	100	EPHA3	100	JNK1	63	NEK1	100	PRKD2	100	TLK2	100		
CAMK1G	100	EPHA4	100	JNK2	77	NEK10	50	PRKD3	100	TNIK	100		
CAMK2A	100	EPHA5	100	JNK3	76	NEK11	82	PRKG1	88	TNK1	41		
CAMK2B	100	EPHA6	100	KIT	100	NEK2	87	PRKG2	100	TNK2	100		
CAMK2D	100	EPHA7	100	KIT	100	NEK3	77	PRKR	100	TNNI3K	100		
CAMK2G	100	EPHA8	100	LATS1	44	NEK4	93	PRKX	100	TRKA	71		
CAMK4	100	EPHB1	100	LATS2	100	NEK5	100	PRP4	100	TRKB	100		
CAMKK1	100	EPHB2	100	LCK	95	NEK6	100	PYK2	100	TRKC	100		
CAMKK2	100	EPHB3	100	LIMK1	98	NEK7	100	QSK	74	TRPM6	81		
CASK	80	EPHB4	100	LIMK2	100	NEK9	100	RAF1	100	TSSK1B	100		
CDC2L1	19	EPHB6	9.1	LKB1	100	NIK	78	RET	84	TSSK3	92		
CDC2L2	100	ERBB2	63	LOK	100	NIM1	82	RIOK1	100	TTK	100		
CDC2L5	99	ERBB3	77	LRRK2	96	NLK	100	RIOK2	95	TXK	7.2		
CDK11	100	ERBB4	22	LRRK2	93	OSR1	100	RIOK3	100	domain-c	45		
CDK2	100	ERK1	100	LTK	95	p38-alpha	100	RIPK1	100	domain-pse	72		
CDK3	100	ERK2	100	LYN	100	p38-beta	100	RIPK2	100	TYRO3	96		
CDK4	85	ERK3	100	LZK	100	p38-delta	100	RIPK4	65	ULK1	84		
CDK4	77	ERK4	5.9	MAK	100	p38-gamma	100	RIPK5	70	ULK2	76		
CDK4	100	ERK5	0	MAP3K1	81	PAK1	100	ROCK1	83	ULK3	95		
CDK5	100	ERK8	100	MAP3K15	83	PAK2	100	ROCK2	82	VEGFR2	63		
CDK7	100	ERN1	66	MAP3K2	30	PAK3	100	ROS1	56	VPS34	73		
CDK8	100	FAK	100	MAP3K3	87	PAK4	100	RPS6KA4	80	VRK2	70		
CDK9	22	FER	100	MAP3K4	100	PAK6	100	RPS6KA5	94	WEE1	100		
CDKL1	98	FES	100	MAP4K2	70	PAK7	100	RPS6KA5	100	WEE2	100		
CDKL2	100	FGFR1	100	MAP4K3	100	PCTK1	95	RPS6KA5	100	WNK1	93		
CDKL3	100	FGFR2	100	MAP4K4	41	PCTK2	0	RSK1	100	WNK2	100		
CDKL5	100	FGFR3	100	MAP4K5	100	PCTK3	100	RSK1	100	WNK3	100		
				% Control remaining	>50%		<50% ->30%		≤30%				

Table S10. Summary of K_d Values for BIIB129 (**25**) for Kinases Identified from the Kinome Screen

Kinase Target	K_d (μM)	Selectivity versus BTK
Bruton's tyrosine kinase (BTK)	0.00057	-
Protein Tyrosine Kinase (TEC)	0.0014	2.6
Tyrosine-protein kinase (TXK)	0.011	19
Colony stimulating factor 1 receptor (CSFR1)	0.073	>100
Fms like tyrosine kinase 3 (FLT3)	0.068	>100
Janus Kinase 3 (JAK3)	0.058	>100
Phosphatidylinositol-4-Phosphate 5-Kinase Type 1 (PIP5K1A)	0.50	>100
SNF1/AMP kinase-related kinase (SNARK)	0.077	>100
Aurora A kinase (AURKA)	0.150	278
Ephrin type-B receptor 6 (EPHB6)	0.170	>300
Polo-like kinase 4 (PLK4)	0.16	>300
Mitogen-activated protein kinase kinase kinase 19 (YSK4)	0.16	320
Aurora C kinase (AURKC)	0.190	>500
B-lymphoid tyrosine kinase (BLK)	0.310	>500
AMP-activated protein kinase-related kinase 5 (ARK5)	0.380	>700
BMP2 inducible kinase (BIKE)	0.38	>700
Janus kinase 2 (JAK2)	1.10	>2000
G-Protein-Coupled receptor kinase 4 (GRK4)	3.7	>6000
Cyclin-dependent kinase 11B (CDC2L1)	29	>10,000
Cyclin-dependent kinase 9 (CDK9)	>30	>10,000
Mitogen-activation protein kinase 4 (ERK4)	>30	>10,000
Extracellular signal-regulated kinase 5 (ERK5)	>30	>10,000
PCTAIRE protein kinase 2 (PCTK2)	>30	>10,000

References:

1. Ma, B.; Bohnert, T.; Otipoby, K. L.; Tien, E.; Arefayene, M.; Bai, J.; Bajrami, B.; Bame, E.; Chan, T. R.; Humora, M.; MacPhee, J. M.; Marcotte, D.; Mehta, D.; Metrick, C. M.; Moniz, G.; Polack, E.; Poreci, U.; Prefontaine, A.; Sheikh, S.; Schroeder, P.; Smirnakis, K.; Zhang, L.; Zheng, F.; Hopkins, B. T., Discovery of BIIB068: A Selective, Potent, Reversible Bruton's Tyrosine Kinase Inhibitor as an Orally Efficacious Agent for Autoimmune Diseases. *Journal of Medicinal Chemistry* **2020**, *63* (21), 12526-12541.
2. Hopkins, B. T.; Bame, E.; Bajrami, B.; Black, C.; Bohnert, T.; Boisselle, C.; Burdette, D.; Burns, J. C.; Delva, L.; Donaldson, D.; Grater, R.; Gu, C.; Hoemberger, M.; Johnson, J.; Kapadnis, S.; King, K.; Lulla, M.; Ma, B.; Marx, I.; Magee, T.; Meissner, R.; Metrick, C. M.; Mingueneau, M.; Murugan, P.; Otipoby, K. L.; Polack, E.; Poreci, U.; Prince, R.; Roach, A. M.; Rowbottom, C.; Santoro, J. C.; Schroeder, P.; Tang, H.; Tien, E.; Zhang, F.; Lyssikatos, J., Discovery and Preclinical Characterization of BIIB091, a Reversible, Selective BTK Inhibitor for the Treatment of Multiple Sclerosis. *J Med Chem* **2022**, *65* (2), 1206-1224.
3. Williams, C. J.; Headd, J. J.; Moriarty, N. W.; Prisant, M. G.; Videau, L. L.; Deis, L. N.; Verma, V.; Keedy, D. A.; Hintze, B. J.; Chen, V. B.; Jain, S.; Lewis, S. M.; Arendall III, W. B.; Snoeyink, J.; Adams, P. D.; Lovell, S. C.; Richardson, J. S.; Richardson, D. C., MolProbity: More and better reference data for improved all-atom structure validation. *Protein Science* **2018**, *27* (1), 293-315.
4. Hamilton, R. A.; Garnett, W. R.; Kline, B. J., Determination of mean valproic acid serum level by assay of a single pooled sample. *Clin Pharmacol Ther* **1981**, *29* (3), 408-413.
5. Hop, C. E.; Wang, Z.; Chen, Q.; Kwei, G., Plasma-pooling methods to increase throughput for in vivo pharmacokinetic screening. *J Pharm Sci* **1998**, *87* (7), 901-3.
6. Haselmayer, P.; Camps, M.; Liu-Bujalski, L.; Nguyen, N.; Morandi, F.; Head, J.; O'Mahony, A.; Zimmerli, S. C.; Bruns, L.; Bender, A. T.; Schroeder, P.; Grenningloh, R., Efficacy and Pharmacodynamic Modeling of the BTK Inhibitor Evobrutinib in Autoimmune Disease Models. *The Journal of Immunology* **2019**, *202* (10), 2888-2906.
7. Fabian, M. A.; Biggs, W. H.; Treiber, D. K.; Atteridge, C. E.; Azimioara, M. D.; Benedetti, M. G.; Carter, T. A.; Ciceri, P.; Edeen, P. T.; Floyd, M.; Ford, J. M.; Galvin, M.; Gerlach, J. L.; Grotzfeld, R. M.; Herrgard, S.; Insko, D. E.; Insko, M. A.; Lai, A. G.; Lélias, J.-M.; Mehta, S. A.; Milanov, Z. V.; Velasco, A. M.; Wodicka, L. M.; Patel, H. K.; Zarrinkar, P. P.; Lockhart, D. J., A small molecule-kinase interaction map for clinical kinase inhibitors. *Nature Biotechnology* **2005**, *23* (3), 329-336.